


May 2019

Quantitative Evaluation of Geared Manual Wheelchair Mobility in Individuals with Spinal Cord Injury: An Integrative Approach

Omid Jahanian

University of Wisconsin-Milwaukee

Follow this and additional works at: <https://dc.uwm.edu/etd>

 Part of the [Biomechanics Commons](#), [Biomedical Engineering and Bioengineering Commons](#), and the [Medicine and Health Sciences Commons](#)

Recommended Citation

Jahanian, Omid, "Quantitative Evaluation of Geared Manual Wheelchair Mobility in Individuals with Spinal Cord Injury: An Integrative Approach" (2019). *Theses and Dissertations*. 2080.
<https://dc.uwm.edu/etd/2080>

This Dissertation is brought to you for free and open access by UWM Digital Commons. It has been accepted for inclusion in Theses and Dissertations by an authorized administrator of UWM Digital Commons. For more information, please contact open-access@uwm.edu.

QUANTITATIVE EVALUATION OF GEARED MANUAL WHEELCHAIR MOBILITY IN
INDIVIDUALS WITH SPINAL CORD INJURY: AN INTEGRATIVE APPROACH

by

Omid Jahanian

A Dissertation Submitted in
Partial Fulfillment of the
Requirements for the Degree of

Doctor of Philosophy
in Health Sciences

at

The University of Wisconsin-Milwaukee

May 2019

ABSTRACT

QUANTITATIVE EVALUATION OF GEARED MANUAL WHEELCHAIR MOBILITY IN INDIVIDUALS WITH SPINAL CORD INJURY: AN INTEGRATIVE APPROACH

by

Omid Jahanian

The University of Wisconsin-Milwaukee, 2019

Under the Supervision of Professor Brooke Slavens

The purpose of this dissertation is to quantify the effects of using geared wheelchair wheels on upper extremity biomechanics and energy expenditure during functional mobility tasks in individuals with spinal cord injury (SCI). The effects of using geared wheels on hand-rim biomechanics, glenohumeral joint dynamics, and shoulder muscle activity were investigated during manual wheelchair propulsion over tiled and carpeted level-floors and up a ramp in low gear (1.5:1) and standard gear (1:1) conditions. The results for the hand-rim biomechanics indicated that regardless of the terrain, using the geared wheels in the low gear condition significantly decreased the propulsion speed, stroke distance, and hand-rim kinetics, including the peak hand-rim resultant force, propulsive moment, and rate of the rise of the resultant force. The significant decrease in the normalized integrated hand-rim propulsive moment suggests that the low gear condition is less demanding than the standard gear condition, in spite of the higher repetition during propulsion in low gear. Analysis of the glenohumeral joint dynamics and shoulder muscle activity during geared manual wheelchair propulsion over carpeted floor showed that the peak glenohumeral joint inferior force and flexion moment, as well as the shoulder flexors muscle activity, decreased significantly during the low gear condition. Manual

wheelchair users with SCI were tested during the six-minute push tests on passive wheelchair rollers to evaluate the effects of using geared wheels on energy expenditure. The results indicated that using geared wheels in the low gear condition significantly increased the energy cost of propulsion and decreased the intensity of wheelchair propulsion. The findings of this dissertation demonstrate that using geared wheels in comparison to standard wheels decreases the demands on the upper extremity of manual wheelchair users, which may ultimately help preserve upper limb function leading to higher levels of activity, independence and quality of life.

© Copyright by Omid Jahanian, 2019
All Rights Reserved

I dedicate this work:

In memory of my father; Mohammad Bagher Jahanian

To my beloved mother; Mahnaz, and my dear brothers; Ali & Amin

TABLE OF CONTENTS

List of Figures	ix
List of Tables	xiv
Acknowledgments.....	xvi
Chapter 1: Introduction	1
Background	1
Manual Wheelchairs	4
Statement of the Problem	8
Specific Aims and Hypotheses	9
Significance and Innovation	10
Content Presentation	12
References	15
Chapter 2: A Comparison of Glenohumeral Joint Kinematics and Muscle Activation During Standard and Geared Manual Wheelchair Mobility	18
Introduction	18
Methods	20
Subjects	20
Experimental Protocol	20
Data Collection	21
Data Processing	23
Data Analysis	25
Results	26
Discussion	31

Conclusion	35
References	36
Chapter 3: Hand-Rim Biomechanics during Geared Manual Wheelchair Propulsion over Different Ground Conditions in Individuals with Spinal Cord Injury	39
Introduction	39
Methods	43
Subjects	43
Data Collection	44
Data Analysis	45
Statistical Analysis	49
Results	51
Discussion	61
Conclusion	63
References	64
Chapter 4: Glenohumeral Joint Dynamics and Shoulder Muscle Activity During Geared Manual Wheelchair Propulsion on Carpeted Floor in Individuals with Spinal Cord Injury	67
Introduction	67
Methods	71
Subjects	71
Experimental Protocol	72
Data Collection	73
Data Processing	76
Data and Statistical Analysis	79
Results	80
Discussion	87
Conclusion	90
References	92

Chapter 5: The Effects of Using Geared Wheelchair Wheels on Energy Cost of Propulsion in Adults with Spinal Cord Injury	96
Introduction	96
Methods	99
Subjects	99
Experimental Protocol and Instrumentation	99
Data Processing	103
Statistical Analysis	105
Results	105
Discussion	109
Conclusion	111
References	113
 Chapter 6: Overall Summary and Conclusions	 116
Summary and Discussion	116
Practical Implications	120
Limitations and Future Directions	123
 References	 125
 Curriculum Vitae	 126

LIST OF FIGURES

Figure 1. Interaction between the components of ICF. 2

Figure 2. The three domains of the wheelchair evaluation and their interactions. 4

Figure 3. Different types of manual wheelchairs. (a) Breezy standard manual wheelchair (Sunrise Medical LLC.), (b) E-Motion M15 PAPA W (Alber USA LLC), (C) geared manual wheelchair with IntelliWheels geared wheels (IntelliWheels, Inc.), (d) lever-propelled wheelchair with Wijit lever drive (Wijit, inc.), and (e) handcycle wheelchair, Top End Excelerator™ (Invacare Corporation). 6

Figure 4. A subject ascending a ramp using a manual wheelchair, instrumented with motion capture markers and surface electromyography electrodes (left); and corresponding Vicon rendering of the custom upper extremity biomechanical model (right).
..... 21

Figure 5. Glenohumeral joint kinematics in sagittal, coronal and transverse planes of motion. Group mean profiles (solid line) +/- one standard deviation (dotted line) of 14 subjects (dominant side) for the standard and geared manual wheelchairs during propulsion on level floor are depicted. The vertical dash-dot lines indicate the transition from the end of the push phase to the start of the recovery phase for each wheel type. 29

Figure 6. Glenohumeral joint kinematics in sagittal, coronal and transverse planes of motion. Group mean profiles (solid line) +/- one standard deviation (dotted line) of 14 subjects (dominant side) for the standard and geared manual wheelchairs during propulsion on a ramp are depicted. The vertical dash-dot lines indicate the transition from the end of the push phase to the start of the recovery phase for each wheel type. 29

Figure 7. Group mean peak muscle activity of the anterior deltoid, pectoralis major, and infraspinatus during one stroke cycle of standard and geared manual wheelchair propulsion on level floor and on ramp. Error bars indicate the standard deviations as reported as percent of maximum voluntary isometric contraction (%MVIC). 32

Figure 8. IntelliWheels geared manual wheelchair wheel (left) and the planetary gear train from a prototype IntelliWheels geared manual wheelchair wheel (right). 45

Figure 9. Orientation of instrumental hand rim coordinate system when wheel is mounted on the right side of the wheelchair. 46

Figure 10. A subject propelling on a carpeted level floor using the IntelliWheels geared manual wheelchair wheels. 47

Figure 11. A subject propelling on a tiled level floor using the IntelliWheels geared manual wheelchair wheels. 47

Figure 12. A subject ascending a ramp using the IntelliWheels geared manual wheelchair wheels.	48
Figure 13. A sample hand-rim propulsive moment reaction curve for propulsion on the carpeted floor used for detecting the semi-state stroke cycles, and the push and recovery phases for each stroke cycle. Moments that cause wheelchair to move forward (propulsive moment) are negative, and moments that act in opposite direction are positive.	49
Figure 14. Group mean values and standard deviations for the propulsion speed during manual wheelchair propulsion on tile and carpeted level floor and up the ramp in the standard gear and low gear conditions.	53
Figure 15. Group mean values and standard deviations for the stroke cycle frequency during manual wheelchair propulsion on tile and carpeted level floor and up the ramp in the standard gear and low gear conditions.	54
Figure 16. Group mean values and standard deviations for the peak hand-rim resultant force mean values and standard deviations during manual wheelchair propulsion on tile and carpeted level floor and up the ramp in the standard gear and low gear conditions.	54
Figure 17. Group mean values and standard deviations for the peak hand-rim propulsive moment during manual wheelchair propulsion on tile and carpeted level floor and up the ramp in the standard gear and low gear conditions.	55
Figure 18. Group mean values and standard deviations for the peak rate of rise of hand-rim resultant force during manual wheelchair propulsion on tile and carpeted level floor and up the ramp in the standard gear and low gear conditions.	55
Figure 19. Group mean values and standard deviations for the fraction of effective force during manual wheelchair propulsion on tile and carpeted level floor and up the ramp in the standard gear and low gear conditions.	56
Figure 20. Group mean values and standard deviations for the normalized stroke cycle frequency during manual wheelchair propulsion on tile and carpeted level floor and up the ramp in the standard gear and low gear conditions.	57
Figure 21. Group mean values and standard deviations for the normalized integrated hand-rim resultant force during manual wheelchair propulsion on tile and carpeted level floor and up the ramp in the standard gear and low gear conditions.	57
Figure 22. Group mean values and standard deviations for the normalized integrated hand-rim propulsive moment during manual wheelchair propulsion on tile and carpeted level floor and up the ramp in the standard gear and low gear conditions.	58
Figure 23. Propulsion speed during manual wheelchair propulsion on tile and carpeted level floor and up the ramp. In each graph the box plot on the left is for the standard gear and on the right is for the low gear condition. The bottom and top edges of the box indicate the intra-quartile range. The diamond inside the box indicates the mean value. The line inside the box indicates the	

median value. the whiskers that extend from each box indicate the entire range of values. The measurements for each subject are shown with a circle and the subject number next to it. . 58

Figure 24. Peak hand-rim resultant force during manual wheelchair propulsion on tile and carpeted level floor and up the ramp. In each graph the box plot on the left is for the standard gear and on the right is for the low gear condition. The bottom and top edges of the box indicate the intra-quartile range. The diamond inside the box indicates the mean value. The line inside the box indicates the median value. the whiskers that extend from each box indicate the entire range of values. The measurements for each subject are shown with a circle and the subject number next to it. 59

Figure 25. Peak hand-rim propulsive moment during manual wheelchair propulsion on tile and carpeted level floor and up the ramp. In each graph the box plot on the left is for the standard gear and on the right is for the low gear condition. The bottom and top edges of the box indicate the intra-quartile range. The diamond inside the box indicates the mean value. The line inside the box indicates the median value. the whiskers that extend from each box indicate the entire range of values. The measurements for each subject are shown with a circle and the subject number next to it. 59

Figure 26. Peak rate of rise of hand-rim resultant force during manual wheelchair propulsion on tile and carpeted level floor and up the ramp. In each graph the box plot on the left is for the standard gear and on the right is for the low gear condition. The bottom and top edges of the box indicate the intra-quartile range. The diamond inside the box indicates the mean value. The line inside the box indicates the median value. the whiskers that extend from each box indicate the entire range of values. The measurements for each subject are shown with a circle and the subject number next to it. 60

Figure 27. Fracture effective force during manual wheelchair propulsion on tile and carpeted level floor and up the ramp. In each graph the box plot on the left is for the standard gear and on the right is for the low gear condition. The bottom and top edges of the box indicate the intra-quartile range. The diamond inside the box indicates the mean value. The line inside the box indicates the median value. the whiskers that extend from each box indicate the entire range of values. The measurements for each subject are shown with a circle and the subject number next to it. 60

Figure 28. Normalized stroke cycle frequency during manual wheelchair propulsion on tile and carpeted level floor and up the ramp. In each graph the box plot on the left is for the standard gear and on the right is for the low gear condition. The bottom and top edges of the box indicate the intra-quartile range. The diamond inside the box indicates the mean value. The line inside the box indicates the median value. the whiskers that extend from each box indicate the entire range of values. The measurements for each subject are shown with a circle and the subject number next to it. 61

Figure 29. Normalized integrated hand-rim propulsive moment during manual wheelchair propulsion on tile and carpeted level floor and up the ramp. In each graph the box plot on the left is for the standard gear and on the right is for the low gear condition. The bottom and top edges of the box indicate the intra-quartile range. The diamond inside the box indicates the mean value. The line inside the box indicates the median value. The whiskers that extend from each box indicate the entire range of values. The measurements for each subject are shown with a circle and the subject number next to it. 61

Figure 30. A subject propelling on a carpeted level floor using the IntelliWheels geared manual wheelchair wheels.73

Figure 31. A subject propelling the instrumented geared wheel on a carpeted level floor. The instrumented hand-rim global coordinate system follows the right-hand rule with the positive X-axis anterior, positive Y-axis superior, and positive Z-axis pointing out of the wheel along the axle. The picture also depicts the subject instrumented with the motion capture markers and surface electromyography electrodes.74

Figure 32. Three-dimensional glenohumeral joint angles, forces and moments. Group mean profiles (solid line) +/- one standard deviation (dotted line) of seven subjects (dominant side) for the standard gear and low gear conditions are depicted. The vertical dash-dot lines indicate the transition from the end of the push phase to the start of the recovery phase for each condition. 82

Figure 33. Three-dimensional sternoclavicular (top row) and acromioclavicular (bottom row) joint angles. Group mean profiles (solid line) +/- one standard deviation (dotted line) of seven subjects (dominant side) for the standard gear and low gear conditions are depicted. The vertical dash-dot lines indicate the transition from the end of the push phase to the start of the recovery phase for each condition. 83

Figure 34. (A-C) Muscle activity of the anterior deltoid and pectoralis major muscles during manual wheelchair propulsion. (A) Group mean peak muscle activity, (B) integrated muscle activity, and (C) normalized integrated activity of the anterior deltoid and pectoralis major during the stroke cycle of the standard gear and low gear conditions. Error bars indicate the standard deviations as reported as percent of maximum voluntary isometric contraction (MVIC) for the peak and integrated muscle activity and as percent of maximum voluntary contraction per meter (%MVIC/m) for the normalized integrated muscle activity. Statistical results (z = test statistics; p = significance level; r = effect size; *: $p < 0.05$) are reported for each muscle. 85

Figure 35. Peak hand-rim resultant force (left) and peak hand-rim propulsive moment (right). The bottom and top edges of the box indicate the intra-quartile range between the first and third quartiles (25th and 75th percentiles). The diamond inside the box indicates the mean value. The line inside the box indicates the median value. The whiskers that extend from each box indicate the entire range of values. The metrics for each subject are shown with a circle and the corresponding subject number. 86

Figure 36. Peak glenohumeral joint inferior force (left) and peak glenohumeral joint flexion moment (right). The bottom and top edges of the box indicate the intra-quartile range between the first and third quartiles (25th and 75th percentiles). The diamond inside the box indicates the mean value. The line inside the box indicates the median value. The whiskers that extend from each box indicate the entire range of values. The metrics for each subject are shown with a circle and the corresponding subject number. 86

Figure 37. Peak glenohumeral joint inferior force (left) and peak glenohumeral joint flexion moment (right). The bottom and top edges of the box indicate the intra-quartile range between the first and third quartiles (25th and 75th percentiles). The diamond inside the box indicates the mean value. The line inside the box indicates the median value. The whiskers that extend from each box indicate the entire range of values. The metrics for each subject are shown with a circle and the corresponding subject number. 87

Figure 38. Energy expenditure assessment during manual wheelchair propulsion on passive wheelchair rollers; the COSMED mask and data acquisition Holter are also shown. 101

Figure 39. Total energy expenditure (left) and distance travelled for the low gear (G) and standard gear (DD) conditions. Each bar along the y-axis represents an individual participant, the top bars show the group mean values. 107

Figure 40. Cost of transport (left) and rate of oxygen consumption (SCI METs) for the low gear (G) and standard gear (DD) conditions. Each bar along the y-axis represents an individual participant, the top bars show the group mean values. 108

Figure 41. Average heart rate (left) and rate of perceived exertion for the low gear (G) and standard gear (DD) conditions. Each bar along the y-axis represents an individual participant, the top bars show the group mean values. 108

Figure 42. Distance travelled (top left), cost of transport (top right), rate of oxygen consumption (SCI MET, bottom left), and rate of perceived exertion (RPE, bottom right) which was measured for each subject during the standard gear and low gear conditions. In each graph the box plot on the left is for the standard gear and on the right is for the low gear condition. In each graph the measurements for each subject are shown with a circle and the subject ID next to it.109

LIST OF TABLES

Table 1. Subjects' characteristics.	14
Table 2. Specifications of the standard and geared wheels.	21
Table 3. Group mean wheelchair propulsion spatiotemporal parameters (mean \pm 1 SD) for each experimental condition (standard and geared wheels on a level floor and on a ramp).	26
Table 4. Group mean glenohumeral joint ranges of motion (mean \pm 1 SD) during the standard and geared manual wheelchair propulsion on level floor and on a ramp (degrees).	29
Table 5. Group mean peak glenohumeral joint kinematics (mean \pm 1 SD) during the standard and geared manual wheelchair propulsion on level floor and on a ramp (degrees).	30
Table 6. Group mean integrated shoulder muscle activity (mean \pm 1 SD) during one stroke cycle of the standard and geared manual wheelchair propulsion on level floor and on a ramp, reported as percent of maximum voluntary isometric contraction (%MVIC).	31
Table 7. Group mean normalized integrated shoulder muscle activity (mean \pm 1 SD) during the standard and geared manual wheelchair propulsion on level floor and on a ramp, reported as percent of maximum voluntary isometric contraction per meter (%MVIC/m).	31
Table 8. Subject characteristics and wheelchair user's shoulder pain index (WUSPI) total scores.	44
Table 9. Summary of all calculations for the metrics of interest.	50
Table 10. Stroke cycle characteristics and hand-rim kinetics mean values and standard deviations during manual wheelchair propulsion on tile and carpeted level floor and up the ramp in the standard gear and low gear conditions.	52
Table 11. Group mean values and standard deviations for the normalized frequency, normalized integrated force, and normalized integrated moment during manual wheelchair propulsion on tile and carpeted level floor and up the ramp in the standard gear and low gear conditions.	56
Table 12. Subject characteristics and wheelchair user's shoulder pain index (WUSPI) total scores.	72
Table 13. Group mean temporal-spatial parameters and rate of perceived exertion for the standard gear and low gear conditions.	82
Table 14. Group mean peak glenohumeral joint kinematics for the standard gear and low gear conditions.	83

Table 15. Group mean peak hand-rim (HR) resultant force and peak glenohumeral (GH) joint forces during push phase for the standard gear and low gear conditions.	84
Table 16. Group mean peak hand-rim (HR) propulsive moment and peak glenohumeral (GH) joint moments during push phase for the standard gear and low gear conditions.	84
Table 17. Group mean hand-rim (HR) normalized integrated resultant force and propulsive moment, and group mean glenohumeral (GH) normalized integrated resultant force and resultant moment during push phase for the standard gear and low gear conditions.	84
Table 18. Subjects characteristics.	100
Table 19. Locations of retroreflective markers for calculation of the distance traveled and stroke cycle frequency, as well as characterization of propulsion pattern.	102
Table 20. The Borg RPE scale, the 15-grade scale for ratings of perceived Exertion (RPE).	103
Table 21. Mean and standard deviation of total distance (Tot. Distance), cost of transport (CT), metabolic equivalent (SCI MET), average heart rate (HR), stroke cycle frequency (cadence), and rate of perceived exertion (RPE) for the standard gear and low gear conditions.	107
Table 22. Propulsion patterns during standard gear and geared conditions.	109

ACKNOWLEDGMENTS

First and most of all, I would like to thank my advisor and mentor Dr. Brooke Slavens for her support and guidance. I truly appreciate the time and effort she has devoted to helping me reach my full potential. It has been an honor to work with her. I would like to thank my committee members Dr. Roger Smith, Dr. Kristian O'Connor, Dr. Gerald Harris, Dr. Scott Strath, and Dr. Bhagwant Sindhu for their support, suggestions and encouragement. Their support in this project and throughout my time as a graduate student has been invaluable. I would also like to thank Dr. Liz Hsiao-Wecksler, Dr. Vaishnavi Muqet, Dr. Barbara Silver-Thorn, Chris C. Cho, Alan Gaglio, and Scott Daigle for their support and collaboration in this project. A special thank you to Alyssa Schnorenberg, Lianna Hawi, Justin Riebe, and all graduate and undergraduate students at the UWM Mobility lab for their generous help in this project. Finally, I would like to thank the faculty and students at the department of Occupational Science and Technology that I had a chance to work with and/or alongside during my time at the UW-Milwaukee.

Chapter 1

Introduction

Background

Mobility is an essential ability for everyone, influencing all aspects of life. Mobility provides a means to learn, interact with others, earn a living and participate in society (Calhoun, Schottler, & Vogel, 2013). Pathologies such as spinal cord injury (SCI) could have devastating effects on mobility and consequently on quality of life. Hence, mobility must be considered one of the most significant aspects of the rehabilitation of individuals with SCI. The number of people with SCI in the U.S. is estimated to be up to 358,000. The recent estimates have shown that the annual incidence of SCI is approximately 17,000 new SCI cases each year (White & Black, 2016).

The overall purpose of rehabilitation for patients with SCI is to improve health related quality of life, which can be achieved by improving the patient's ability to participate in activities of daily life. The barriers to participation are impairment and associated motor and sensory loss (Harvey, 2008). To provide a unified and standard language for those working in the areas of disability, the purpose of rehabilitation for patients with SCI could be defined within the framework of international classification of Functioning, Disability and Health (ICF). The ICF defines components of the health from the perspective of the body, individual and society (World Health Organization, 2001). For SCI health condition, the associated impairment is poor strength (Harvey, 2008) which directly impacts on the ability to perform mobility activities such as walking and moving (Harvey, 2008). This in turn has implications for participation, such as working, engaging in family life and participating in community activities. According to ICF, impairment, activity

limitation and participation restriction are all effected by environmental and personal factors (Figure 1). Among environmental factors, access to appropriate assistive products and technology for personal indoor and outdoor mobility and transportation could have a great significance in the process of rehabilitation and restoration of function and mobility in persons with SCI. Most individuals who sustain an SCI require manual or power wheelchairs as a means of mobility.

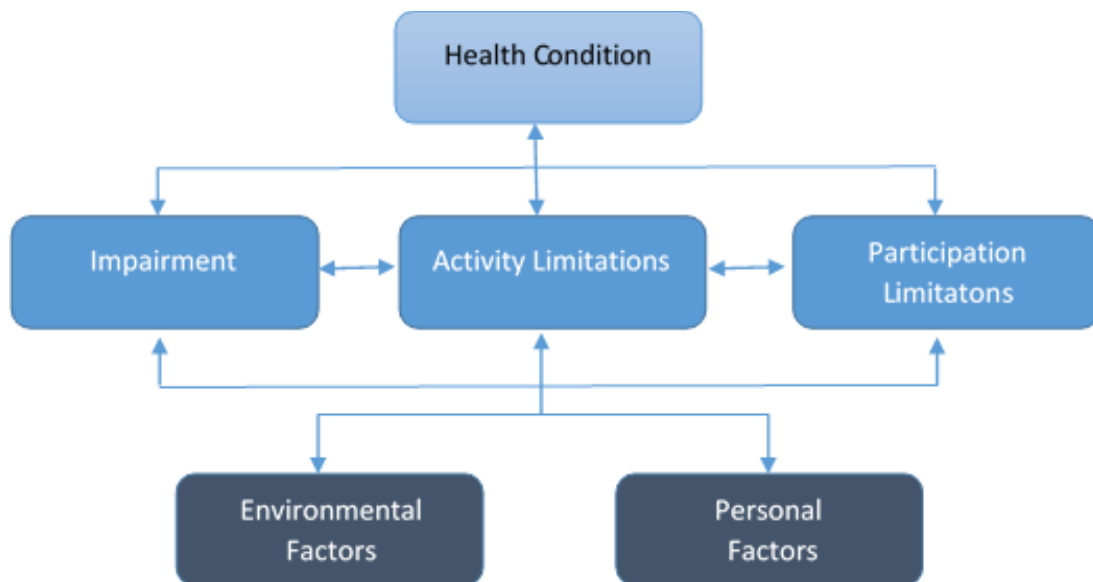


Figure 1. Interaction between the components of ICF (World Health Organization, 2001).

Spinal cord injury (SCI) is one of the leading conditions associated with wheelchair use (Kaye, Kang, & LaPlante, 2000). More than half of the individuals with SCI in the U.S. are non-ambulatory and wheelchair users (Stover, DeLisa, & Whiteneck, 1995); manual wheelchairs are the most common alternative mode of mobility chosen by people with SCI (Beekman, Miller-Porter, & Schoneberger, 1999). To optimize users' functions and minimize the risk of injuries and traumas associated with wheelchair mobility, prescription of a wheelchair as an intervention should match the user's current expectations, preferences, and physical needs. Often clinicians prescribe the appropriate form of mobility and type of wheelchair through subjective methods by

considering factors such as age, level of severity of injury, environment and personal preferences. Transition to other forms of wheeled mobility is often prescribed too late when a patient has endured an injury or presented with pain, which could have negative effects on their quality of life. Understanding the mechanism of intervention and its effect on impairment, coupled with knowledge of the model of disablement, are necessary for optimized prescription of an adaptive equipment (e.g. wheelchair) or transitioning to a new equipment targeted to the intervention (Marino, 2007). For this reason, all three domains of individual (personal factors), environment (environmental factors) and adaptive equipment (e.g. wheelchair) and their interactions need to be adequately considered (Batavia, Batavia, & Friedman, 2001). The intervention target in the rehabilitation process needs to be structured in a way that increase the interaction between the individual and the adaptive equipment (fit between person and wheelchair) and the interaction between environment and the adaptive equipment (access of the wheelchair within the environment) (Batavia et al., 2001). Therefore, the user can function optimally in his or her world (Figure 2). To achieve this goal, it is necessary to develop an integrative approach based on biomechanical and physiological analyses, and functional assessments of manual wheelchair users. The main goal of biomechanical and physiological analysis of wheelchair propulsion should be the generation of knowledge that can be used to improve performance, prevent secondary injuries, and ultimately increase the quality of life of wheelchair users.

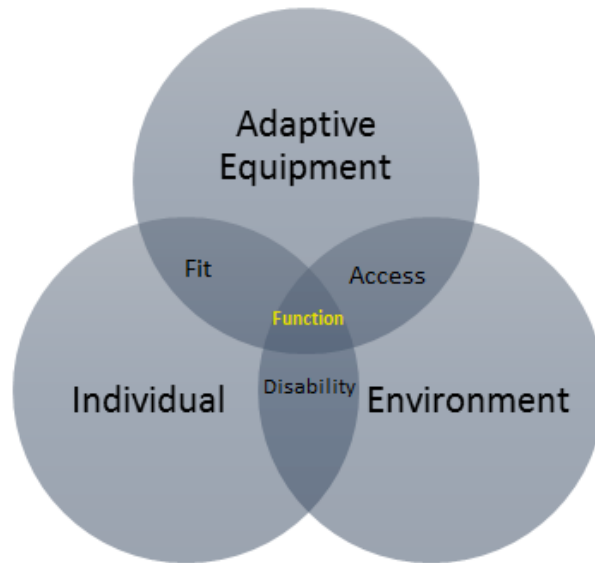


Figure 2. The three domains of the wheelchair evaluation and their interactions (Batavia et al., 2001).

Manual Wheelchairs

About 90% of daily wheelchairs are basic hand-rim propelled wheelchairs (standard manual wheelchairs), (Kaye et al., 2000). As standard manual wheelchairs are relatively inexpensive, highly maneuverable on flat surfaces, relatively light, and convenient to transport, they are the most commonly prescribed type of wheelchair (Flemmer & Flemmer, 2016). van der Woude described the hand-rim propulsion mechanism as the device which has the closest possible interaction with the human system (van der Woude, Lucas HV, de Groot, & Janssen, 2006) “each stroke of the hands propels, brakes, or turns the wheelchair with direct visual, proprioceptive, and kinesthetic feedback to the user, directly expressing information about position, speed and spatial orientation of the body.” On the other hand, standard manual wheelchair mobility has been described as a low efficient and physically straining form of mobility (van der Woude, Lucas HV et al., 2006). Hand-rim propulsion is very stressful for musculoskeletal (Boninger, Koontz, Sisto,

& Dyson-Hudson, 2005; van der Woude, Lucas HV & de Groot, 2005) and cardiopulmonary (Hildebrandt, Voight, Bahn, Berendes, & Kroger, 1970) systems. Manual wheelchair users are at high risk of repetitive strain injuries, primarily in the shoulder and hand-wrist area (Burnham & Steadward, 1994; Mercer et al., 2006). The solution to this problem might be alternative wheelchair propulsion mechanisms (Figure 3).

Lever and Crank propelled wheelchairs are among the most common alternatives. Several researches have shown that the efficiency of these alternatives varies from slightly lower than standard manual wheelchair propulsion to much higher when gearing is included (Dallmeijer, Zentgraaff, Zijp, & van der Woude, 2004; Flemmer & Flemmer, 2016; van der Woude, Lucas HV, Botden, Vriend, & Veeger, 1997). Lever and crank propulsion mechanisms allow a much more natural position of the hands and shoulders than standard hand-rim propulsion mechanism during propulsion. Therefore, they could be less straining, particularly for outdoor use (Flemmer & Flemmer, 2016; van der Woude, LHV, Veeger, Dallmeijer, Janssen, & Rozendaal, 2001; van der Woude, Lucas HV et al., 2006). However, the use of these alternative manual wheelchairs is limited in comparison with standard manual wheelchairs due to disadvantages such as weight, size, and limited maneuverability as well as being less friendly for transferring (Kloosterman, M. G., Snoek, van der Woude, L H, Buurke, & Rietman, 2013; van der Woude, Lucas HV et al., 2006). Pushrim-activated power assist wheelchairs and geared manual wheelchairs are the most recent alternatives, which use the same propulsion techniques as standard manual wheelchairs but equipped with additional assistance (battery power sources in power assist wheelchairs and mechanical gearing in geared manual wheelchairs). Transition to a power assist wheelchair or a geared manual wheelchair might be an interesting alternative in the context of the preservation of the arm function as well as the need to remain physically active (Finley & Rodgers, 2007; Howarth,

Pronovost, Polgar, Dickerson, & Callaghan, 2010; Karmarkar, Cooper, Liu, Connor, & Puhlman, 2008).



Figure 3. Different types of manual wheelchairs. (a) Breezy standard manual wheelchair (Sunrise Medical LLC.), (b) E-Motion M15 PAPA W (Alber USA LLC), (c) geared manual wheelchair with IntelliWheels geared wheels (IntelliWheels, Inc.), (d) lever-propelled wheelchair with Wijit lever drive (Wijit, inc.), and (e) handcycle wheelchair, Top End Excelerator™ (Invacare Corporation).

need to remain physically active (Finley & Rodgers, 2007; Howarth, Pronovost, Polgar, Dickerson, & Callaghan, 2010; Karmarkar, Cooper, Liu, Connor, & Puhlman, 2008).

Power assist wheelchairs have become a viable option for manual wheelchair users to reduce deconditioning and injuries associated with standard manual wheelchair propulsion. Using power assist wheelchairs combines many of the advantages of both the standard manual wheelchairs and

the powered wheelchairs while increasing mechanical efficiency (Kloosterman et al., 2013). The power assist wheelchair is a hybrid between standard manual wheelchair and powered wheelchairs. It consists of a hand-rim wheelchair with electro-motors embedded into the wheels or wheelchair frame, when a subject exerts power on the hand-rim, the motor is activated and augments the delivered power (Karmarkar et al., 2008). Power assist wheelchairs reduce the user's metabolic energy significantly (Algood, Cooper, Fitzgerald, Cooper, & Boninger, 2004). Kinematic analysis of the arm during power-assisted manual wheelchair propulsion compared to standard manual wheelchair propulsion has been done in several studies (Algood et al., 2004; Corfman, Cooper, Boninger, Koontz, & Fitzgerald, 2003; Kloosterman, Marieke GM, Eising, Schaake, Buurke, & Rietman, 2012). Significant decreases in wrist (Corfman et al., 2003), and shoulder (Algood et al., 2004) ranges of motion have been reported in these studies. Kloosterman and colleagues reported that using power assisted manual wheelchairs significantly decreased the peak force on the hand-rim, resulting in decreased shoulder flexion, adduction and internal rotation moments as well as decreased forces at the shoulder in the posterior, superior and lateral directions (Kloosterman et al., 2012). Significant decreased muscle activity in pectoralis major and triceps brachii during power-assisted manual wheelchair propulsion has been reported by the majority of researchers who studied muscle activation patterns during power-assisted propulsion (Kloosterman et al., 2012; Levy et al., 2004). Precision tasks are easier with a standard manual wheelchair, while tasks which require more torque are easier with a power assist wheelchair (Kloosterman et al., 2013). In general, power-assisted propulsion reduces the strain on the arms and cardiovascular system compared to standard manual wheelchair propulsion. Therefore, using power assist wheelchairs could decrease the risk of secondary UE injuries and may allow the user to delay the transition to a fully powered wheelchair. However, power assist wheelchairs are 37-

53 pounds heavier than standard manual wheelchairs (Flemmer & Flemmer, 2016) , which makes them less friendly for transferring. They are harder to propel when the battery is discharged and as it was mentioned previously they are less maneuverable in tight turns and are relatively expensive. Currently, power assist wheelchairs are not widely used (Flemmer & Flemmer, 2016) because of the aforementioned disadvantages, particularly their heavy weight.

The geared manual wheelchair is one of the recently developed options available to manual wheelchair users (Chow & Levy, 2011). Similar to a multi-speed bicycle, geared wheels allow users to choose the option of wheeling in a lower gear, which might make propulsion easier. The geared wheels add 2-10 pounds to the weight of a standard manual wheelchair. Geared manual wheelchairs may be a promising alternative wheel technology that increases the users' accessibility and participation while reducing the biomechanical demands on the human body. Our group has shown that using geared manual wheelchairs may be beneficial for demanding tasks such as ramp ascent (Jahanian, Schnorenberg, & Slavens, 2016) and propulsion on carpeted floors (Jahanian, Schnorenberg, Hawi, & Slavens, 2015) . Howarth and colleagues (Howarth et al., 2010) reported similar results for using geared manual wheelchairs during ramp ascent. Decreased shoulder pain is also one of the potential advantages of geared manual wheelchair mobility (Finley & Rodgers, 2007).

Statement of the Problem

Physicians and therapists require quantifiable reasons for prescription of sophisticated wheelchairs and novel technologies (Mortenson, Miller, & Auger, 2008) such as geared wheels. However, geared manual wheels are relatively new, and there is still limited scientific evidence supporting the advantages of geared manual wheelchair mobility. There are no guidelines available for

prescription or transition to geared manual wheelchairs. Little to nothing is known in literature about using geared wheels on biomechanics and physiology of manual wheelchair users that may explain the pros and cons of using geared manual wheelchairs. The use of geared manual wheelchair wheels has the potential to preserve upper limb function and decrease the risk of secondary injuries in manual wheelchair users and allow them to maintain an optimal level of activity and independence necessary for high quality of life. To elucidate the biomechanical and physiological mechanisms affected by using geared manual wheelchairs, development of an integrative approach for systematic (combined physiological and biomechanical) evaluation of manual wheelchair mobility is necessary.

The purpose of this dissertation is to quantitatively investigate the effects of using geared wheels on hand-rim biomechanics, joint dynamics, muscle activity and energetics during propulsion over different ground conditions and mobility tasks in individuals with SCI.

Specific Aims and Hypotheses

Aim #1: To evaluate and compare the glenohumeral joint kinematics and shoulder muscle activity during standard and geared manual wheelchair propulsion on tile level floor and on a ramp in able-bodied subjects.

Hypothesis: There will be significant differences in kinematic metrics and muscle activation parameters between standard and geared wheels during propulsion over the ground and on a ramp.

Aim #2: To evaluate the hand-rim biomechanics during geared manual wheelchair propulsion on tile and carpeted level floors and a ramp in the low gear and standard gear conditions in adults with SCI.

Hypothesis: The propulsion speed and hand-rim kinetics will be significantly less during the low gear condition in comparison with the standard gear condition. The gear condition will not be significantly effective on the stroke cycle frequency.

Aim #3: To evaluate the glenohumeral joint dynamics and shoulder muscle activity during geared manual wheelchair propulsion on carpeted level floor in adults with SCI.

Hypothesis: The peak glenohumeral joint kinetics and shoulder muscle activity will be significantly less during the low gear condition in comparison with the standard gear condition. The gear condition will not be significantly effective on the glenohumeral joint kinematics.

Aim #4: To quantify the effects of using geared wheelchair wheels on energy cost and intensity of manual wheelchair propulsion in adults with SCI.

Hypothesis 1: Using geared wheels in the low gear condition will significantly increase energy cost of propulsion in comparison to the standard gear condition.

Hypothesis 2: Using geared wheels in the low gear condition will significantly decrease the intensity of wheelchair propulsion in comparison to the standard gear condition.

Significance and Innovation

This study will enable us to better understand the impact of using geared wheels on manual wheelchair propulsion biomechanics and energetics and how it may affect the incidence of secondary injuries and pain associated with manual wheelchair mobility. To the author's

knowledge it is for the first time that the effects of geared manual wheelchair mobility on wheelchair propulsion biomechanics and energetics are being evaluated in adult manual wheelchair users with SCI using an integrative approach. This study has the potential to change the clinical practice paradigms. Currently therapists and physicians prescribe the appropriate form of mobility and type of wheelchair through subjective methods by considering static guidelines and factors such as age, level of severity of injury, environment and user preferences. Transition to other forms of wheeled mobility is often prescribed too late when a patient has endured an injury or presented with pain which could have negative effects on quality of life. This project is innovative because of the integrative approach that will be used for evaluating manual wheelchair mobility. This research could significantly impact the SCI rehabilitation approaches concerning prescribing the optimal mobility device, monitoring, and transitioning to other forms of mobility.

To achieve our aims, we collaborated with experienced researchers and scientists with expertise in biomechanics, engineering, occupational therapy, physical medicine and rehabilitation, and biostatistics. The novel features of this project include the interdisciplinary nature of the research and utilization of state-of-the-art technologies for data collection and analysis. We used Delsys trigno wearable sensors for electromyography; Vicon T-series motion capture system for motion analysis; a custom instrumented hand-rim, previously developed and validated by our team (Gaglio, Liang, Daigle, & Hsiao-Wecksler, 2016; Gaglio et al., 2017) for kinetic data collection; and COSMED k4b2 indirect calorimeter for energy expenditure measurement.

The proposed integrative approach in this research could be implemented for developing commercially available toolkits to assist clinicians with manual wheelchair prescription, use, training, and transition. The outcomes of this study could be helpful for clinicians (therapists and physicians), wheelchair users, rehabilitation engineers, manufacturers, and insurers. The

outcomes from this research will have clinical implications for augmenting manual wheelchair prescription guidelines. The results from this study will also be used for design modifications and development of new geared wheels for manual wheelchair users.

Content Presentation

In the following, the results of this study are presented in five chapters, anticipating their subsequent modification into a format for journal manuscript submission.

To evaluate the biomechanical effects of novel propulsion mechanisms such as geared wheels, it is warranted to first investigate able-bodied, non-wheelchair users (van der Woude et al., 2001; van der Woude, Luc HV, Veeger, & Rozendal, 1989). Able-bodied subjects are equally well untrained and are physically homogenous (van der Woude, Luc HV et al., 1989). To test the hypotheses for Aim #1, fourteen able-bodied individuals, seven females and seven males, with an average age of 22.5 ± 3.4 years, were tested. Chapter 2 provides the details of this study. The results of this study also were used to refine the data collection protocol for the main study with individuals with SCI.

To test the hypotheses for Aims #2-4, thirteen veterans with SCI were recruited through the Clement J. Zablocki Veterans Affairs Center in Milwaukee. This study was approved by the Clement J. Zablocki Veterans Affairs Center and the University of Wisconsin-Milwaukee (UWM) Institutional Review Boards. All subjects signed the approved informed consent forms prior to participation. The inclusion criteria for subjects were to be between 18 and 70 years old, use a manual wheelchair as the primary mode of mobility, have a minimum of six months experience as a manual wheelchair user, and have the ability to perform independent transfers.

Thirteen veterans with paraplegic SCI who met the inclusion criteria participated in this study.

Wheelchair propulsion testing was completed at the UWM Mobility Lab. Table 1 provides subjects' characteristics.

To test the hypotheses for Aims #2 & 3, hand-rim biomechanics, UE joint dynamics, and muscle activity during geared manual wheelchair propulsion in two conditions (standard gear, and low gear) on tiled / carpeted level floor and on a ramp were evaluated. Chapters 3&4 provide the details of this part of the study. All the analyses for Aims #2 & 3 are based on the data from a sample of seven (7) subjects (a subset of thirteen adult manual wheelchair users who were recruited for this study).

To test the hypotheses for Aim #4, geared manual wheelchair energetics was evaluated in two conditions (standard gear, and low gear) during 6-minute propulsion test on passive rollers. The details of this part of the study are provided in chapter 5. All the analyses for Aim #4 are based on the data from a sample of eleven (11) subjects (a subset of thirteen adult manual wheelchair users who were recruited for this study). Chapter 6 provides a summary of the outcomes and conclusions of the studies that were conducted in this research.

Table 1. Subjects' characteristics.

Subject	Age (years)	Weight (kg)	Height (cm)	Arm Dominance	SCI level	Years as wheelchair user
1	64	117	172	R	T10, ASIA D	30
2	52	75	180	R	T10, ASIA A	27
3	53	87	178	L	T4, ASIA A	27
4	42	84.8	188	R	T10, ASIA C	21
5	55	97.7	185	R	T5, ASIA <u>A</u>	31
6	36	80.2	175	R	L2, ASIA <u>C</u>	12
7	68	73	170	R	T10, ASIA A	1.5
8	57	81.2	180	R	T11, ASIA <u>C</u>	0.6
9	50	66	180	R	T6, ASIA C	9.5
10	24	71.2	180	R	T5, ASIA <u>A</u>	2
11	51	112	188	L	T12, ASIA <u>C</u>	30
12	29	93	188	R	T1, ASIA A	10
13	54	136	193	R	T12, ASIA A	36

References

- Algood, S. D., Cooper, R. A., Fitzgerald, S. G., Cooper, R., & Boninger, M. L. (2004). Impact of a pushrim-activated power-assisted wheelchair on the metabolic demands, stroke frequency, and range of motion among subjects with tetraplegia. *Archives of Physical Medicine and Rehabilitation*, 85(11), 1865-1871.
- Batavia, M., Batavia, A. I., & Friedman, R. (2001). Changing chairs: Anticipating problems in prescribing wheelchairs. *Disability and Rehabilitation; Disabil.Rehabil.*, 23(12), 539-548.
- Beekman, C. E., Miller-Porter, L., & Schoneberger, M. (1999). Energy cost of propulsion in standard and ultralight wheelchairs in people with spinal cord injuries. *Physical Therapy*, 79(2), 146-158.
- Boninger, M. L., Koontz, A. M., Sisto, S. A., & Dyson-Hudson, T. A. (2005). Pushrim biomechanics and injury prevention in spinal cord injury: Recommendations based on CULP-SCI investigations. *Journal of Rehabilitation Research and Development*, 42(3), 9.
- Burnham, R. S., & Steadward, R. D. (1994). Upper extremity peripheral nerve entrapments among wheelchair athletes: Prevalence, location, and risk factors. *Archives of Physical Medicine and Rehabilitation*, 75(5), 519-524.
- Calhoun, C., Schottler, J., & Vogel, L. (2013). Recommendations for mobility in children with spinal cord injury. *Topics in Spinal Cord Injury Rehabilitation*, 19(2), 142-151.
- Chow, J. W., & Levy, C. E. (2011). Wheelchair propulsion biomechanics and wheelers' quality of life: An exploratory review. *Disability and Rehabilitation: Assistive Technology*, 6(5), 365-377.
- Corfman, T. A., Cooper, R. A., Boninger, M. L., Koontz, A. M., & Fitzgerald, S. G. (2003). Range of motion and stroke frequency differences between manual wheelchair propulsion and pushrim-activated power-assisted wheelchair propulsion. *The Journal of Spinal Cord Medicine*, 26(2), 135-140.
- Dallmeijer, A., Zentgraaff, I., Zijp, N., & van der Woude, L. (2004). Submaximal physical strain and peak performance in handcycling versus handrim wheelchair propulsion. *Spinal Cord*, 42(2), 91-98.
- Finley, M. A., & Rodgers, M. M. (2007). Effect of 2-speed geared manual wheelchair propulsion on shoulder pain and function. *Archives of Physical Medicine and Rehabilitation*, 88(12), 1622-1627.
- Flemmer, C. L., & Flemmer, R. C. (2016). A review of manual wheelchairs. *Disability and Rehabilitation: Assistive Technology*, 11(3), 177-187.

- Gaglio, A., Daigle, S., Gacek, E., Jahanian, O., Slavens, B., Rice, I., et al. (2017). Validation of an instrumented wheelchair hand rim. *2017 Design of Medical Devices Conference*, pp. V001T05A012.
- Gaglio, A., Liang, J., Daigle, S., & Hsiao-Weckslar, E. (2016). Design of a universal instrumented wheelchair hand rim. *Journal of Medical Devices*, *10*(3), 030956.
- Harvey, L. (2008). *Management of spinal cord injuries: A guide for physiotherapists* Elsevier Health Sciences.
- Hildebrandt, G., Voight, E. D., Bahn, D., Berendes, B., & Kroger, J. (1970). Energy costs of propelling wheelchair at various speeds: Cardiac response and effect on steering accuracy. *Archives of Physical Medicine and Rehabilitation*, *51*(3), 131-136.
- Howarth, S. J., Pronovost, L. M., Polgar, J. M., Dickerson, C. R., & Callaghan, J. P. (2010). Use of a geared wheelchair wheel to reduce propulsive muscular demand during ramp ascent: Analysis of muscle activation and kinematics. *Clinical Biomechanics*, *25*(1), 21-28.
- Jahanian, O., Schnorenberg, A. J., Hawi, L., & Slavens, B. A. (2015). Upper extremity joint dynamics and electromyography (EMG) during standard and geared manual wheelchair propulsion. *Proceeding of the 39th Annual Meeting of American Society of Biomechanics*,
- Jahanian, O., Schnorenberg, A. J., & Slavens, B. A. (2016). Evaluation of shoulder joint kinematics and muscle activity during geared and standard manual wheelchair mobility. *Engineering in Medicine and Biology Society (EMBC), 2016 IEEE 38th Annual International Conference of The*, pp. 6162-6165.
- Karmarkar, A., Cooper, R., Liu, H., Connor, S., & Puhlman, J. (2008). Evaluation of pushrim-activated power-assisted wheelchairs using ANSI/RESNA standards. *Archives of Physical Medicine and Rehabilitation; Arch.Phys.Med.Rehabil.*, *89*(6), 1191-1198.
- Kaye, H. S., Kang, T., & LaPlante, M. P. (2000). Mobility device use in the united states. disability statistics report 14.
- Kloosterman, M. G., Snoek, G. J., van der Woude, L H, Buurke, J. H., & Rietman, J. S. (2013). A systematic review on the pros and cons of using a pushrim-activated power-assisted wheelchair. *Clinical Rehabilitation*, *27*(4), 299-313.
- Kloosterman, M. G., Eising, H., Schaake, L., Buurke, J. H., & Rietman, J. S. (2012). Comparison of shoulder load during power-assisted and purely hand-rim wheelchair propulsion. *Clinical Biomechanics*, *27*(5), 428-435.
- Levy, C. E., Chow, J. W., Tillman, M. D., Hanson, C., Donohue, T., & Mann, W. C. (2004). Variable-ratio pushrim-activated power-assist wheelchair eases wheeling over a variety of terrains for elders. *Archives of Physical Medicine and Rehabilitation*, *85*(1), 104-112.

- Marino, R. J. (2007). Domains of outcomes in spinal cord injury for clinical trials to improve neurological function. *Journal of Rehabilitation Research and Development*, 44(1), 113.
- Mercer, J. L., Boninger, M., Koontz, A., Ren, D., Dyson-Hudson, T., & Cooper, R. (2006). Shoulder joint kinetics and pathology in manual wheelchair users. *Clinical Biomechanics*, 21(8), 781-789.
- Mortenson, W. B., Miller, W. C., & Auger, C. (2008). Issues for the selection of wheelchair-specific activity and participation outcome measures: A review. *Archives of Physical Medicine and Rehabilitation*, 89(6), 1177-1186.
- Stover, S. L., DeLisa, J. A., & Whiteneck, G. G. (1995). *Spinal cord injury: Clinical outcomes from the model systems* Aspen Publishers.
- van der Woude, L., Veeger, H., Dallmeijer, A., Janssen, T., & Rozendaal, L. (2001). Biomechanics and physiology in active manual wheelchair propulsion. *Medical Engineering & Physics*, 23(10), 713-733.
- van der Woude, Luc HV, Veeger, D. E., & Rozendal, R. H. (1989). Ergonomics of wheelchair design: A prerequisite for optimum wheeling conditions. *Adapted Physical Activity Quarterly*, 6(2), 109-132.
- van der Woude, Lucas HV, Botden, E., Vriend, I., & Veeger, D. (1997). Mechanical advantage in wheelchair lever propulsion: Effect on physical strain and efficiency. *Journal of Rehabilitation Research and Development*, 34(3), 286.
- van der Woude, Lucas HV, & de Groot, S. (2005). Wheelchair propulsion: A straining form of ambulation. *Indian Journal of Medical Research*, 121(6), 719.
- van der Woude, Lucas HV, de Groot, S., & Janssen, T. W. (2006). Manual wheelchairs: Research and innovation in rehabilitation, sports, daily life and health. *Medical Engineering & Physics*, 28(9), 905-915.
- White, N., & Black, N. (2016). Spinal cord injury (SCI) facts and figures at a glance.
- World Health Organization. (2001). *International classification of functioning, disability and health: ICF*. World Health Organization.

Chapter 2

A Comparison of Glenohumeral Joint Kinematics and Muscle Activation During Standard and Geared Manual Wheelchair Mobility

Introduction

An estimated 3.7 million people in the United States use a wheelchair (Brault, 2012). Approximately 90% of which use hand-rim propelled manual wheelchairs (standard manual wheelchairs) (Kaye, Kang, & LaPlante, 2000). Manual wheelchairs are relatively inexpensive, highly maneuverable on flat surfaces, lightweight, and convenient to transport (Flemmer & Flemmer, 2016). However, manual wheelchair mobility has been described as a low efficient and physically straining form of mobility that places manual wheelchair users at high risk of repetitive strain injuries, primarily in the shoulder and wrist (Burnham & Steadward, 1994; Mercer et al., 2006; van der Woude, Lucas HV, de Groot, & Janssen, 2006). This often leads to reduced independence, function, and quality of life (van der Woude, Lucas HV & de Groot, 2005).

The geared manual wheelchair wheel is an alternative propulsion mechanism that may reduce the biomechanical demands of the upper extremity during propulsion, while maximizing function. Similar to a multi-speed bicycle, geared wheels allow users to choose the option of wheeling in a low gear or standard gear. Despite this new rehabilitation technology, there is limited scientific evidence surrounding geared manual wheelchair mobility. Finley and Rodgers studied the effects of geared wheels (i.e., MAGIC Wheels) on shoulder pain in a longitudinal study with full time manual wheelchair users (Finley & Rodgers, 2007). Findings in this study indicated the potential for geared manual wheels to reduce shoulder pain. Furthermore, Howarth and colleagues investigated the effects of using geared manual wheelchair wheels on the muscular demand of

able-bodied individuals during ramp ascent (Howarth, Polgar, Dickerson, & Callaghan, 2010; Howarth, Pronovost, Polgar, Dickerson, & Callaghan, 2010a). They found a significant decrease in peak muscle activity of the shoulder flexors and a significant increase in the integrated muscle activity during ramp ascent (Howarth et al., 2010). They also reported reduced demands of the abdominal muscles, which indicated the potential benefits of geared manual wheelchairs for individuals with compromised activity capacity (Howarth et al., 2010). Preliminary results of the studies conducted by our group demonstrated that using geared manual wheelchair wheels might be beneficial for demanding tasks, such as ramp ascent and propulsion on carpeted floors (Jahanian, Schnorenberg, Hawi, & Slavens, 2015; Jahanian, Schnorenberg, & Slavens, 2016).

To evaluate the biomechanical effects of novel propulsion mechanisms, such as geared wheels, it is warranted to first investigate able-bodied, non-wheelchair users (van der Woude, LHV, Veeger, Dallmeijer, Janssen, & Rozendaal, 2001a; van der Woude, Luc HV, Veeger, & Rozendal, 1989). Able-bodied subjects are equally well un-trained and are physically homogenous (van der Woude, LHV, Veeger, Dallmeijer, Janssen, & Rozendaal, 2001b). To better understand the upper extremity biomechanics during geared manual wheelchair mobility we aimed to evaluate and compare the upper extremity joint kinematics and muscle activity during standard and geared manual wheelchair propulsion on tile level floor and on a ramp in able-bodied subjects. It was hypothesized that there would be significant differences in kinematic metrics and muscle activation parameters between standard and geared wheels during propulsion over ground and on a ramp.

Methods

Subjects

Fourteen individuals, seven females and seven males, with an average age of 22.5 ± 3.4 years (age range from 18 to 29 years) participated in this study. The average weight was 76.1 ± 18.3 kg and the average height was 1.76 ± 0.10 m. All participants were able-bodied and had no prior wheelchair experience. This study was approved by the University of Wisconsin-Milwaukee Institutional Review Board and consent was obtained from participants.

Experimental protocol

A Breezy® Ultra 4 manual wheelchair (Sunrise Medical LLC., Fresno, CA, US) was used with standard wheels and Easy Push (IntelliWheels, Inc., IL) geared wheels for all activities (Table 2). The hand-rim of the Easy Push wheel is connected to the wheel via a planetary gear mechanism with the gear ratio of 1.6:1. The inertial and geometric specifications of the wheels are listed in Table 1.

Data collection was conducted at the University of Wisconsin-Milwaukee Mobility Lab. Subject-specific measurements were obtained for all participants. The wheelchair's seat height was adjusted close to optimum height by satisfying the following criteria, 1) the elbow was flexed at approximately 120 degrees when the hands were on the highest point of the hand-rims; and, 2) the footrests clear the ground by five centimeters (Brubaker, 1990). Participants were provided with an acclimation period to become familiar with the standard and geared wheels over level ground and on a ramp. Participants propelled the manual wheelchair with each type of wheels, along an 8-meter tiled, level floor, and up an 2.5-meter ramp with a 4.8-degree slope (Figure 4; below the American with Disability Act Accessibility Guidelines maximum allowable slope of 5 degrees),

(Board, 2002). They used a self-selected speed and propulsion pattern for all tasks. Each ramp ascent trial began on the level tile floor with the participant positioned one meter from the ramp base (Howarth, Pronovost, Polgar, Dickerson, & Callaghan, 2010b).

Table 2. Specifications of the standard and geared wheels.

Wheel type	Weight (kg)	Wheel width (cm)	Wheel size (cm)
Standard	2.6	6.0	61.0
Geared	4.4	7.7	61.0

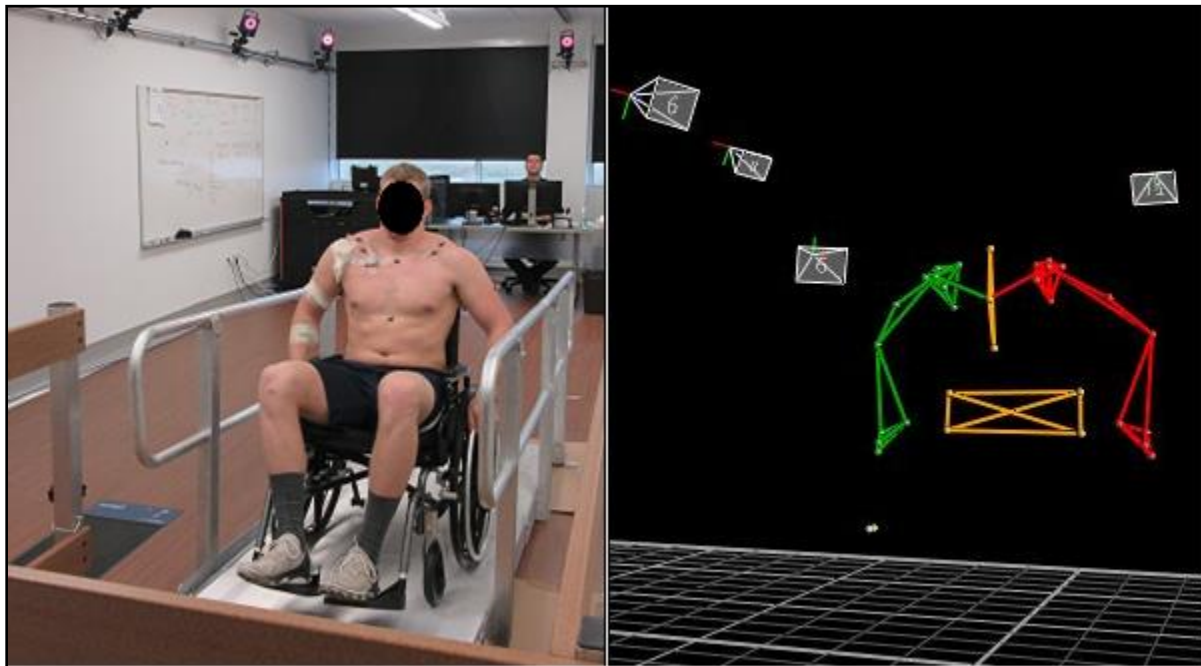


Figure 4. A subject ascending a ramp using a manual wheelchair, instrumented with motion capture markers and surface electromyography electrodes (left); and corresponding Vicon rendering of the custom upper extremity biomechanical model (right).

Data collection

Kinematic data collection

Participants were instrumented with our established upper extremity model consisting of 27 retro-reflective markers on anatomical landmarks of the thorax, clavicles, scapulae, upper arms, forearms, and hands. (Figure 4) (Schnorenberg et al., 2014). Four markers were placed on the backrest and one marker on the dominant side wheel axle. Motion data were collected at 120 Hz using a 15-camera Vicon T-series motion capture system (Vicon Motion Systems, Oxford, UK).

Surface electromyography data collection

Shoulder flexion is the dominant movement during the push phase of manual wheelchair propulsion (Mulroy, Gronley, Newsam, & Perry, 1996; Sabick, Kotajarvi, & An, 2004). Thus, muscle activity of the primary shoulder flexors (anterior deltoid and pectoralis major) and one of the rotator cuff muscles (infraspinatus) were recorded using surface electromyography (EMG), (Criswell, 2010; Dubowsky, Sisto, & Langrana, 2009). Delsys Trigno wireless surface electrodes (Delsys, Inc., Natick, MA) with built-in bandpass filter of 20-450 Hz were used to record EMG data of the anterior deltoid, clavicular head of the pectoralis major, and infraspinatus of the dominant arm.

Prior to EMG electrode placement, the skin surface underlying each electrode was scrubbed and cleaned with an alcohol preparatory pad. Electrodes were placed over the anterior deltoid (anterior aspect of the arm, approximately 4 cm below the clavicle), clavicular head of the pectoralis major (approximately 2 cm below the clavicle, midway between the underarm and suprasternal notch), and infraspinatus (parallel and approximately 4 cm below the spine of the scapula), (Criswell, 2010). The Vicon motion capture system was digitally synchronized with the Delsys EMG system. The EMG signals were acquired at a sampling frequency of 2040 Hz using Vicon Nexus software (Vicon Motion Systems, Oxford, UK).

Before the experimental trials, maximum voluntary isometric contractions (MVIC) were performed for each muscle using a BTE PrimusRS (BTE, Hanover, MD). During the MVIC trials, the participant sat on the BTE chair with the trunk in an upright position and trunk and legs secured to the chair with Velcro straps. Three MVIC trials were performed for each muscle, with contraction durations of three seconds. Verbal encouragement was provided during each trial by the investigator. The MVIC of the anterior deltoid was tested with the upper arm next to the trunk with 45 degrees of shoulder flexion while resistance was applied posteriorly against the distal end of humerus during isometric shoulder flexion. The pectoralis major muscle was tested while the upper arm was horizontal and midway between anterior and lateral directions, and the forearm was flexed 90 degrees at the elbow. Resistance was applied laterally against the elbow during isometric shoulder horizontal flexion (Chow, J. W., Millikan, Carlton, Morse, & Chae, 2001). The MVIC of the infraspinatus was tested with the upper arm next to the trunk with the forearm horizontal and flexed 90 degrees at the elbow. Resistance was applied medially against the wrist during isometric shoulder external rotation. The mean peak EMG magnitude of the three trials was calculated as the MVIC of each muscle.

Data processing

Kinematics

To identify the push and recovery phases of each propulsion stroke, sagittal plane kinematics of the third metacarpal marker was used. The three critical points in time were the 1) initial hand contact, 2) hand release, and 3) second hand contact (Chow, John W. et al., 2009). These were visually inspected and identified using the method of Chow et al., (2009). The push phase was defined as the initial hand contact to hand release, and a complete stroke cycle was defined from

the initial hand contact to the second hand contact. Temporal parameters examined in this study were stroke time, push phase (expressed as percentage of stroke time), and stroke frequency (one second divided by the stroke time). Stroke distance was computed as the distance between the position of the wheel center in the sagittal plane at the time of the initial and second hand contacts. Stroke speed was calculated by dividing the stroke distance by the stroke time. The normalized stroke frequency was obtained by dividing the stroke frequency by the stroke distance. The third or the fourth stroke cycle was analyzed as the semi-steady state condition stroke cycle (Chow et al., 2009). The first full stroke cycle that occurred after the wheelchair castors passed the midpoint of the ramp was used for analysis of ramp ascent (Chow et al., 2009).

Kinematic data were processed using Vicon Nexus software. The marker trajectories were filtered using a Woltring filter with a mean squared error of 20 (Woltring, 1986). Body segment parameters were estimated using equations developed for an adult population (Yeadon & Morlock, 1989). Our inverse dynamics model was used to calculate the three-dimensional (3-D) movements of the glenohumeral joint (Schnorenberg et al., 2014). The kinematic metrics of interest, including 3-D ranges of motion (ROMs) and joint angles of the glenohumeral joint, were calculated using our upper extremity inverse dynamics model developed in MATLAB software (MathWorks, Inc.), (Schnorenberg et al., 2014).

Electromyography

Methods previously described by Beres and Harkema were used to define the EMG burst duration after rectification of the EMG signals (Beres-Jones & Harkema, 2004). The detection threshold was defined as the mean of the baseline plus four standard deviations. The onset of an EMG burst was then defined as the time when the signal amplitude rose above the detection threshold and remained above it for at least 30 ms (Beres-Jones & Harkema, 2004). The end of an EMG burst

was defined as the time when the signal amplitude fell below the detection threshold and remained below it for at least 50 ms (Beres-Jones & Harkema, 2004). Visual examination was also performed.

The raw EMG signals were full wave rectified and processed using a root mean square (RMS) algorithm with a time averaging period of 25 ms. The RMS envelope of the EMG data recorded for each muscle during wheelchair propulsion trials were normalized as a percentage of the MVIC obtained from each respective muscle from the mean RMS envelope of the MVIC trials. The normalized EMG signals were used to determine the peak EMG during the burst duration and the integrated EMG over each stroke cycle using MATLAB software. The normalized integrated muscle activity was calculated by dividing the integrated muscle activity by the distance traveled per stroke cycle.

Data analysis

The subject means and standard deviations of the spatiotemporal parameters, glenohumeral joint kinematics, and peak and integrated muscle activity were computed for each wheel type (standard and geared) and slope (level floor and ramp) for three trials. A two-way analysis of variance (2 wheel types x 2 slopes) with repeated measures was used for statistical analysis. If there was no significant interaction between the factors (wheel type and slope), the main effects of the wheel type factor (regardless of the level of slope) were investigated. When there was significant interaction between factors, simple effects of the wheel type factor within each level of slope were examined using a paired-samples t-test. All statistical analyses were completed with SPSS software (IBM Corporation) using a general linear model with repeated measures and paired sample t-tests (significance level = 0.05).

Results

Spatiotemporal parameters

The statistical analysis results indicated that there was a significant interaction between the wheel type and slope for the stroke distance ($F = 6.65$, $p = 0.023$), speed ($F = 20.26$, $p = 0.001$) and normalized stroke frequency ($F = 16.79$, $p = 0.001$; Table 3). Analysis of the simple effects indicated that when using geared wheels on level floor, there was a 21% decrease in the stroke distance ($t = 7.30$, $p \ll 0.001$) and a 20% decrease in propulsion speed ($t = 9.16$, $p \ll 0.001$), compared to standard wheel use. Additionally, there was a 26% decrease in stroke distance ($t = 7.28$, $p \ll 0.001$) and an 18% decrease in propulsion speed ($t = 5.54$, $p \ll 0.001$) during ramp ascent with geared wheels, compared to standard wheels. Using geared wheels increased the normalized stroke frequency by 33% ($t = -4.68$, $p \ll 0.001$) on level floor and by 43% ($t = -6.93$, $p \ll 0.001$) on the ramp (Table 3).

Table 3. Group mean wheelchair propulsion spatiotemporal parameters (mean \pm 1 SD) for each experimental condition (standard and geared wheels on a level floor and on a ramp).

	Level floor		Ramp	
	Standard wheels	Geared wheels	Standard wheels	Geared wheels
Speed (m/s) #	1.10 \pm 0.16 **	0.88 \pm 0.14 **	0.61 \pm 0.12 **	0.50 \pm 0.08 **
Stroke distance (m) #	1.20 \pm 0.23 **	0.94 \pm 0.22 **	0.68 \pm 0.14 **	0.51 \pm 0.09 **
Stroke cycle time (s) *	1.10 \pm 0.19	1.07 \pm 0.18	1.13 \pm 0.21	1.02 \pm 0.13
Push phase (%) *	47.79 \pm 5.28	41.07 \pm 4.36	62.51 \pm 3.92	55.55 \pm 3.41
Stroke cycle frequency (Hz) *	0.93 \pm 0.14	0.95 \pm 0.14	0.91 \pm 0.15	1.00 \pm 0.12
Normalized stroke cycle frequency (1/ms) #	0.81 \pm 0.24 **	1.09 \pm 0.35 **	1.42 \pm 0.48 **	2.05 \pm 0.54 **

#: Statistically significant interaction between wheel type and slope, $p < 0.05$

*: Statistically significant difference, $p < 0.05$ (wheel type main effect)

**: Statistically significant difference, $p < 0.05$ (wheel type simple effects for level floor and ramp)

The interaction between the wheel type and slope was not statistically significant for the stroke cycle time, frequency and push phase. Analysis of the main effects indicated that regardless of the slope level, geared manual wheelchair propulsion decreased the stroke cycle time by 6% ($F = 5.35$, $p = 0.038$) and push phase by 12% ($F = 128.25$, $p << 0.001$), and increased stroke cycle frequency by 6% ($F = 6.36$, $p = 0.025$), (Table 3).

Kinematics

Mean glenohumeral joint kinematics in each plane of motion for all subjects for each wheel type and slope level are depicted (Figures 5,6). The glenohumeral joint trajectories in each plane of motion had a similar morphology for all tasks. Wheel type did not alter the general trend. In the sagittal plane, the glenohumeral joint started in the push phase from an extended position and exhibited flexion for 40-60% of wheelchair cycle on level floor and 55-70% of wheelchair cycle on the ramp. In the coronal plane, the glenohumeral joint started from an adducted position in push phase and exhibited abduction for 40-50% of wheelchair cycle on level floor and 50-65% of wheelchair cycle on the ramp. In the transverse plane, the glenohumeral joint exhibited external rotation for 45-60% of wheelchair cycle on level floor and 55-70% of wheelchair cycle on the ramp.

The interaction between the wheel type and slope was not statistically significant for the glenohumeral joint ROM and maximum joint angle in the coronal plane and the minimum joint angle in the transverse plane (Tables 3, 4). Analysis of the main effects indicated that regardless of the slope level, the glenohumeral joint coronal plane ROM increased significantly ($F = 11.68$, $p = 0.005$) during geared manual wheelchair propulsion in comparison to standard manual wheelchair propulsion (Table 4). The maximum glenohumeral joint angle in the coronal plane

(peak adduction) increased significantly ($F = 6.64$, $p = 0.023$) and the minimum glenohumeral joint angle in the transverse plane (peak external rotation) increased significantly ($F = 8.47$, $p = 0.012$) during geared manual wheelchair propulsion.

There was a statistically significant interaction between the wheel type and slope factors for the maximum glenohumeral joint angle in the transverse plane (minimum external rotation angle, $F = 10.26$, $p = 0.007$) (Table 5). Analysis of the simple effects indicated that during ramp ascension using the geared wheels significantly decreased the maximum glenohumeral joint angle in the transverse plane ($t = 3.98$, $p = 0.002$). Using geared wheels did not significantly affect glenohumeral joint ROM in the sagittal and transverse planes, nor any glenohumeral joint peak kinematics in the sagittal plane (Tables 3,4).

Shoulder muscle activity

There was a statistically significant interaction between the wheel type and slope factors for the pectoralis major peak EMG ($F = 5.01$, $p = 0.043$) (Figure 7). Analysis of the simple effects indicated that when using geared wheels on level floor, the peak muscle activity of pectoralis major decreased by 39% ($t = 3.09$, $p = 0.08$) in comparison to the standard wheel type. The pectoralis major peak activity decreased notably during geared manual wheelchair propulsion on the ramp, but was not statistically significant ($t = 1.19$, $p = 0.25$).

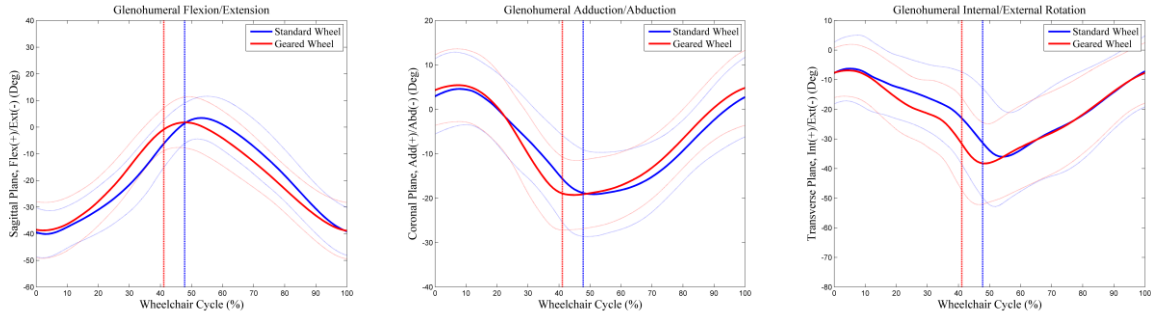


Figure 5. Glenohumeral joint kinematics in sagittal, coronal and transverse planes of motion. Group mean profiles (solid line) +/- one standard deviation (dotted line) of 14 subjects (dominant side) for the standard and geared manual wheelchairs during propulsion on level floor are depicted. The vertical dash-dot lines indicate the transition from the end of the push phase to the start of the recovery phase for each wheel type.

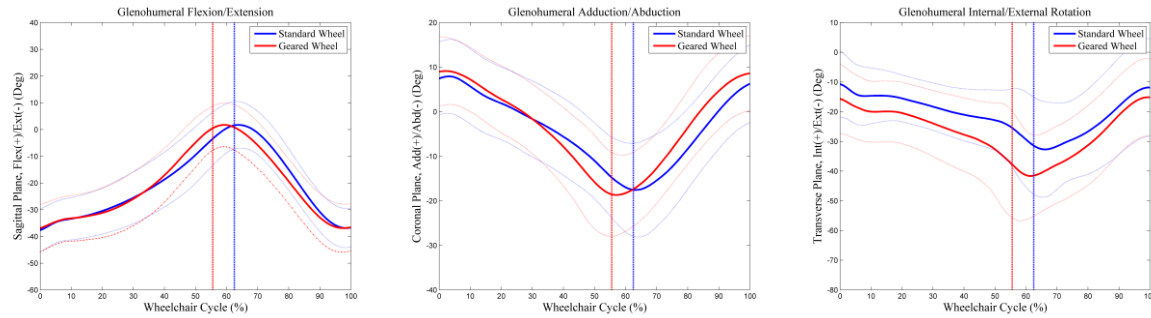


Figure 6. Glenohumeral joint kinematics in sagittal, coronal and transverse planes of motion. Group mean profiles (solid line) +/- one standard deviation (dotted line) of 14 subjects (dominant side) for the standard and geared manual wheelchairs during propulsion on a ramp are depicted. The vertical dash-dot lines indicate the transition from the end of the push phase to the start of the recovery phase for each wheel type.

Table 4. Group mean glenohumeral joint ranges of motion (mean ± 1 SD) during the standard and geared manual wheelchair propulsion on level floor and on a ramp (degrees).

Plane	Level floor		Ramp	
	Standard wheels	Geared wheels	Standard wheels	Geared wheels
Sagittal	43.19 ± 9.42	44.67 ± 9.25	41.77 ± 6.51	41.33 ± 7.10
Coronal *	25.56 ± 10.55	27.44 ± 9.36	27.62 ± 10.28	30.26 ± 9.51
Transverse	35.625 ± 9.63	38.34 ± 7.69	30.38 ± 8.26	33.68 ± 6.26

*: Statistically significant difference, $p < 0.05$ (wheel type main effect, regardless of level of slope)

Table 5. Group mean peak glenohumeral joint kinematics (mean \pm 1 SD) during the standard and geared manual wheelchair propulsion on level floor and on a ramp (degrees).

Plane		Level floor		Ramp	
		Standard wheels	Geared wheels	Standard wheels	Geared wheels
Sagittal	Max flexion	2.42 \pm 7.79	2.84 \pm 8.94	3.21 \pm 8.59	3.13 \pm 7.81
	Max extension	40.77 \pm 8.96	41.83 \pm 8.24	38.56 \pm 8.06	38.19 \pm 8.45
Coronal	Max adduction *	5.72 \pm 9.55	6.70 \pm 7.75	8.87 \pm 8.40	10.20 \pm 7.78
	Max abduction *	19.84 \pm 12.84	20.74 \pm 8.40	18.74 \pm 10.53	20.05 \pm 9.44
Transverse	Min external rotation #	4.21 \pm 11.61	4.19 \pm 10.04	7.39 \pm 10.82 **	12.79 \pm 12.25 **
	Max external rotation *	39.47 \pm 14.93	42.53 \pm 12.37	37.77 \pm 14.64	46.47 \pm 16.02

#: Statistically significant interaction between wheel type and slope, $p < 0.05$

*: Statistically significant difference, $p < 0.05$ (wheel type main effect, regardless of level of slope)

**: Statistically significant difference, $p < 0.05$ (wheel type simple effects for level floor and ramp)

The interaction between the wheel type and slope was not significant for the anterior deltoid and infraspinatus peak and integrated EMG and the infraspinatus normalized integrated EMG. Analysis of the main effects indicated that regardless of the slope level, the peak muscle activity of infraspinatus decreased by 20% ($F = 8.00$, $p = 0.014$) during geared manual wheelchair propulsion in comparison to standard manual wheelchair propulsion (Figure 7). The anterior deltoid peak EMG was not significantly different ($F = 2.75$, $p = 0.17$) between the geared and standard manual wheelchair propulsions. The integrated muscle activity of anterior deltoid and pectoralis major decreased by 20% ($F = 7.97$, $p = 0.014$), and 35% ($F = 7.87$, $p = 0.015$), respectively, during geared manual wheelchair propulsion (Table 6). The infraspinatus integrated muscle activity decreased notably (14%) using geared wheels but was not statistically significant ($F = 4.51$, $p = 0.053$). The results for normalized integrated activity indicated that the infraspinatus normalized integrated muscle activity increased by 13% ($F = 5.24$, $p = 0.039$) during geared manual wheelchair propulsion compared to standard manual wheelchair propulsion (Table 7). Changes in anterior deltoid and pectoralis major integrated normalized muscle activity during the standard and geared manual wheelchair propulsions were not statistically significant.

Table 6. Group mean integrated shoulder muscle activity (mean \pm 1 SD) during one stroke cycle of the standard and geared manual wheelchair propulsion on level floor and on a ramp, reported as percent of maximum voluntary isometric contraction (%MVIC).

	Level floor		Ramp	
	Standard wheels	Geared wheels	Standard wheels	Geared wheels
Anterior deltoid *	179.68 \pm 76.34	150.55 \pm 92.29	339.19 \pm 223.70	267.42 \pm 145.01
Pectoralis major *	120.61 \pm 79.28	72.45 \pm 32.53	246.41 \pm 167.53	167.31 \pm 98.24
Infraspinatus	200.43 \pm 74.42	192.34 \pm 99.82	342.13 \pm 175.03	276.96 \pm 110.31

*: Statistically significant difference, $p < 0.05$ (wheel type main effect)

Table 7. Group mean normalized integrated shoulder muscle activity (mean \pm 1 SD) during the standard and geared manual wheelchair propulsion on level floor and on a ramp, reported as percent of maximum voluntary isometric contraction per meter (%MVIC/m).

	Level floor		Ramp	
	Standard wheels	Geared wheels	Standard wheels	Geared wheels
Anterior deltoid	150.74 \pm 60.44	161.34 \pm 92.81	500.44 \pm 311.67	534.82 \pm 277.13
Pectoralis major	96.73 \pm 55.45	76.93 \pm 32.73	357.15 \pm 243.19	337.30 \pm 206.11
Infraspinatus *	171.08 \pm 71.42	211.07 \pm 114.35	511.96 \pm 252.54	559.28 \pm 228.13

*: Statistically significant difference, $p < 0.05$ (wheel type main effect)

Discussion

We successfully characterized the spatiotemporal parameters, glenohumeral joint kinematics and shoulder muscle activity during manual wheelchair propulsion on level floor and up a ramp in 14 able-bodied individuals using geared and standard wheels.

Use of the geared wheels resulted in reduced stroke distance, speed, stroke time, and push time, and increased stroke frequency when compared to the use of the standard manual wheelchair wheels. The spatiotemporal parameters including propulsion speed, stroke time, stroke distance, push time, and stroke frequency during standard manual wheelchair use on level floor were similar

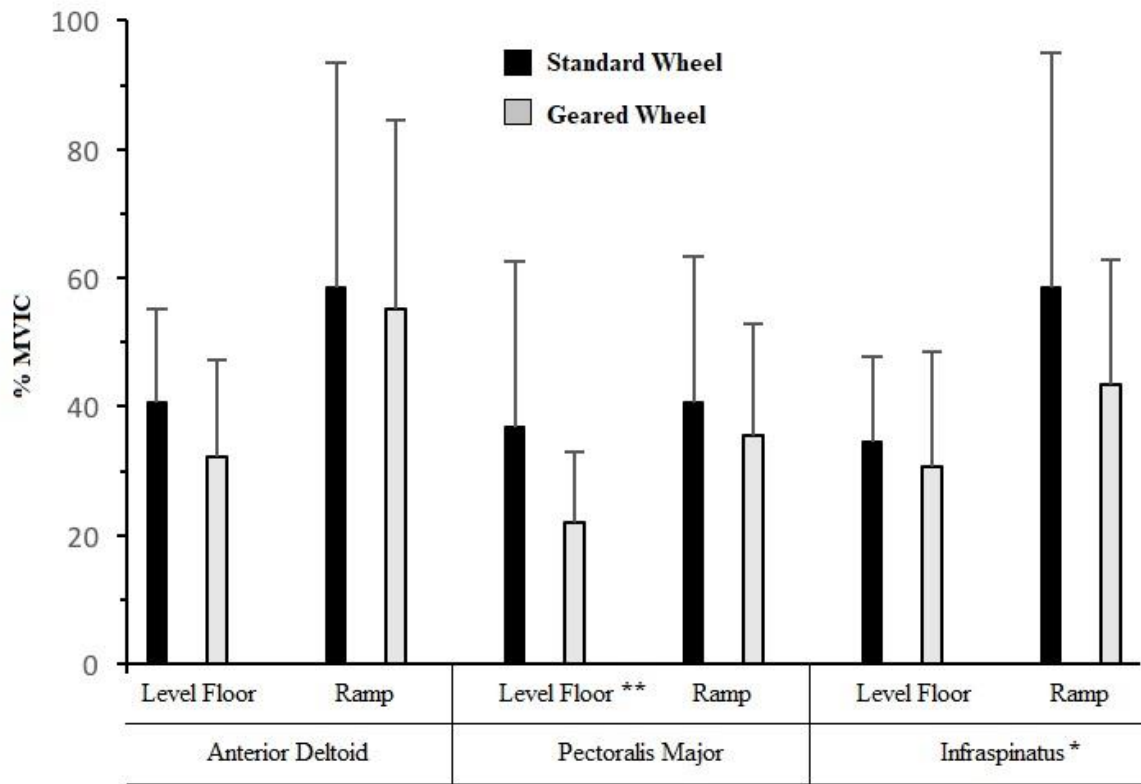


Figure 7. Group mean peak muscle activity of the anterior deltoid, pectoralis major, and infraspinatus during one stroke cycle of standard and geared manual wheelchair propulsion on level floor and on ramp. Error bars indicate the standard deviations as reported as percent of maximum voluntary isometric contraction (%MVIC).

to previously reported values (speed = 1.02-1.29 m/s, stroke time = 1.08-1.17 s, stroke distance = 1.20-1.36 m, push phase = 42.1%, and stroke frequency = 0.9-0.96 Hz), (Chow et al., 2009; Requejo et al., 2015). The propulsion speed, stroke distance, and stroke cycle frequency during the ramp task were less than previously reported values, while the stroke time and push phase were greater (speed = 1.22 m/s, stroke time = 0.98 s, stroke distance = 1.19 m, push phase = 50.6%, and stroke frequency = 1.04 Hz), (Chow et al., 2009). A possible reason for the differences could be due to the participants in our study being able-bodied.

The significantly decreased propulsion speed during the geared wheel use is primarily attributed to the reduction in the stroke distance, a direct effect of the gear reduction (1.6:1) in the geared wheels. Stroke time decreased significantly (stroke frequency increased significantly) during

geared wheel use; the geared wheel had a greater effect during ramp propulsion. The normalized stroke frequency substantially increased during geared wheel use similar to the results reported in the literature (Howarth et al., 2010). Using the geared wheels resulted in a significantly reduced push phase which was different from Howarth et al., in which there was no significant difference between the geared and standard conditions for the push phase (Howarth et al., 2010).

The effects of using the geared wheelchair wheels on the normalized stroke frequency and push phase was significant and should be taken into consideration for manual wheelchair prescription. The scientific evidence previously outlined for recommendations related to wheelchair propulsion emphasize a minimization of cadence or push frequency (Boninger, Koontz, Sisto, & Dyson-Hudson, 2005). Increasing push frequency has been linked to increased risk of secondary upper extremity injuries in manual wheelchair users (Boninger et al., 2005; van der Woude, Lucas HV et al., 2006). Long propulsive strokes (push phase) have been also recommended to minimize the cadence and peak forces (Boninger et al., 2005).

Glenohumeral joint kinematic data were similar to previously reported values for wheelchair biomechanics (Howarth et al., 2010; Morrow, Kaufman, & An, 2011). The increase in the glenohumeral joint ROM in the coronal plane could be due to the larger wheel width of the geared wheels in comparison to the standard wheels (Table 2). Increased glenohumeral joint internal rotation has been associated with a reduction in the subacromial space and impingement (Morrow et al., 2011), which is a main contributor to the development of the shoulder pain in manual wheelchair users (Zhao et al., 2015). Therefore, the significant increase in glenohumeral joint external rotation during geared manual wheelchair mobility, which we observed, could be beneficial for manual wheelchair users.

Using the geared manual wheelchair resulted in substantial reduction in the peak muscle activity of the primary shoulder flexors (pectoralis major, anterior deltoid), and infraspinatus compared to the standard wheels. Similar results were reported in the previous investigation on geared manual wheelchairs (Howarth et al., 2010). Use of the geared wheels had a greater effect on peak activity of the shoulder flexor muscles during propulsion on level floor and on the peak activity of the infraspinatus during ramp propulsion. Reducing peak shoulder muscle activity is the primary benefit of using geared manual wheelchair wheels. A reduction in the peak muscular demands could lead to a reduction in peak forces applied to the glenohumeral joint and consequently a reduction in the risk of shoulder secondary injury and pain, thereby improving independence of wheelchair users (Dallmeijer, Zentgraaff, Zijp, & van der Woude, 2004). Using the geared wheels decreased the integrated shoulder flexors muscle activity substantially in comparison to standard wheels.

Combined metrics, such as normalized integrated muscle activity, incorporate both muscle activity and stroke cycle characteristics. Normalized integrated muscle activity provides a more comprehensive characterization of the impact that the geared wheel system has on upper extremity biomechanics. This metric, among others, may provide a better understanding of how geared wheel use affects wheelchair propulsion. The normalized integrated muscle activity for the shoulder flexor muscles was not significantly different between the geared and standard wheel conditions. However, the normalized muscle activity was significantly higher for the geared condition in the investigation by Howarth et al., (2010). The difference in gear ratio (2:1 vs. 1.6:1) and slower velocity with the geared wheel with larger gear reduction (2:1) could be the main reasons for this difference. This might be evidence that the smaller gear reduction (1.6:1) could be a more optimized gear ratio for manual wheelchair users, particularly for longer distances.

Conclusion

This study indicated that using geared manual wheelchair wheels resulted in substantial reduction of shoulder muscle activity and improvement in glenohumeral joint kinematics during manual wheelchair propulsion. These benefits may have the potential to decrease the risk of secondary musculoskeletal injuries and joint pain in manual wheelchair users. We also found a significant increase in the normalized stroke frequency which translates to a more repetitive task. Transition to a geared manual wheelchair could be an alternative to standard manual wheelchair mobility in the context of the preservation of upper limb function as well as the need to remain physically active. However, further biomechanical investigations including hand-rim biomechanics, upper extremity joint dynamics and muscle activity with manual wheelchair users with SCI are warranted.

The results of this study were used to refine the data collection protocol for the main study with individuals with SCI (Aims #2 & 3, chapters 3 & 4).

References

- Beres-Jones, J. A., & Harkema, S. J. (2004). The human spinal cord interprets velocity-dependent afferent input during stepping. *Brain*, *127*(10), 2232-2246.
- Board, U. A. (2002). ADA accessibility guidelines for buildings and facilities.
- Boninger, M. L., Koontz, A. M., Sisto, S. A., & Dyson-Hudson, T. A. (2005). Pushrim biomechanics and injury prevention in spinal cord injury: Recommendations based on CULP-SCI investigations. *Journal of Rehabilitation Research and Development*, *42*(3), 9.
- Brault, M. W. (2012). Americans with disabilities: 2010. *Current Population Reports*, *7*, 0-131.
- Brubaker, C. (1990). Technical consideration--ergonomic considerations. *Journal of Rehabilitation Research and Development*, *27*, 37.
- Burnham, R. S., & Steadward, R. D. (1994). Upper extremity peripheral nerve entrapments among wheelchair athletes: Prevalence, location, and risk factors. *Archives of Physical Medicine and Rehabilitation*, *75*(5), 519-524.
- Chow, J. W., Millikan, T. A., Carlton, L. G., Morse, M. I., & Chae, W. S. (2001). Biomechanical comparison of two racing wheelchair propulsion techniques. *Medicine and Science in Sports and Exercise*, *33*(3), 476-484.
- Chow, J. W., Millikan, T. A., Carlton, L. G., Chae, W., Lim, Y., & Morse, M. I. (2009). Kinematic and electromyographic analysis of wheelchair propulsion on ramps of different slopes for young men with paraplegia. *Archives of Physical Medicine and Rehabilitation*, *90*(2), 271-278.
- Criswell, E. (2010). *Cram's introduction to surface electromyography* Jones & Bartlett Publishers.
- Dallmeijer, A., Zentgraaff, I., Zijp, N., & van der Woude, L. (2004). Submaximal physical strain and peak performance in handcycling versus handrim wheelchair propulsion. *Spinal Cord*, *42*(2), 91-98.
- Dubowsky, S. R., Sisto, S. A., & Langrana, N. A. (2009). Comparison of kinematics, kinetics, and EMG throughout wheelchair propulsion in able-bodied and persons with paraplegia: An integrative approach. *Journal of Biomechanical Engineering*, *131*(2), 021015.
- Finley, M. A., & Rodgers, M. M. (2007). Effect of 2-speed geared manual wheelchair propulsion on shoulder pain and function. *Archives of Physical Medicine and Rehabilitation*, *88*(12), 1622-1627.
- Flemmer, C. L., & Flemmer, R. C. (2016). A review of manual wheelchairs. *Disability and Rehabilitation: Assistive Technology*, *11*(3), 177-187.

- Howarth, S. J., Polgar, J. M., Dickerson, C. R., & Callaghan, J. P. (2010). Trunk muscle activity during wheelchair ramp ascent and the influence of a geared wheel on the demands of postural control. *Archives of Physical Medicine and Rehabilitation*, 91(3), 436-442.
- Howarth, S. J., Pronovost, L. M., Polgar, J. M., Dickerson, C. R., & Callaghan, J. P. (2010a). Use of a geared wheelchair wheel to reduce propulsive muscular demand during ramp ascent: Analysis of muscle activation and kinematics. *Clinical Biomechanics*, 25(1), 21-28.
- Howarth, S. J., Pronovost, L. M., Polgar, J. M., Dickerson, C. R., & Callaghan, J. P. (2010b). Use of a geared wheelchair wheel to reduce propulsive muscular demand during ramp ascent: Analysis of muscle activation and kinematics. *Clinical Biomechanics*, 25(1), 21-28.
- Jahanian, O., Schnorenberg, A. J., Hawi, L., & Slavens, B. A. (2015). Upper extremity joint dynamics and electromyography (EMG) during standard and geared manual wheelchair propulsion. *Proceeding of the 39th Annual Meeting of American Society of Biomechanics*,
- Jahanian, O., Schnorenberg, A. J., & Slavens, B. A. (2016). Evaluation of shoulder joint kinematics and muscle activity during geared and standard manual wheelchair mobility. *Engineering in Medicine and Biology Society (EMBC), 2016 IEEE 38th Annual International Conference of The*, pp. 6162-6165.
- Kaye, H. S., Kang, T., & LaPlante, M. P. (2000). Mobility device use in the united states. disability statistics report 14.
- Mercer, J. L., Boninger, M., Koontz, A., Ren, D., Dyson-Hudson, T., & Cooper, R. (2006). Shoulder joint kinetics and pathology in manual wheelchair users. *Clinical Biomechanics*, 21(8), 781-789.
- Morrow, M. M., Kaufman, K. R., & An, K. (2011). Scapula kinematics and associated impingement risk in manual wheelchair users during propulsion and a weight relief lift. *Clinical Biomechanics*, 26(4), 352-357.
- Mulroy, S. J., Gronley, J. K., Newsam, C. J., & Perry, J. (1996). Electromyographic activity of shoulder muscles during wheelchair propulsion by paraplegic persons. *Archives of Physical Medicine and Rehabilitation*, 77(2), 187-193.
- Requejo, P. S., Mulroy, S. J., Ruparel, P., Hatchett, P. E., Haubert, L. L., Eberly, V. J., et al. (2015). Relationship between hand contact angle and shoulder loading during manual wheelchair propulsion by individuals with paraplegia. *Topics in Spinal Cord Injury Rehabilitation*, 21(4), 313-324.
- Sabick, M. B., Kotajarvi, B. R., & An, K. (2004). A new method to quantify demand on the upper extremity during manual wheelchair propulsion. *Archives of Physical Medicine and Rehabilitation*, 85(7), 1151-1159.

- Schnorenberg, A. J., Slavens, B. A., Wang, M., Vogel, L. C., Smith, P. A., & Harris, G. F. (2014). Biomechanical model for evaluation of pediatric upper extremity joint dynamics during wheelchair mobility. *Journal of Biomechanics*, 47(1), 269-276.
- van der Woude, L., Veeger, H., Dallmeijer, A., Janssen, T., & Rozendaal, L. (2001a). Biomechanics and physiology in active manual wheelchair propulsion. *Medical Engineering & Physics*, 23(10), 713-733.
- van der Woude, L., Veeger, H., Dallmeijer, A., Janssen, T., & Rozendaal, L. (2001b). Biomechanics and physiology in active manual wheelchair propulsion. *Medical Engineering & Physics*, 23(10), 713-733.
- van der Woude, Luc HV, Veeger, D. E., & Rozendal, R. H. (1989). Ergonomics of wheelchair design: A prerequisite for optimum wheeling conditions. *Adapted Physical Activity Quarterly*, 6(2), 109-132.
- van der Woude, Lucas HV, & de Groot, S. (2005). Wheelchair propulsion: A straining form of ambulation. *Indian Journal of Medical Research*, 121(6), 719.
- van der Woude, Lucas HV, de Groot, S., & Janssen, T. W. (2006). Manual wheelchairs: Research and innovation in rehabilitation, sports, daily life and health. *Medical Engineering & Physics*, 28(9), 905-915.
- Woltring, H. J. (1986). A fortran package for generalized, cross-validatory spline smoothing and differentiation. *Advances in Engineering Software* (1978), 8(2), 104-113.
- Yeadon, M. R., & Morlock, M. (1989). The appropriate use of regression equations for the estimation of segmental inertia parameters. *Journal of Biomechanics*, 22(6-7), 683-689.
- Zhao, K. D., Van Straaten, M. G., Cloud, B. A., Morrow, M. M., An, K. N., & Ludewig, P. M. (2015). Scapulothoracic and glenohumeral kinematics during daily tasks in users of manual wheelchairs. *Frontiers in Bioengineering and Biotechnology*, 3, 183.

Chapter 3

Hand-Rim Biomechanics during Geared Manual Wheelchair Propulsion over Different Ground Conditions in Individuals with Spinal Cord Injury

Introduction

Approximately 90% of wheelchair users use hand-rim propelled manual wheelchairs (Kaye, Kang, & LaPlante, 2000). However, manual wheelchair mobility has been described as a low efficient and physically straining form of mobility, with high risk of repetitive strain injuries and pain (Mercer et al., 2006; van der Woude, Lucas HV, de Groot, & Janssen, 2006). This often leads to reduced independent function and quality of life. The high prevalence of upper extremity pain and secondary injuries among manual wheelchair users with spinal cord injury (SCI) is a clear indication of unfavorably high loading during manual wheelchair propulsion (van der Woude, LHV, Veeger, Dallmeijer, Janssen, & Rozendaal, 2001). Several strategies have been explored and recommended to decrease the upper limb loading and the frequency of the propulsive stroke during wheelchair propulsion. To minimize the biomechanical demands of wheelchair propulsion, manual wheelchair users are recommended to maintain an ideal weight and to utilize the efficient propulsion techniques such as using long, smooth strokes that limit high impacts on the hand-rim, allowing the hand to drift down naturally and keeping it below the hand-rim during the recovery phase of propulsion. Other methods such as using the lightweight wheelchairs, and proper fit can also reduce the upper extremity injury risk for manual wheelchair users (Paralyzed Veterans of America Consortium for Spinal Cord Medicine, 2005). However, these strategies cannot decrease the forces and moments required for overcoming the rolling resistance and gravity during manual wheelchair propulsion over different ground conditions and mobility tasks. Manual wheelchairs

with alternative propulsion designs and add-on assistive technologies could alleviate the forces and moments required for manual wheelchair propulsion. Use of the alternative wheelchair propulsion mechanisms may help to preserve upper limb function and decrease the risk of secondary injuries in manual wheelchair users (Requejo et al., 2008).

Lever and crank propelled wheelchairs are among the most common alternatives, which allow a much more natural position of the hands and shoulders than standard hand-rim propulsion mechanism during propulsion. Therefore, they could be less straining, particularly for outdoor use (Flemmer & Flemmer, 2016; van der Woude, Lucas HV, Dallmeijer, Janssen, & Veeger, 2001; van der Woude, Lucas HV et al., 2006). However, the use of these alternative manual wheelchairs is limited in comparison with standard manual wheelchairs due to disadvantages such as weight, size, and limited maneuverability as well as being less friendly for transferring (Kloosterman, M. G., Snoek, van der Woude, L H, Buurke, & Rietman, 2013; van der Woude, Lucas HV et al., 2006). Pushrim-activated power assist wheelchairs are one of the most recent alternatives, which use the same propulsion techniques as standard manual wheelchairs but equipped with additional assistance. The power assist wheelchair is a hybrid between standard manual wheelchairs and powered wheelchairs. It consists of a hand-rim wheelchair with electro-motors embedded into the wheels or wheelchair frame, when a subject exerts power on the hand-rim, the motor is activated and augments the delivered power (Karmarkar, Cooper, Liu, Connor, & Puhlman, 2008). Kloosterman and colleagues reported that using the power assisted manual wheelchairs significantly decreased the hand-rim kinetics, resulting in decreased upper extremity kinetics during start-up and steady state propulsion (Kloosterman, Marieke GM, Eising, Schaake, Buurke, & Rietman, 2012; Kloosterman, Marieke GM, Buurke, de Vries, van der Woude, Lucas HV, & Rietman, 2015; Kloosterman, Marieke GM, Buurke, Schaake, van der Woude, Lucas HV, &

Rietman, 2016). Using the power assist wheelchairs could decrease the risk of secondary upper extremity injuries and may allow the user to delay the transition to a fully powered wheelchair. However, as power assist wheelchairs are less friendly for transferring, harder to propel when the battery is discharged, less maneuverable in tight turns and relatively expensive, they are not widely used (Flemmer & Flemmer, 2016).

Geared manual wheelchairs are one of the recently developed alternative propulsion mechanisms that may reduce the biomechanical demands of the upper extremity while maximizing function. Similar to a multi-speed bicycle, geared wheels allow users to choose the option of wheeling in a lower gear, which might make propulsion easier. The geared wheels add 2-10 pounds to the weight of a standard manual wheelchair. Geared manual wheels are relatively new, and there is still limited scientific evidence supporting the advantages of geared manual wheelchair mobility. There are no guidelines available for prescription or transition to geared manual wheelchairs. The pilot studies conducted by our group has shown that using geared manual wheelchairs may be beneficial for demanding tasks such as ramp ascent and propulsion on carpet (Jahanian, Schnorenberg, Hawi, & Slavens, 2015; Jahanian, Schnorenberg, & Slavens, 2016) . Howarth and colleagues reported similar results for using geared manual wheelchairs during ramp ascent (Howarth, Pronovost, Polgar, Dickerson, & Callaghan, 2010). Another study with manual wheelchair users indicated the potential for shoulder pain reduction with the use of geared manual wheelchairs (Finley & Rodgers, 2007).

The mechanical stresses from propulsion over uneven ground, ramps and carpet, and during starting from rest have been reported to be more demanding and detrimental to the upper limbs (Koontz, Cooper, Boninger, & Yang, 2005; Morrow, Hurd, Kaufman, & An, 2010) . The pilot studies we conducted with able-bodied subjects indicated that using the geared manual wheelchair

wheels for propulsion on carpeted floor and on a ramp (chapter 2), decreased the shoulder muscle activity. The use of the geared wheels has the potential to preserve the upper limb function of the manual wheelchair users and allow them to maintain an optimal level of activity and independence. However, no research has evaluated the effects of using geared manual wheelchair wheels on hand-rim and upper extremity joint kinetics in manual wheelchair users.

To investigate the effects of using geared manual wheelchair wheels on upper extremity joint dynamics, it is necessary first to measure and calculate the hand-rim biomechanics including the hand-rim kinetics and stroke cycle characteristics. Additionally, parameters of hand-rim biomechanics such as propulsion forces and wheel torque, rate of force application, fractional effective force, and stroke cycle frequency have all been associated with manual wheelchair efficiency and development of upper extremity limb pain and injuries in manual wheelchair users (Boninger, Cooper, Baldwin, Shimada, & Koontz, 1999; Boninger, Koontz, Sisto, & Dyson-Hudson, 2005). Our primary goal in this study is to evaluate the hand-rim biomechanics during geared manual wheelchair propulsion on tile and carpeted level floors and a ramp in the low gear and standard gear conditions in adults with SCI. It is hypothesized that the propulsion speed and hand-rim kinetics including the peak hand-rim resultant force, peak hand-rim propulsive moment, and maximum rate of resultant hand-rim force will be significantly less during the low gear condition in comparison with the standard gear condition. Gear condition will not be significantly effective on the stroke cycle frequency.

Previous studies with able-bodied subjects indicated that to comprehensively understand the impact that the geared wheel system has on upper extremity biomechanics, it is necessary to calculate and evaluate combined biomechanical metrics such as normalized integrated hand-rim resultant force and propulsive moment. Our secondary goal in this study is to investigate the effects

of using geared wheels on hand-rim combined biomechanical metrics during manual wheelchair propulsion on tile and carpeted level floors and up a ramp in adults with SCI. It is hypothesized that using the geared wheels in the lower gear condition will significantly increase the normalized integrated frequency in comparison to the standard gear condition. Gear condition will not be significantly effective on the normalized integrated hand-rim resultant force and normalized integrated hand-rim propulsive moment.

Methods

This study was approved by the Clement J. Zablocki Veterans Affairs Center and the University of Wisconsin-Milwaukee (UWM) Institutional Review Boards. All subjects signed the approved informed consent forms prior to participation.

Subjects

The inclusion criteria for subjects were to be between 18 and 70 years old, use a manual wheelchair as the primary mode of mobility, have a minimum of six months experience as a manual wheelchair user, and have the ability to perform independent transfers. Seven (7) veterans with paraplegic SCI who met the inclusion criteria participated in this study. Shoulder pain assessment was administered after clinical examination by the physiatrist at the SCI unit at the Clement J. Zablocki Veterans Administration Medical Center (VAMC) using the Wheelchair User's Shoulder Pain Index (Curtis et al., 1995). Wheelchair propulsion testing was completed at the UWM Mobility Lab. Table 8 provides subjects' characteristics and their WUSPI scores.

Table 8. Subject characteristics and wheelchair user's shoulder pain index (WUSPI) total scores.

#	Subject ID	Age (years)	Weight (kg)	Height (cm)	Arm Dominance	SCI level	Years as a wheelchair user	WUSPI total score (cm)
1	5	55	97.7	185	Right	T5	31	21.2
2	6	36	80.2	175	Right	L2	12	8.7
3	8	57	81.2	180	Right	T11	0.6	N/A
4	10	24	71.2	180	Right	T5	2	53.9
5	11	51	112.0	188	Left	T12	30	19.7
6	12	29	93.0	188	Right	T1	10	1.2
7	13	54	136.0	193	Right	T12	36	3.0
Mean ± SD		43.7 ± 13.7	95.9 ± 22.1	184.1 ± 6.1	-----	-----	17.3 ± 14.6	18.0 ± 19.5

T#: Thoracic spinal injury level, L#: Lumbar spinal injury level

Data collection

Instrumented hand-rim

Subjects used their personal standard manual wheelchairs equipped with the IntelliWheels geared wheels (IntelliWheels, Inc., Champaign, IL), which allowed them to propel in standard gear (gear ratio of 1:1) or shift into a low gear (gear ratio of 1.5:1). Using an in-hub planetary gear train between the hand-rim and wheel, the IntelliWheels geared wheels could reduce the load required for wheelchair propulsion (Figure 8). For measuring propulsion kinetics, an IntelliWheels geared wheel equipped with a custom instrumented hand-rim, previously developed and validated by our team (Gaglio, Liang, Daigle, & Hsiao-Wecksler, 2016; Gaglio et al., 2017), was mounted to the wheelchair on the subject's dominant side to measure hand-rim kinetics. A non-instrumented IntelliWheels geared wheel, with the same geometry and inertia as the instrumented geared wheel, was mounted on the opposite side.



Figure 8. IntelliWheels geared manual wheelchair wheel (left) and the planetary gear train from a prototype IntelliWheels geared manual wheelchair wheel (right).

Experimental Protocol

After acclimation time of 15-30 minutes, subjects propelled their wheelchairs over an 8-meter, carpeted level floor (Figure 10; padding thickness: 9.5 mm and carpet thickness: 17.5 mm), a 10-meter, tiled level floor (Figure 11), and up a 2.5-meter ramp with a 4.8-degree slope (Figure 12; below the American with Disability Act Accessibility Guidelines maximum allowable slope of 5 degrees (Board, 2002) in both standard and low gear conditions in random order. They were instructed to start propelling their wheelchairs from a resting position up to their self-selected normal speed in a straight line and to end the trial at the designated finish line. For the trials on the carpet, subjects were instructed to start propelling their wheelchair from a resting position on the carpet and to end the trial at the designated finish line on the carpet as well. Each ramp ascent trial began on the level tile floor with the subject positioned one meter from the ramp base. Subjects performed the tasks in a random order, there were five trials for each task.

Data Analysis

Three components of the applied hand-rim forces (F_x , F_y , and F_z), the propulsive moment about

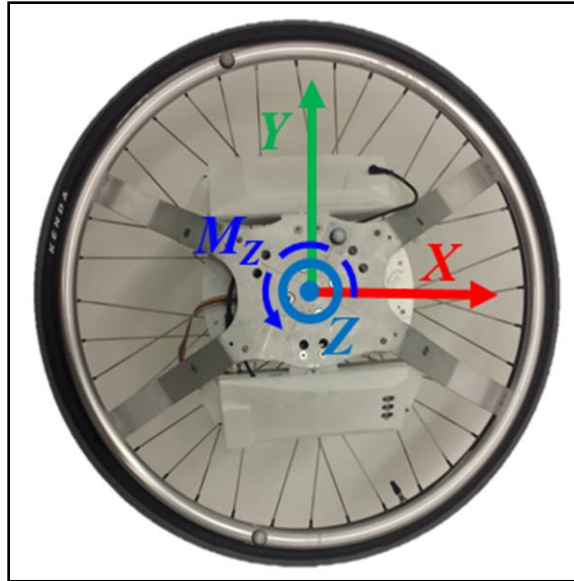


Figure 9. Orientation of instrumental hand rim coordinate system when wheel is mounted on the right side of the wheelchair.

the hub (T_z), and the hand-rim angular position data (θ) from the instrumented hand-rim during each trial were used for calculating hand-rim kinetics and the stroke cycle characteristics of geared manual wheelchair propulsion. The hand-rim kinetic characteristics included the peak hand-rim resultant force, peak hand-rim propulsive moment, fractional effective force, and maximum rate of rise of the hand-rim resultant force. The stroke cycle characteristics included the propulsion speed and stroke frequency. The stroke cycle was divided into the push and recovery phases using the propulsive moment. Using a custom MATLAB program, the onset of the push phase was identified as the point at which the propulsive moment exceeded the detection threshold, which was the mean of the moment baseline plus 3 standard deviations. The end of the push phase was the point at which the propulsive moment returned to the baseline and remained under the threshold (Figure 13). For the propulsion condition (semi-steady state), the first two and the last strokes of each trial were removed and the averaged values over the rest of the trials were used for analysis (Figure 13).



Figure 10. A subject propelling on a carpeted level floor using the IntelliWheels geared manual wheelchair wheels.



Figure 11. A subject propelling on a tiled level floor using the IntelliWheels geared manual wheelchair wheels.



Figure 12. A subject ascending a ramp using the IntelliWheels geared manual wheelchair wheels.

The kinematic parameters including the stroke distance and linear velocity were determined from the hand-rim angular position data for each stroke cycle. Because of the relative motion between the hand-rim and the wheel during the geared condition, the calculated kinematic values were divided by 1.5 for these trials (geared condition). The stroke cycle frequency was computed based on the stroke cycle time. The normalized stroke cycle frequency was calculated as the ratio of stroke cycle frequency to the stroke distance which indicates the number of stroke cycles over time and distance. The rate of rise of the resultant force was determined by differentiating the resultant force with respect to the time (Koontz et al., 2005). The fractional effective force is the percentage of the tangential force that contributed to the resultant force, where tangential force was obtained by dividing the propulsive moment by the radius of the hand-rim (0.275 m). This definition of tangential force assumes that the grip moment during push phase is negligible (Koontz et al., 2005). To investigate the kinetic demands of manual wheelchair propulsion, the integration of the forces

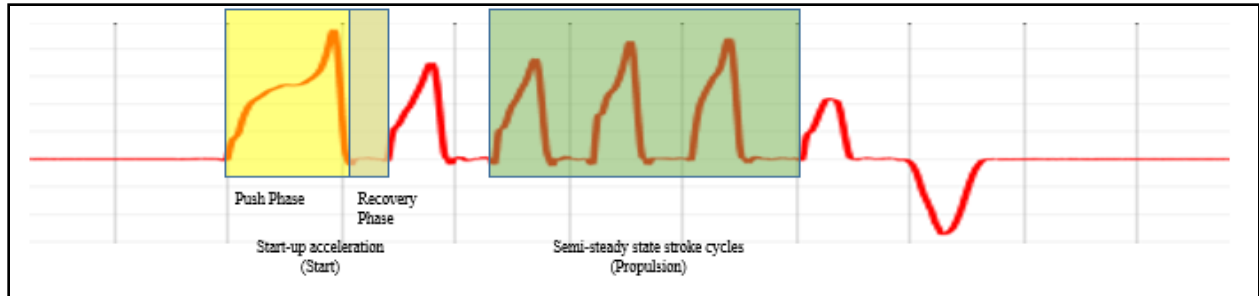


Figure 13. A sample hand-rim propulsive moment reaction curve for propulsion on the carpeted floor used for detecting the semi-state stroke cycles, and the push and recovery phases for each stroke cycle. Moments that cause wheelchair to move forward (propulsive moment) are negative, and moments that act in opposite direction are positive.

(linear impulse) and moments (angular impulse) during the push phase were calculated during both conditions. To compare the two conditions, the integrated force and moment were divided by the travelled distance (normalized integrated force and moment) and were analyzed for the propulsion task. A summary of all calculations for the metrics of interest are listed in Table 9.

Statistical analysis

The subject means, and standard deviations of the hand-rim kinetics and stroke cycle characteristics were computed for each gear condition (standard gear and low gear) and terrain (tile level floor, carpeted level floor, and ramp) for five trials. A two-way analysis of variance (2 gear conditions x 3 terrains) with repeated measures was used for statistical analysis. If there was no significant interaction between the factors (gear condition and terrain), the main effects of the gear condition factor (regardless of the terrain) were investigated. When there was a significant interaction between factors, simple effects of the gear condition factor within each terrain were examined using repeated measures analysis of variance (ANOVA). All statistical analyses were completed with SPSS software (IBM Corporation) using a general linear model with repeated measures (significance level = 0.05).

Table 9. Summary of all calculations for the metrics of interest.

Metric	Calculation
Hand-rim Resultant Force (F)	$\sqrt{F_x^2 + F_y^2 + F_z^2}$
Hand-rim Propulsive Moment (T_z)	Directly measured by the instrumented hand-rim
Rate of rise of the resultant Force	$\frac{dF}{dt}$
Tangential Force (F_t)	$\frac{T_z}{\text{Handrim radius}}$
Fractional Effective Force	$\frac{F_t}{F} \times 100$
Integrated Force (linear impulse)	The area under the resultant force time (F-t) graph during one stroke cycle (calculated using numerical integration)
Integrated Moment (angular impulse)	The area under the propulsive moment time (T_z -t) graph during one stroke cycle (calculated using numerical integration)
Stroke Time (t)	The time from the beginning of the push phase to the end of the recovery phase in each stroke cycle
Stroke Angle	The angular displacement of the wheel during one stroke cycle, measured directly by the instrumented hand-rim
Stroke Distance (D)	The linear distance that the wheelchair travelled during one stroke cycle, calculated based on the stroke angle and the circumference of the wheel
Frequency (Frq)	$\frac{1}{t}$
Propulsion Speed	$\frac{D}{t}$
Normalized Frequency	$\frac{Frq}{D}$
Normalized Integrated Force	$\frac{\text{Integrated Force}}{D}$
Normalized Integrated Moment	$\frac{\text{Integrated Moment}}{D}$

Results

Mean values and the standard deviations for the stroke cycle characteristics and hand-rim kinetics during manual wheelchair propulsion on tile and carpeted level floor and up the ramp in the standard gear and low gear conditions are reported in Table 10 and Figures 14-19. Mean values and the standard deviations for the combined biomechanical metrics including the normalized stroke frequency, and the normalized integrated hand-rim resultant force and propulsive moment are reported in Table 11 and Figures 20-22. The box plot graphs combined with the individual measurements for the hand-rim kinetics, stroke cycle characteristics, and combined biomechanical metrics that are significantly affected by gear condition are depicted in Figures 23-29.

The interaction between the gear condition and terrain was not statistically significant for the propulsion speed, frequency, peak hand-rim resultant force, peak rate of rise of the hand-rim resultant force, and fractional effective force. Analysis of the main effects indicated that regardless of the terrain, the low gear condition significantly decreased the propulsion speed ($F = 12.28$, $p = 0.013$), peak hand-rim resultant force ($F = 18.25$, $p = 0.005$), peak rate of rise of the hand-rim resultant force ($F = 7.36$, $p = 0.035$), and fractionation effective force ($F = 16.38$, $p = 0.007$); (Table 10). Frequency was not significantly affected by the gear condition ($F = 1.57$, $p = 0.256$); (Table 10).

The statistical analysis results indicated that there was a significant interaction between the gear condition and terrain for the peak hand-rim propulsive moment ($F = 8.21$, $p = 0.006$). Analysis of the simple effects indicated that during the low gear condition the peak hand-rim propulsive moment decreased significantly on tile level floor ($F = 55.46$, $p < 0.001$), carpeted level floor ($F = 93.60$, $p < 0.001$), and up the ramp ($F = 16.68$, $p = 0.006$), compared to the standard gear condition (Table 10).

Table 10. Stroke cycle characteristics and hand-rim kinetics mean values and standard deviations during manual wheelchair propulsion on tile and carpeted level floor and up the ramp in the standard gear and low gear conditions.

Metric	Environment	Standard Gear	Low Gear	<i>p</i>
		Mean + SD	Mean + SD	
Speed (m/s)*	Tile	1.51 + 0.18	1.23 + 0.23	0.013
	Carpet	0.96 + 0.12	0.77 + 0.12	
	Ramp	1.01 + 0.16	0.85 + 0.22	
Frequency (1/s)	Tile	0.93 + 0.15	0.96 + 0.12	0.256
	Carpet	1.00 + 0.18	1.03 + 0.23	
	Ramp	1.10 + 0.18	1.16 + 0.28	
Peak Force (N)*	Tile	92.72 + 23.22	65.36 + 24.16	0.005
	Carpet	125.45 + 25.53	104.83 + 25.86	
	Ramp	148.04 + 39.83	128.97 + 24.10	
Peak Moment (N.m) #	Tile **	21.31 + 6.55	13.45 + 5.48	< 0.001
	Carpet **	29.19 + 4.32	22.96 + 4.20	< 0.001
	Ramp **	35.43 + 6.43	30.36 + 5.29	0.006
Peak Rate of Rise of the Force (N/s)*	Tile	1334.13 + 392.13	961.80 + 642.90	0.035
	Carpet	1822.29 + 700.03	1372.28 + 564.61	
	Ramp	2573.07 + 864.01	1989.20 + 898.89	
Fractional Effective Force (%) *	Tile	70.36 + 7.85	67.87 + 11.90	0.007
	Carpet	81.54 + 9.79	68.49 + 7.45	
	Ramp	90.36 + 14.20	83.35 + 17.88	

#: Statistically significant interaction between gear condition and terrain, $p < 0.05$

*: Statistically significant difference, $p < 0.05$ (gear condition main effect)

** : Statistically significant difference, $p < 0.05$ (gear condition simple effects for tile, carpet and ramp)

The interaction between the gear condition and terrain was not statistically significant for the normalized frequency, normalized integrated hand-rim resultant force, and normalized integrated propulsive moment. Analysis of the main effects indicated that regardless of the terrain, the low gear condition significantly increased the normalized frequency ($F = 7.62$, $p = 0.033$), and significantly decreased the normalized integrated propulsive moment ($F = 8.07$, $p = 0.030$); (Table 11). The normalized integrated hand-rim resultant force was not significantly affected by the gear condition ($F = 1.70$, $p = 0.239$); (Table 11).

The box plot graphs combined with the individual measurements for the hand-rim kinetics, stroke cycle characteristics, and combined biomechanical metrics indicate that all or a pronounced majority of subjects individually followed the group trends (Figures 23-29).

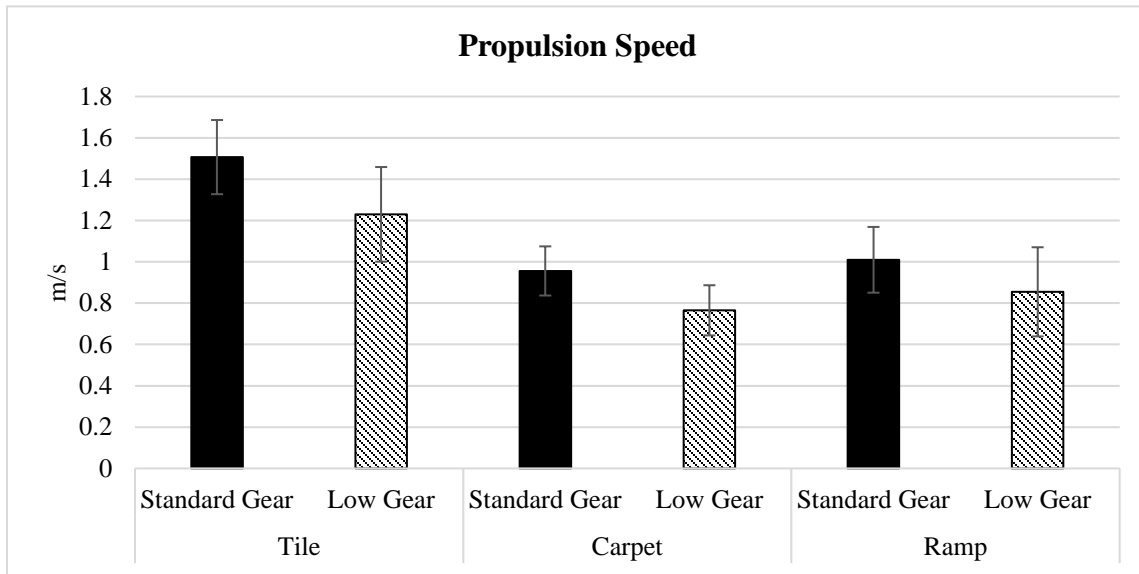


Figure 14. Group mean values and standard deviations for the propulsion speed during manual wheelchair propulsion on tile and carpeted level floor and up a ramp in the standard gear and low gear conditions.

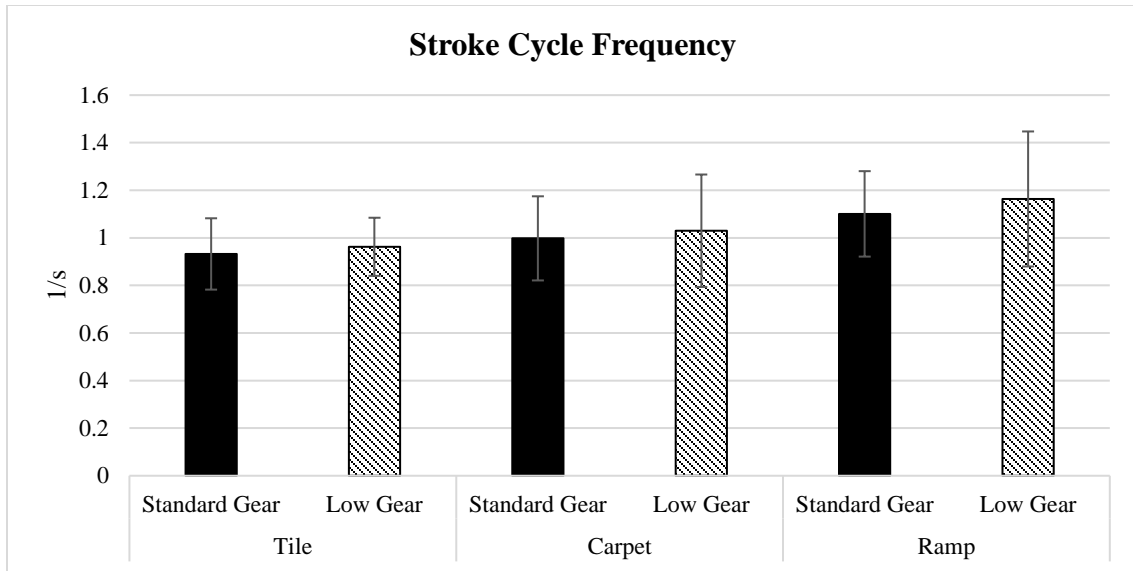


Figure 15. Group mean values and standard deviations for the stroke cycle frequency during manual wheelchair propulsion on tile and carpeted level floor and up a ramp in the standard gear and low gear conditions.

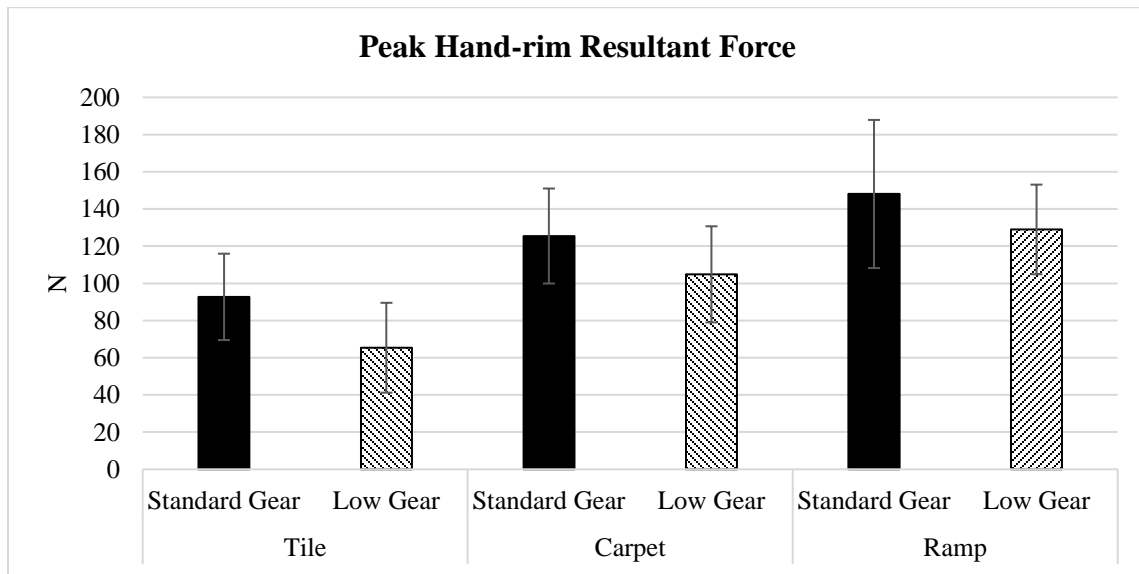


Figure 16. Group mean values and standard deviations for the peak hand-rim resultant force mean values and standard deviations during manual wheelchair propulsion on tile and carpeted level floor and up a ramp in the standard gear and low gear conditions.

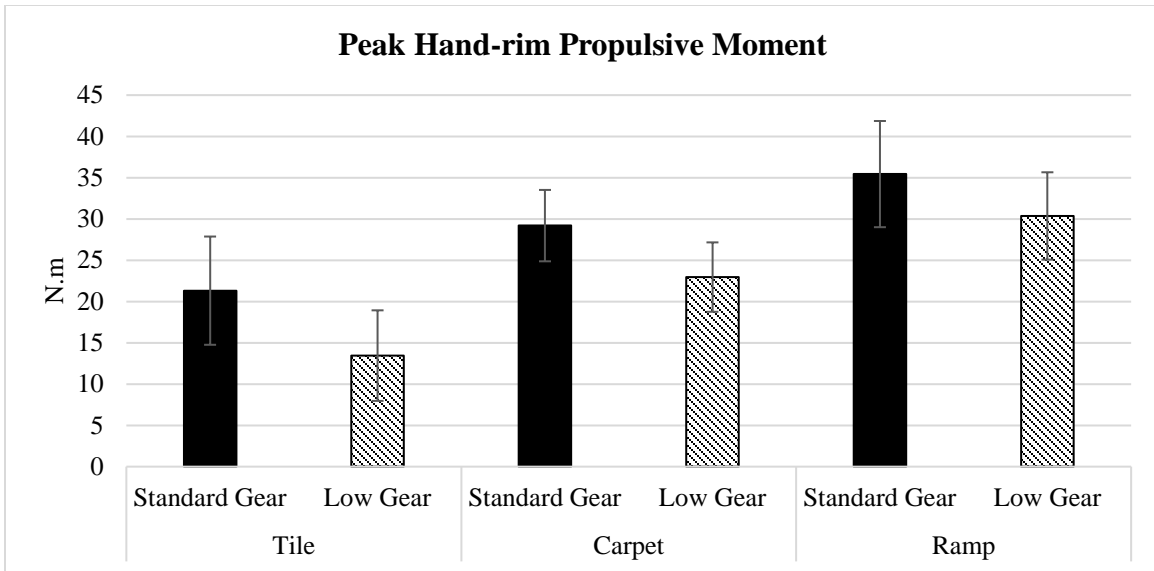


Figure 17. Group mean values and standard deviations for the peak hand-rim propulsive moment during manual wheelchair propulsion on tile and carpeted level floor and up a ramp in the standard gear and low gear conditions.

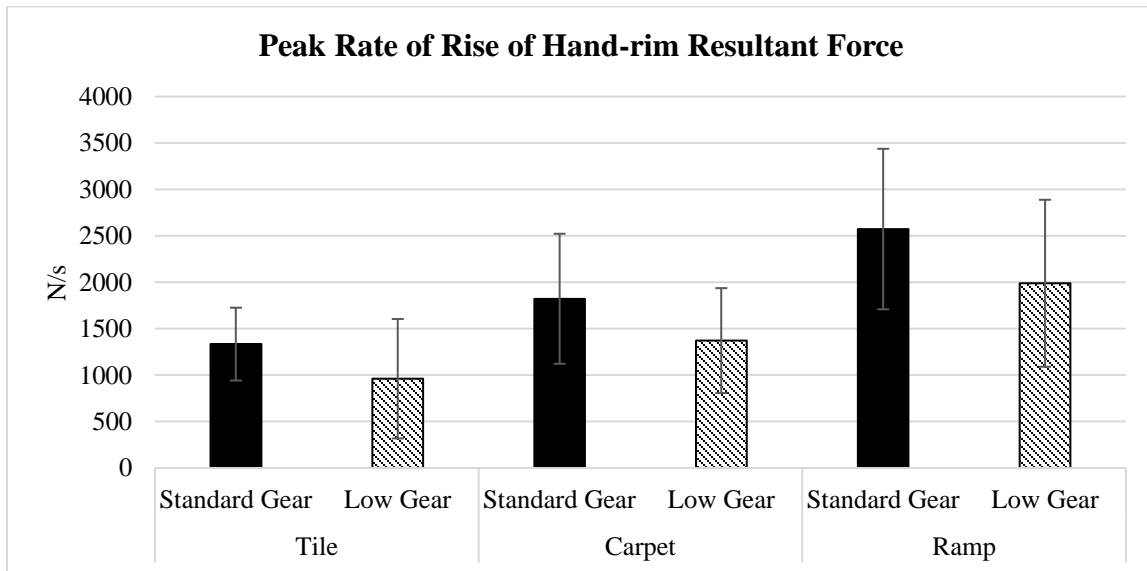


Figure 18. Group mean values and standard deviations for the peak rate of rise of hand-rim resultant force during manual wheelchair propulsion on tile and carpeted level floor and up a ramp in the standard gear and low gear conditions.

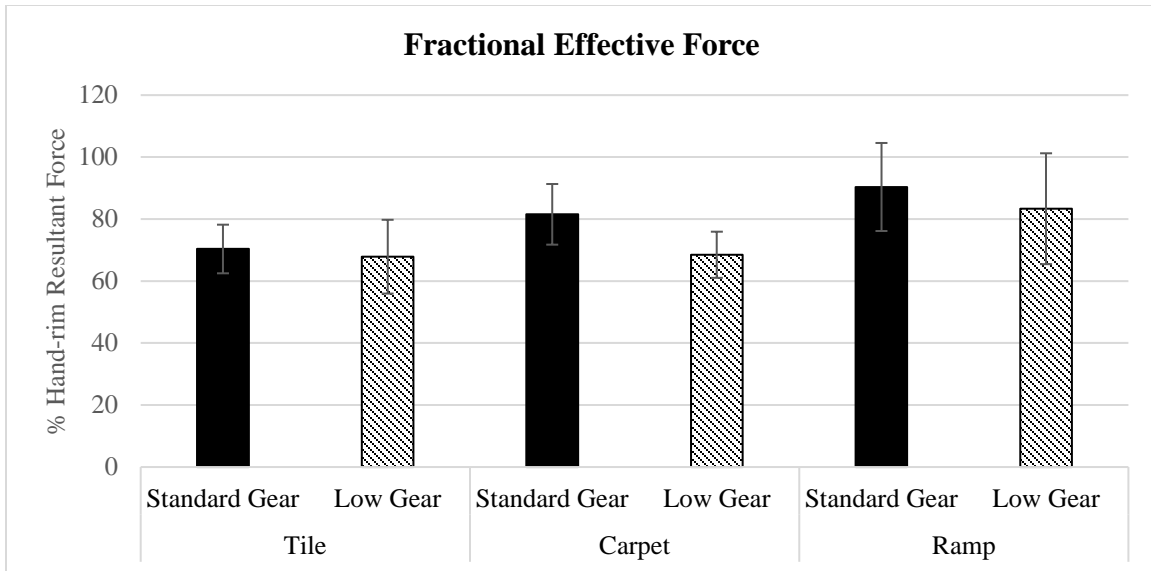


Figure 19. Group mean values and standard deviations for the fraction of effective force during manual wheelchair propulsion on tile and carpeted level floor and up the ramp in the standard gear and low gear conditions.

Table 11. Group mean values and standard deviations for the normalized frequency, normalized integrated force, and normalized integrated moment during manual wheelchair propulsion on tile and carpeted level floor and up the ramp in the standard gear and low gear conditions.

Metric	Environment	Standard Gear	Low Gear	<i>p</i>
		Mean + SD	Mean + SD	
Normalized Frequency ([1/s].m) *	Tile	0.61 + 0.23	0.79 + 0.25	0.033
	Carpet	1.11 + 0.51	1.47 + 0.76	
	Ramp	1.29 + 0.60	1.79 + 1.23	
Normalized Integrated Force ([N].s/m)	Tile	13.06 + 3.20	9.00 + 2.83	0.239
	Carpet	45.35 + 10.27	42.91 + 9.33	
	Ramp	51.00 + 12.33	49.19 + 13.90	
Normalized Integrated Moment ([N.m].s/m) *	Tile	2.75 + 0.62	1.77 + 0.47	0.030
	Carpet	10.35 + 2.04	8.70 + 1.46	
	Ramp	12.60 + 3.51	11.38 + 3.75	

#: Statistically significant interaction between gear condition and terrain, $p < 0.05$

*: Statistically significant difference, $p < 0.05$ (gear condition main effect)

** : Statistically significant difference, $p < 0.05$ (gear condition simple effects for tile, carpet and ramp)

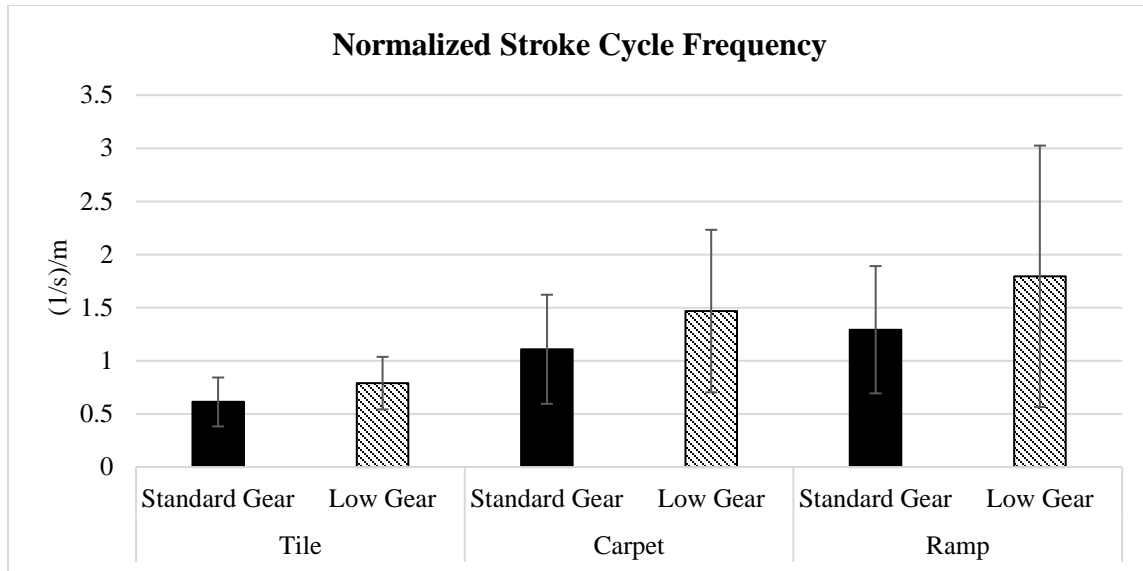


Figure 20. Group mean values and standard deviations for the normalized stroke cycle frequency during manual wheelchair propulsion on tile and carpeted level floor and up the ramp in the standard gear and low gear conditions.

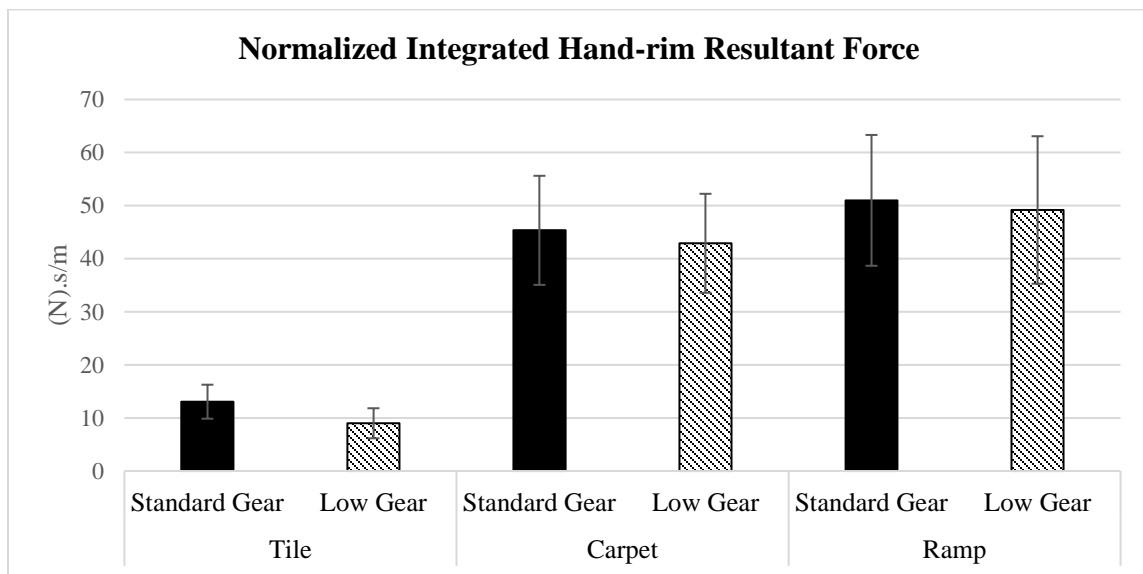


Figure 21. Group mean values and standard deviations for the normalized integrated hand-rim resultant force during manual wheelchair propulsion on tile and carpeted level floor and up the ramp in the standard gear and low gear conditions.

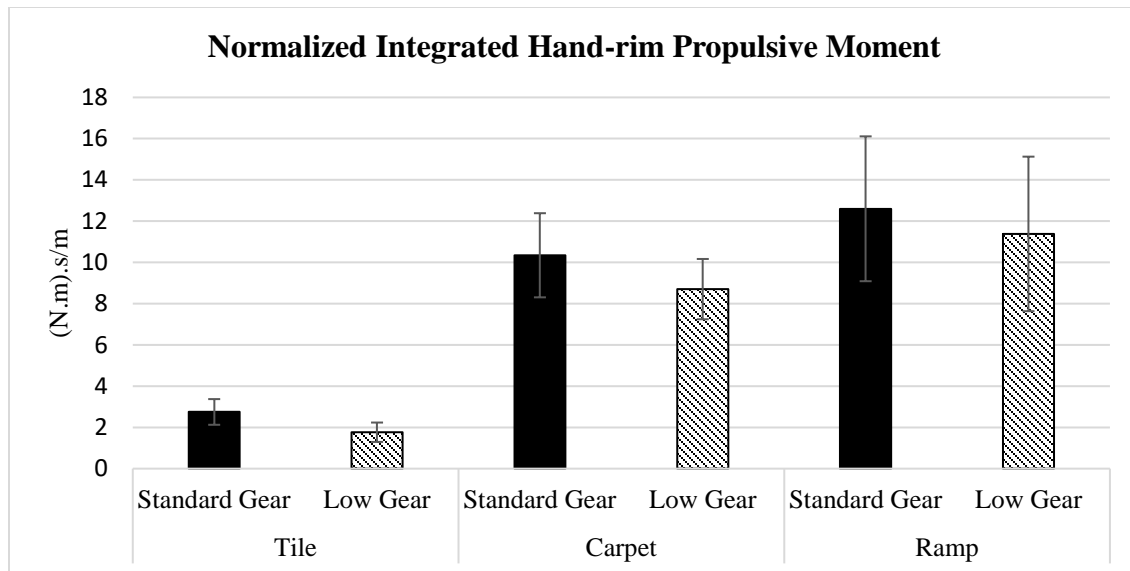


Figure 22. Group mean values and standard deviations for the normalized integrated hand-rim propulsive moment during manual wheelchair propulsion on tile and carpeted level floor and up the ramp in the standard gear and low gear conditions.

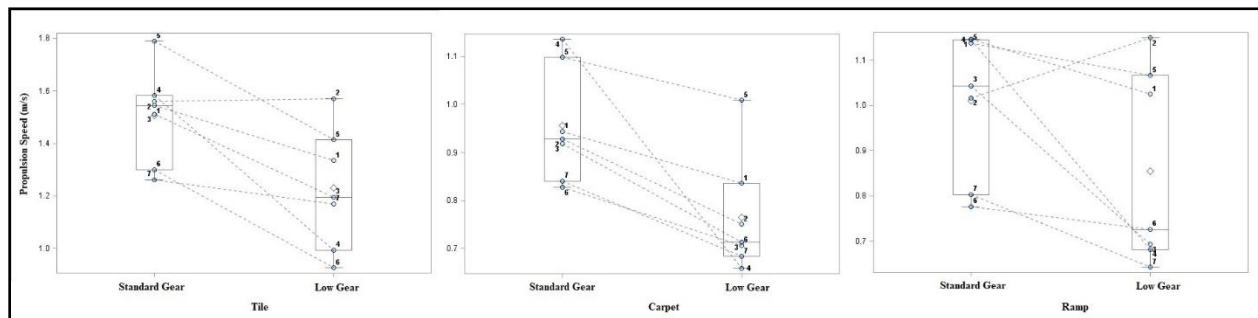


Figure 23. Propulsion speed during manual wheelchair propulsion on tile and carpeted level floor and up the ramp. In each graph the box plot on the left is for the standard gear and on the right is for the low gear condition. The bottom and top edges of the box indicate the intra-quartile range. The diamond inside the box indicates the mean value. The line inside the box indicates the median value. The whiskers that extend from each box indicate the entire range of values. The measurements for each subject are shown with a circle and the subject number next to it.

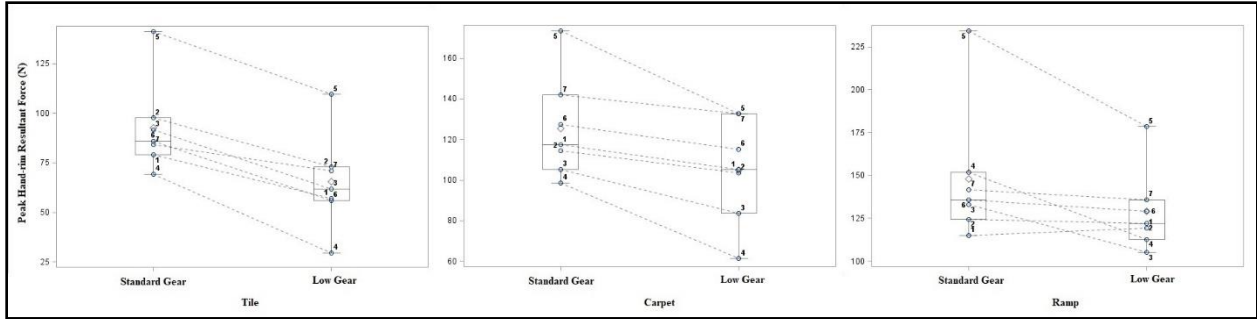


Figure 24. Peak hand-rim resultant force during manual wheelchair propulsion on tile and carpeted level floor and up the ramp. In each graph the box plot on the left is for the standard gear and on the right is for the low gear condition. The bottom and top edges of the box indicate the intra-quartile range. The diamond inside the box indicates the mean value. The line inside the box indicates the median value. the whiskers that extend from each box indicate the entire range of values. The measurements for each subject are shown with a circle and the subject number next to it.

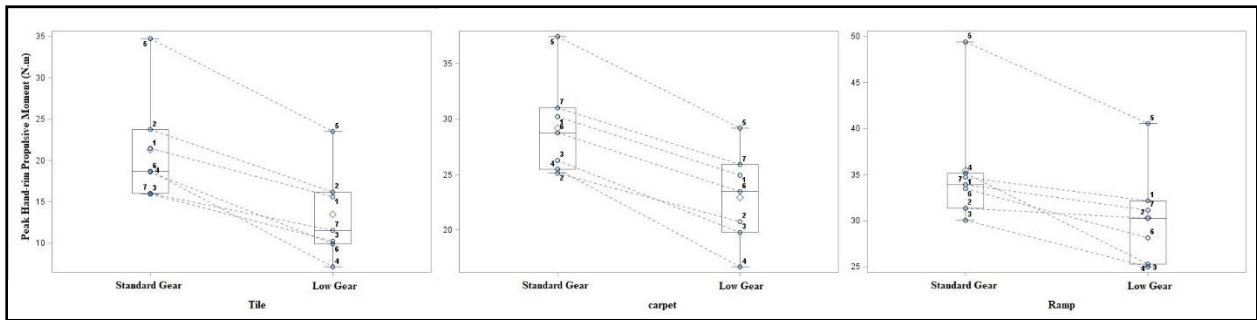


Figure 25. Peak hand-rim propulsive moment during manual wheelchair propulsion on tile and carpeted level floor and up the ramp. In each graph the box plot on the left is for the standard gear and on the right is for the low gear condition. The bottom and top edges of the box indicate the intra-quartile range. The diamond inside the box indicates the mean value. The line inside the box indicates the median value. the whiskers that extend from each box indicate the entire range of values. The measurements for each subject are shown with a circle and the subject number next to it.

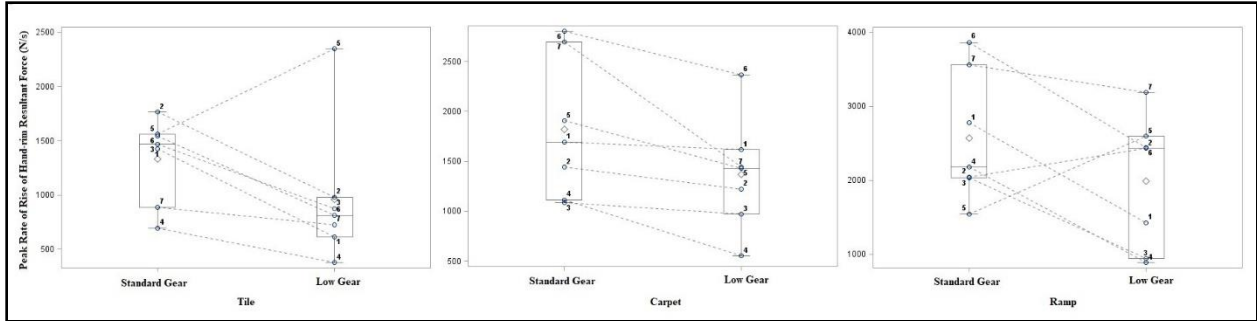


Figure 26. Peak rate of rise of hand-rim resultant force during manual wheelchair propulsion on tile and carpeted level floor and up the ramp. In each graph the box plot on the left is for the standard gear and on the right is for the low gear condition. The bottom and top edges of the box indicate the intra-quartile range. The diamond inside the box indicates the mean value. The line inside the box indicates the median value. The whiskers that extend from each box indicate the entire range of values. The measurements for each subject are shown with a circle and the subject number next to it.

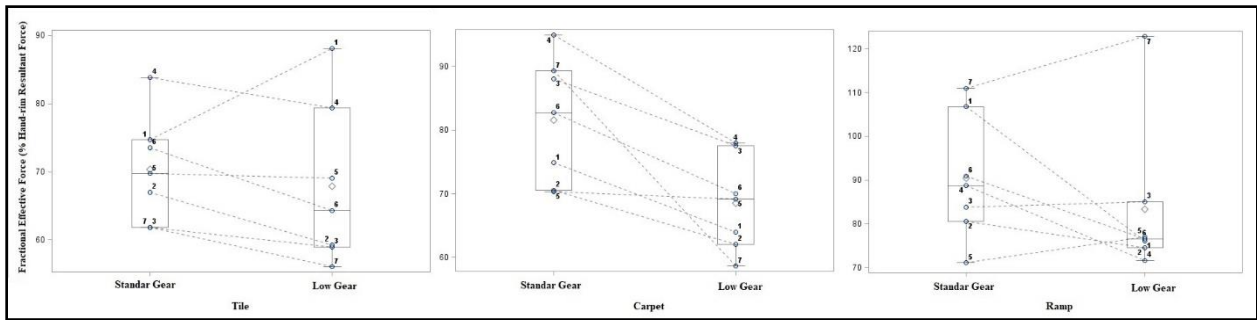


Figure 27. Fracture effective force during manual wheelchair propulsion on tile and carpeted level floor and up the ramp. In each graph the box plot on the left is for the standard gear and on the right is for the low gear condition. The bottom and top edges of the box indicate the intra-quartile range. The diamond inside the box indicates the mean value. The line inside the box indicates the median value. The whiskers that extend from each box indicate the entire range of values. The measurements for each subject are shown with a circle and the subject number next to it.

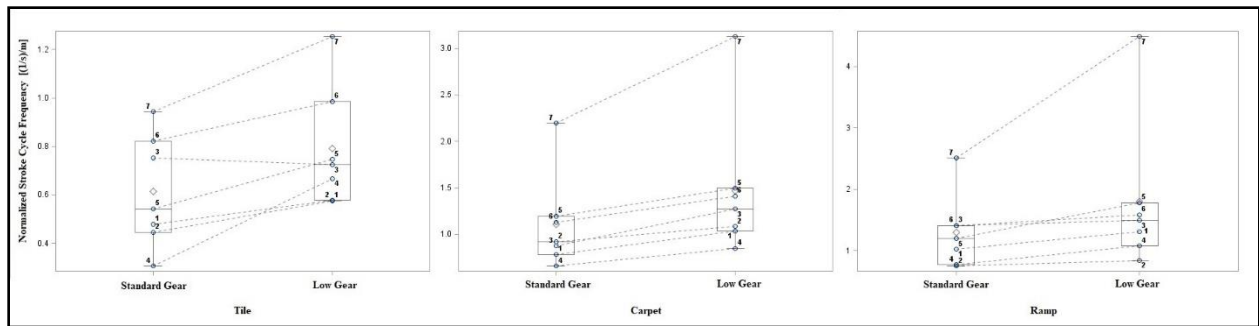


Figure 28. Normalized stroke cycle frequency during manual wheelchair propulsion on tile and carpeted level floor and up the ramp. In each graph the box plot on the left is for the standard gear and on the right is for the low gear condition. The bottom and top edges of the box indicate the intra-quartile range. The diamond inside the box indicates the mean value. The line inside the box indicates the median value. the whiskers that extend from each box indicate the entire range of values. The measurements for each subject are shown with a circle and the subject number next to it.

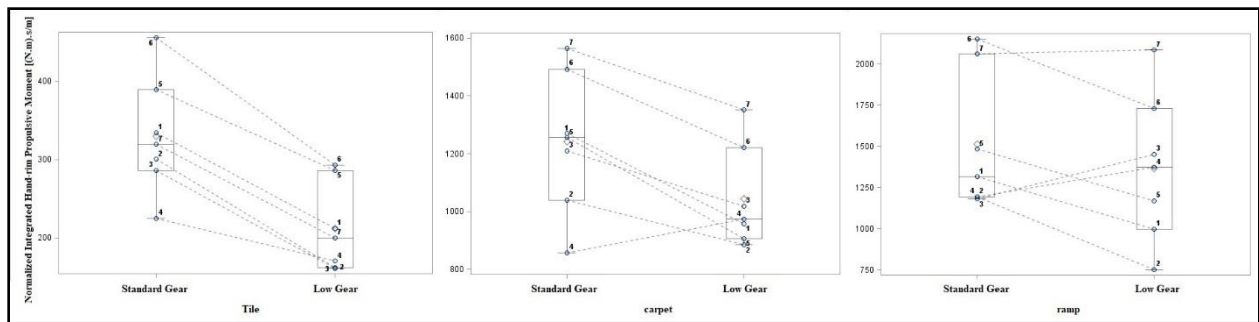


Figure 29. Normalized integrated hand-rim propulsive moment during manual wheelchair propulsion on tile and carpeted level floor and up the ramp. In each graph the box plot on the left is for the standard gear and on the right is for the low gear condition. The bottom and top edges of the box indicate the intra-quartile range. The diamond inside the box indicates the mean value. The line inside the box indicates the median value. the whiskers that extend from each box indicate the entire range of values. The measurements for each subject are shown with a circle and the subject number next to it.

Discussion

We successfully characterized the hand-rim kinetics and stroke cycle characteristics during geared manual wheelchair propulsion on tile and carpeted level floors and up a ramp in veterans with SCI. Similar to previous studies, we found that high hand-rim kinetics occur during manual

wheelchair propulsion (standard gear) on the carpeted floor, and up the ramp (Hurd, Morrow, Kaufman, & An, 2008; Koontz et al., 2005).

Consistent with the hypotheses, using the geared wheels in the low gear condition significantly decreased the propulsion speed, and hand-rim kinetics including the peak hand-rim resultant force, peak hand-rim propulsive moment, and peak rate of rise of the hand-rim resultant force, in comparison with the standard gear condition. The gear condition was not significantly effective on the stroke cycle frequency. The fractional effective force decreased significantly during the low gear condition. However, the large values reported for the fractional effective force indicate that the assumption of the negligible hand moment during push phase was not valid.

Using the geared wheels in the low gear condition significantly increased the normalized stroke cycle frequency and significantly decreased the normalized integrated hand-rim propulsive moment, which the later one was not consistent with what we had hypothesized. The gear condition was not significantly effective on the normalized integrated hand-rim resultant force.

The significant differences in hand-rim kinetics seen between the standard gear and low gear conditions indicate potential benefits of using geared wheels regardless of the terrain. Previous studies have shown that the reduction of hand-rim propulsion forces, wheel torque, and rate of force application could increase the manual wheelchair efficiency and decrease the risk of development of upper extremity limb injuries such as carpal tunnel syndrome (Jahanian, Gaglio, Schnorenberg, Muqet, Hsiao-Wecksler, & Slavens, 2019) and upper extremity joint pain (Boninger et al., 1999; Boninger et al., 2005). The significant increase in the normalized stroke cycle frequency during the low gear condition demonstrate that for a given distance, a higher number of stroke cycles are required. High-repetition of upper extremity joint motions have been significantly related to increased risk of upper limb injuries in manual wheelchair users

(Boninger et al., 2005; Requejo et al., 2008).

Evaluation of combined hand-rim biomechanical metrics could provide a more comprehensive characterization of the impact that the geared wheel system has on upper extremity biomechanics. In this study, the normalized integrated hand-rim propulsive moment and normalized integrated hand-rim resultant force decreased during the low gear condition in comparison with the standard gear condition. This indicates that although a higher number of stroke cycles are required for travelling a given distance in the low gear condition than the standard gear condition, the low gear condition might be less demanding than the standard gear condition. This might be interpreted as lower cumulative load during the low gear condition than the standard gear condition.

Conclusion

The current investigation suggests that using geared wheels could be beneficial for manual wheelchair users to independently accomplish propulsion tasks such as propulsion on carpeted floor, and ramp ascension while reducing the risk of secondary upper extremity injuries. This work has the potential to impact clinical decision making for wheelchair prescription, training, and usage. Further investigation of hand-rim biomechanics, joint dynamics, muscle activity and energetics is warranted to elucidate the effects of using the geared wheels on upper extremity biomechanics, physiology and function in manual wheelchair users with SCI.

References

- Board, U. A. (2002). ADA accessibility guidelines for buildings and facilities.
- Boninger, M. L., Cooper, R. A., Baldwin, M. A., Shimada, S. D., & Koontz, A. (1999). Wheelchair pushrim kinetics: Body weight and median nerve function. *Archives of Physical Medicine and Rehabilitation*, 80(8), 910-915.
- Boninger, M. L., Koontz, A. M., Sisto, S. A., & Dyson-Hudson, T. A. (2005). Pushrim biomechanics and injury prevention in spinal cord injury: Recommendations based on CULP-SCI investigations. *Journal of Rehabilitation Research and Development*, 42(3), 9.
- Curtis, K., Roach, K., Applegate, E. B., Amar, T., Benbow, C., Genecco, T., et al. (1995). Development of the wheelchair user's shoulder pain index (WUSPI). *Spinal Cord*, 33(5), 290-293.
- Finley, M. A., & Rodgers, M. M. (2007). Effect of 2-speed geared manual wheelchair propulsion on shoulder pain and function. *Archives of Physical Medicine and Rehabilitation*, 88(12), 1622-1627.
- Flemmer, C. L., & Flemmer, R. C. (2016). A review of manual wheelchairs. *Disability and Rehabilitation: Assistive Technology*, 11(3), 177-187.
- Gaglio, A., Daigle, S., Gacek, E., Jahanian, O., Slavens, B., Rice, I., et al. (2017). Validation of an instrumented wheelchair hand rim. *2017 Design of Medical Devices Conference*, pp. V001T05A012.
- Gaglio, A., Liang, J., Daigle, S., & Hsiao-Wecksler, E. (2016). Design of a universal instrumented wheelchair hand rim. *Journal of Medical Devices*, 10(3), 030956.
- Howarth, S. J., Pronovost, L. M., Polgar, J. M., Dickerson, C. R., & Callaghan, J. P. (2010). Use of a geared wheelchair wheel to reduce propulsive muscular demand during ramp ascent: Analysis of muscle activation and kinematics. *Clinical Biomechanics*, 25(1), 21-28.
- Hurd, W. J., Morrow, M. M., Kaufman, K. R., & An, K. (2008). Biomechanic evaluation of upper-extremity symmetry during manual wheelchair propulsion over varied terrain. *Archives of Physical Medicine and Rehabilitation*, 89(10), 1996-2002.
- Jahanian, O., Gaglio, A., Daigle, S., Muqet, V., Schnorenberg, A. J., Hsiao-Wecksler, E. T., et al. (2018). Hand-rim biomechanics of geared manual wheelchair mobility. *Proceeding of the Rehabilitation Engineering and Assistive Technology Society of North America (RESNA) 2018 Annual Conference*.

- Jahanian, O., Gaglio, A., Schnorenberg, A. J., Muqet, V., Hsiao-Wecksler, E. T., & Slavens, B. A. (2019). Evaluation of Hand-rim and Wrist Joint Kinetics During Geared Manual Wheelchair Propulsion in Veterans with Spinal Cord Injury. *Biomedical sciences instrumentation*, 55(2), 324-329.
- Jahanian, O., Schnorenberg, A. J., Hawi, L., & Slavens, B. A. (2015). Upper extremity joint dynamics and electromyography (EMG) during standard and geared manual wheelchair propulsion. *Proceeding of the 39th Annual Meeting of American Society of Biomechanics*,
- Jahanian, O., Schnorenberg, A. J., & Slavens, B. A. (2016). Evaluation of shoulder joint kinematics and muscle activity during geared and standard manual wheelchair mobility. *Engineering in Medicine and Biology Society (EMBC), 2016 IEEE 38th Annual International Conference of The*, pp. 6162-6165.
- Karmarkar, A., Cooper, R., Liu, H., Connor, S., & Puhlman, J. (2008). Evaluation of pushrim-activated power-assisted wheelchairs using ANSI/RESNA standards. *Archives of Physical Medicine and Rehabilitation; Arch.Phys.Med.Rehabil.*, 89(6), 1191-1198.
- Kaye, H. S., Kang, T., & LaPlante, M. P. (2000). Mobility device use in the united states. disability statistics report 14.
- Kloosterman, M. G., Snoek, G. J., van der Woude, L H, Buurke, J. H., & Rietman, J. S. (2013). A systematic review on the pros and cons of using a pushrim-activated power-assisted wheelchair. *Clinical Rehabilitation*, 27(4), 299-313.
- Kloosterman, M. G., Buurke, J. H., de Vries, W., van der Woude, Lucas HV, & Rietman, J. S. (2015). Effect of power-assisted hand-rim wheelchair propulsion on shoulder load in experienced wheelchair users: A pilot study with an instrumented wheelchair. *Medical Engineering & Physics*, 37(10), 961-968.
- Kloosterman, M. G., Buurke, J. H., Schaake, L., van der Woude, Lucas HV, & Rietman, J. S. (2016). Exploration of shoulder load during hand-rim wheelchair start-up with and without power-assisted propulsion in experienced wheelchair users. *Clinical Biomechanics*, 34, 1-6.
- Kloosterman, M. G., Eising, H., Schaake, L., Buurke, J. H., & Rietman, J. S. (2012). Comparison of shoulder load during power-assisted and purely hand-rim wheelchair propulsion. *Clinical Biomechanics*, 27(5), 428-435.
- Koontz, A. M., Cooper, R. A., Boninger, M. L., & Yang, Y. (2005). A kinetic analysis of manual wheelchair propulsion during start-up on select indoor and outdoor surfaces. *Journal of Rehabilitation Research and Development*, 42(4), 447.
- Mercer, J. L., Boninger, M., Koontz, A., Ren, D., Dyson-Hudson, T., & Cooper, R. (2006). Shoulder joint kinetics and pathology in manual wheelchair users. *Clinical Biomechanics*, 21(8), 781-789.

- Morrow, M. M., Hurd, W. J., Kaufman, K. R., & An, K. (2010). Shoulder demands in manual wheelchair users across a spectrum of activities. *Journal of Electromyography and Kinesiology*, 20(1), 61-67.
- Paralyzed Veterans of America Consortium for Spinal Cord Medicine. (2005). Preservation of upper limb function following spinal cord injury: A clinical practice guideline for health-care professionals. *The Journal of Spinal Cord Medicine*, 28(5), 434-470.
- Requejo, P., Mulroy, S., Haubert, L. L., Newsam, C., Gronley, J., & Perry, J. (2008). Evidence-based strategies to preserve shoulder function in manual wheelchair users with spinal cord injury. *Topics in Spinal Cord Injury Rehabilitation*, 13(4), 86-119.
- van der Woude, L., Veeger, H., Dallmeijer, A., Janssen, T., & Rozendaal, L. (2001). Biomechanics and physiology in active manual wheelchair propulsion. *Medical Engineering & Physics*, 23(10), 713-733.
- van der Woude, Lucas HV, Dallmeijer, A. J., Janssen, T. W., & Veeger, D. (2001). Alternative modes of manual wheelchair ambulation: An overview. *American Journal of Physical Medicine & Rehabilitation*, 80(10), 765-777.
- van der Woude, Lucas HV, de Groot, S., & Janssen, T. W. (2006). Manual wheelchairs: Research and innovation in rehabilitation, sports, daily life and health. *Medical Engineering & Physics*, 28(9), 905-915.

Chapter 4

Glenohumeral Joint Dynamics and Shoulder Muscle Activity During Geared Manual Wheelchair Propulsion on Carpeted Floor in Individuals with Spinal Cord Injury

Introduction

Wheelchairs are one of the most prevalent mobility devices among adult individuals with a disability in the United States, with 90% of all wheelchair users using a manual wheelchair (Kaye, Kang, & LaPlante, 2000). Unfortunately, manual wheelchair use is a physically straining form of mobility, placing wheelchair users at a high risk of repetitive strain injuries (Collinger, Fullerton, Impink, Koontz, & Boninger, 2010; Mercer et al., 2006; van der Woude, Lucas HV, de Groot, & Janssen, 2006).

The environment and surface quality (i.e. carpet) are confounding factors that can affect force, repetition, and velocity during manual wheelchair propulsion (Sawatzky, DiGiovine, Berner, Roesler, & Katte, 2015). The surface rolling resistance has been shown to significantly affect wheelchair biomechanics (Cowan, Nash, Collinger, Koontz, & Boninger, 2009; Hurd, Morrow, Kaufman, & An, 2008; Koontz, Cooper, Boninger, & Yang, 2005). Carpeted floors have higher rolling resistance than the tile surfaces. In addition, the carpeted floor is softer, which results in greater deformation and dissipation of energy at the wheel-floor interface and shorter stroke distances (Hurd et al., 2008; van der Woude, LHV, Veeger, Dallmeijer, Janssen, & Rozendaal, 2001). Therefore, the mechanical stresses from propulsion over carpet are more demanding to the upper limbs than propulsion on a smooth level surface (Hurd et al., 2008; Koontz et al.,

2005). These additional demands may increase the risk of secondary injuries in manual wheelchair users and further deteriorate their function and quality of life.

Among manual wheelchair users with spinal cord injury (SCI), the shoulder is the most common site of pain with prevalence of 30% to 73% (Boninger, Towers, Cooper, Dicianno, & Munin, 2001; Dyson-Hudson & Kirshblum, 2004; van Drongelen et al., 2006). Subacromial impingement is the major contributor to shoulder pain in this population (Bayley, Cochran, & Sledge, 1987; Dyson-Hudson & Kirshblum, 2004). Previous studies have shown that people who experienced higher shoulder forces and moments were more likely to exhibit shoulder pathology (Mercer et al., 2006). High superiorly directed external forces and the increased internal rotation of the glenohumeral joint during manual wheelchair propulsion have been linked to the incidence of shoulder impingement and high prevalence of shoulder pain in manual wheelchair users (Mercer et al., 2006; Morrow, Kaufman, & An, 2011; Zhao et al., 2015). The increased activity of shoulder muscles has been shown to result in high resultant joint forces in the shoulder joint and potentially increase the risk of shoulder injury (Dubowsky, Sisto, & Langrana, 2009). To minimize the injury risk, manual wheelchair users are recommended to maintain an ideal weight, use lightweight wheelchairs, and utilize efficient propulsion techniques (Paralyzed Veterans of America Consortium for Spinal Cord Medicine, 2005). However, these strategies alone cannot decrease the forces and moments which are required for overcoming the rolling resistance during manual wheelchair propulsion over different terrains. Manual wheelchairs with alternative propulsion designs and add-on assistive technologies could alleviate the high demands required for manual wheelchair propulsion. The use of the alternative wheelchair propulsion mechanisms may help to preserve upper limb function and decrease the risk of secondary injuries in manual wheelchair users (Requejo, Philip et al., 2008)

Lever and crank propelled wheelchairs are among the most common alternatives, which allow a more natural position of the hands and shoulders than standard hand-rim propulsion mechanisms. The efficiency of these wheelchairs is higher than standard manual wheelchairs when gearing is included. Therefore, they could be less demanding (Flemmer & Flemmer, 2016; van der Woude et al., 2001; van der Woude, Lucas HV et al., 2006). However, the use of these alternative manual wheelchairs is limited in comparison with standard manual wheelchairs due to disadvantages such as weight, size, and limited maneuverability and being challenging for transfers (Kloosterman, M. G., Snoek, van der Woude, L H, Buurke, & Rietman, 2013; van der Woude, Lucas HV et al., 2006). The pushrim-activated power assist wheelchair is a hybrid between a standard manual wheelchair and a powered wheelchair (Karmarkar, Cooper, Liu, Connor, & Puhlman, 2008). Power assist wheelchairs are one of the more recent wheel technologies, which use the same propulsion techniques as standard manual wheelchairs but equipped with additional assistance. It has been reported that using power assisted manual wheelchairs significantly decreases the hand-rim kinetics, resulting in decreased upper extremity kinetics during start-up and steady state propulsion (Kloosterman et al., 2013; Kloosterman, Marieke GM, Buurke, de Vries, van der Woude, Lucas HV, & Rietman, 2015; Kloosterman, Marieke GM, Buurke, Schaake, van der Woude, Lucas HV, & Rietman, 2016). Using pushrim-activated power assist wheelchairs may decrease the injury risk for manual wheelchair users; however, as the power assist wheelchairs are less friendly for transferring (heavier and larger) and relatively expensive, they are not widely used (Flemmer & Flemmer, 2016).

Geared manual wheelchair wheels are an assistive device that may reduce the biomechanical demands of the upper extremity required for propulsion while maximizing function. Similar to a multi-speed bicycle, geared wheels allow users to choose the option of wheeling in a lower gear

which may make propulsion less demanding for the upper limbs. The use of geared wheels has the potential to preserve the shoulders of manual wheelchair users and allow them to maintain an optimal level of activity and independence necessary for high quality of life. However, current research is lacking on the biomechanical and functional effects of using geared manual wheelchair wheels. Specifically, the investigation of geared wheels in individuals with spinal cord injury on various surfaces for mobility in the home and community. The findings of a longitudinal study with full-time manual wheelchair users indicated shoulder pain reduction with the use of geared wheels (MagicWheels®, gear ratio of 2:1) in comparison to standard wheels (Finley & Rodgers, 2007). Another study investigated the effects of using geared manual wheelchair wheels (MagicWheels®, gear ratio of 2:1) on muscular demand of able-bodied non-wheelchair users during ramp ascent with four different grades (Howarth, Pronovost, Polgar, Dickerson, & Callaghan, 2010). A significant decrease in the peak muscle activity of the shoulder flexors, including the anterior deltoid and pectoralis major, was found during ramp ascent. However, the integrated muscle activity increased significantly, which was mainly due to the notable increase in the ramp ascent duration during the geared wheel condition in comparison to the standard wheel condition (Howarth et al., 2010). Despite these works, the effects of using geared wheels on upper extremity joint dynamics and muscle activity in manual wheelchair users have not yet been investigated.

Decreasing the frequency of the propulsive stroke and minimizing the forces and moments required for wheelchair propulsion could significantly decrease the injury risk in manual wheelchair users (Boninger, Koontz, Sisto, & Dyson-Hudson, 2005). It is expected that using the geared wheels decreases the kinetic loads being applied to the upper limbs during wheelchair

propulsion while decreasing the stroke distance. Thus, the trade-off between the stroke distance and upper limb load will be investigated.

The purpose of this study was to quantitatively elucidate the effects of using geared wheels (IntelliWheels®) on shoulder biomechanics and muscle activity during propulsion on carpeted floor in individuals with SCI. We hypothesized that the glenohumeral joint forces and moments as well as the anterior deltoid and pectoralis major muscle activity would be significantly less during the low gear condition compared to the standard gear condition, and that glenohumeral joint angles would be similar during both conditions.

Methods

This study was approved by the Clement J. Zablocki Veterans Affairs Center and the University of Wisconsin-Milwaukee (UWM) Institutional Review Boards. At the beginning of the data collection session, the study was explained to the participants in layman's terms "the aim of this study is to investigate the effects of using geared wheels on the loads being applied to the upper limbs during manual wheelchair propulsion." All subjects signed the approved informed consent forms prior to participation.

Subjects

The inclusion criteria for subjects were to be between 18 and 70 years old, use a manual wheelchair as the primary mode of mobility, have a minimum of six months experience as a manual wheelchair user, and have the ability to perform independent transfers. Seven (7) veterans with paraplegic SCI who met the inclusion criteria participated in this study. Shoulder pain assessment was administered after clinical examination by the physiatrist at the SCI unit at

the Clement J. Zablocki VA Medical Center using the Wheelchair User’s Shoulder Pain Index (WUSPI; Curtis et al., 1995). Wheelchair propulsion testing was completed at the UWM Mobility Lab. Table 12 provides subjects’ characteristics and their WUSPI scores.

Experimental protocol

Subjects used their personal standard manual wheelchairs equipped with IntelliWheels geared wheels (IntelliWheels, Inc., Champaign, IL), which allowed them to propel in standard gear (gear ratio of 1:1) or shift into a low gear (gear ratio of 1.5:1). Prior to data collection subjects were given 15-30 minutes to be familiarized with the wheels and the experimental protocol. Subjects propelled their wheelchair over an 8-meter, carpeted level floor (padding thickness: 9.5 mm and carpet thickness: 17.5 mm) in both standard gear and low gear conditions, in a random order (Figure 30). The gear was shifted from the standard gear to the low gear or vice versa by the investigator. Subjects were instructed to start propelling their wheelchair from a resting position on the carpet, move up to their self-selected normal speed and to end the trial at the designated finish line on the carpet. Five trials were captured for each condition.

Table 12. Subject characteristics and wheelchair user’s shoulder pain index (WUSPI) total scores.

#	Subject ID	Age (years)	Weight (kg)	Height (cm)	Arm Dominance	SCI level	Years as a wheelchair user	WUSPI total score (cm)
1	5	55	97.7	185	Right	T5	31	21.2
2	6	36	80.2	175	Right	L2	12	8.7
3	8	57	81.2	180	Right	T11	0.6	N/A
4	10	24	71.2	180	Right	T5	2	53.9
5	11	51	112.0	188	Left	T12	30	19.7
6	12	29	93.0	188	Right	T1	10	1.2
7	13	54	136.0	193	Right	T12	36	3.0
Mean ± SD		43.7 ± 13.7	95.9 ± 22.1	184.1 ± 6.1	-----	----- ---	17.3 ± 14.6	18.0 ± 19.5

T#: Thoracic spinal injury level, L#: Lumbar spinal injury level



Figure 30. A subject propelling on a carpeted level floor using the IntelliWheels geared manual wheelchair wheels.

Data collection

Electromyography (EMG) data collection

Muscle activity of the primary shoulder flexors were recorded using surface EMG (Mulroy, Gronley, Newsam, & Perry, 1996; Sabick, Kotajarvi, & An, 2004). Trigno wireless surface electrodes (Delsys, Inc., Natick, MA) with a built-in bandpass filter of 20-450 Hz were used to record EMG data of the anterior deltoid, and the clavicular head of the pectoralis major for the dominant arm. The motion capture system was digitally synchronized with the EMG system and the EMG signals were digitized at a sampling frequency of 2040 Hz using Nexus software (Vicon Motion Systems, Oxford, UK).

Prior to EMG electrode placement, the skin surface underlying each electrode was scrubbed and cleaned with an alcohol preparatory pad. Electrodes were placed over the anterior deltoid



Figure 31. A subject propelling the instrumented geared wheel on a carpeted level floor. The instrumented hand-rim global coordinate system follows the right-hand rule with the positive X -axis anterior, positive Y -axis superior, and positive Z -axis pointing out of the wheel along the axle. The picture also depicts the subject instrumented with the motion capture markers and surface electromyography electrodes.

(anterior aspect of the arm, approximately 4 cm below the clavicle) and clavicular head of the pectoralis major (approximately 2 cm below the clavicle, midway between the underarm and suprasternal notch), (Criswell, 2010). Maximum voluntary isometric contractions (MVIC) were performed for each muscle using an isokinetic BTE PrimusRS (BTE, Hanover, MD) prior to the experimental trials. During the MVIC trials, the subject sat on the BTE chair with their trunk in an upright position and trunk and legs secured to the chair with Velcro straps. Three MVIC trials were performed for each muscle, with contraction durations of 3 seconds; verbal encouragement was provided during each trial by the investigator. The MVIC of the anterior deltoid was tested with the upper arm next to the trunk with 45 degrees of shoulder flexion while resistance was applied posteriorly against the distal end of humerus during isometric shoulder flexion. The

pectoralis major muscle was tested while the upper arm was horizontal and midway between anterior and lateral directions, and the forearm was flexed 90 degrees at the elbow. Resistance was applied laterally against the elbow during isometric shoulder horizontal flexion (Chow, Millikan, Carlton, Morse, & Chae, 2001; Criswell, 2010).

Upper extremity kinematic data collection

Subject-specific measurements including height, weight, and bilateral upper extremity segments lengths and circumferences were obtained. Participants were instrumented with 27 passive retro-reflective markers (Figure 31) on anatomical landmarks of the hands, forearms, upper arms, scapulae, clavicles, and thorax to prepare for motion capture. The markers were placed on the following anatomical locations: spinal process (C7), xiphoid process, suprasternal notch, acromion process, acromial angle, trigonum spinae, scapular spine, acromion angle, scapula inferior angle, coracoid process, humerus, olecranon process, radial styloid, ulnar styloid, third metacarpal, and fifth metacarpal. Four markers were placed on the top corners and the bottom corners of wheelchair back, and one marker was placed on the center of wheel hub (Schnorenberg et al., 2014). Motion data were collected at 120 Hz using a 15-camera Vicon T-series motion capture system (Vicon Motion Systems, Oxford, UK).

Hand-rim kinetics data collection

A custom instrumented geared wheel previously developed and validated (Gaglio, Liang, Daigle, & Hsiao-Wecksler, 2016; Gaglio et al., 2017) was mounted to the wheelchair on the subject's dominant side to measure hand-rim kinetics during propulsion (Figure 31). A non-instrumented IntelliWheels geared wheel, with the same geometry and inertia as the instrumented geared wheel was mounted on the opposite side. Hand-rim kinetics and kinematic data were collected at 120 Hz and transferred wirelessly via Bluetooth.

Rate of perceived exertion

At the end of each test condition, the rate of perceived exertion was measured using the Borg 6-20 scale (Borg, 1998). Borg 6-20 is a subjective rating scale that has been used as a valid method for rating perceived exertion and measuring exercise intensity in people with SCI and manual wheelchair users (Goosey-Tolfrey et al., 2010; Ward, Bar-Or, Longmuir, & Smith, 1995).

Data processing

Hand-rim kinetics and stroke cycle characteristics

Hand-rim data were filtered with a 4th-order, low-pass Butterworth filter with a 20 Hz cutoff frequency. The three components of the applied hand-rim force, the propulsive moment about the hub, and the hand-rim angular position during each trial were used for calculating the hand-rim biomechanics metrics of interest. These metrics included the resultant force and propulsive moment, and the stroke cycle characteristics which are the stroke time, stroke distance, push time (expressed as percentage of stroke time), and linear velocity. The stroke cycle was divided into the push and recovery phases using the propulsive moment. The first two and the last strokes of each trial were excluded to eliminate acceleration and deceleration effects. The remaining stroke cycles, representing semi-steady state propulsion, were used for analysis. The stroke distance and linear velocity were determined from the hand-rim angular position data for each stroke cycle. The resultant force was determined by vector sum of the three component forces of the hand-rim forces during the push phase. The normalized stroke cycle frequency was calculated as the ratio of stroke cycle frequency (1/stroke cycle time) to the stroke distance, which indicates the number of stroke cycles required to propel one meter. The integrated hand-rim resultant force was calculated based on the area under the resultant force time graph during one stroke cycle. The

integrated hand-rim propulsive moment was calculated in an analogous way. The normalized integrated hand-rim resultant force and propulsive moment were computed by dividing the integrated hand-rim resultant force and propulsive moment by the stroke distance.

Glenohumeral joint dynamics

Upper extremity kinematic data were processed using Nexus software. The marker trajectories were filtered using a Woltring filter with a mean squared error of 20 (Woltring, 1986). The three components of the applied hand-rim forces and moments as well as the marker trajectories were used to calculate the upper extremity joint dynamics during wheelchair propulsion. Schnorenberg model for pediatric wheelchair mobility (Schnorenberg et al., 2014) was modified to be used in an adult population. The mass and segment center of mass location of the hands, forearms and upper arms, were calculated using the equations developed for an adult population (Winter, 2009). Segment inertias for each subject were calculated using the regression equations for adult population (Yeadon & Morlock, 1989). The modified inverse dynamics model was used to calculate 3-D glenohumeral joint angles, forces, and moments.

The glenohumeral joint resultant force and resultant moment were determined by the vector sum of the three component glenohumeral forces and moments during the push phase. The integrated glenohumeral resultant force was calculated as the area under the resultant force-time graph during one stroke cycle. The integrated glenohumeral joint moment was calculated in an analogous way. The normalized integrated glenohumeral joint resultant force and moment during the push phase were computed by dividing the integrated glenohumeral joint resultant force and moment by the stroke distance.

Electromyography

The raw EMG signals were full wave rectified and smoothed using a root mean square (RMS) algorithm with a time averaging period of 25 milliseconds. The RMS envelope of the EMG data was used to determine the onset and end of an EMG burst. The detection threshold was defined as the mean of the baseline plus three standard deviations. The onset of an EMG burst was then defined as the time when the signal amplitude rose above the detection threshold and remained above it for at least 30 ms. The end of an EMG burst was defined as the time when the signal amplitude fell below the detection threshold and remained below it for at least 50 ms (Beres-Jones & Harkema, 2004; Hodges & Bui, 1996). Visual examination was also performed for verification and if necessary, the detection threshold was modified by adding or subtracting one standard deviation.

The RMS envelope of the MVIC trials were smoothed with an averaging filter with the time averaging period of 500 milliseconds. The MVIC value for each muscle was calculated as the average of the peak value of the three MVIC trials. The RMS envelope for each muscle during wheelchair propulsion trials were normalized to the percentage of the MVIC obtained from each respective muscle.

The normalized EMG signals were used to determine the peak EMG during the burst duration and the integrated EMG over each stroke cycle using MATLAB software (R2017a; The MathWorks, Inc., Natick, Massachusetts, United States). The normalized integrated muscle activity was calculated by dividing the integrated muscle activity by the distance traveled per stroke cycle.

Data and statistical analysis

All subjects performed the experiments according to the experimental protocol. All subjects had a complete data set except for one subject lacking EMG data of the anterior deltoid muscle. Subject's mean glenohumeral joint dynamics were calculated by averaging the values of at least seven stroke cycles for each condition, except for one subject during the standard gear condition which had just one stroke cycle.

To test the respective research hypotheses, the differences between the stroke cycle characteristics, peak hand-rim kinetics, peak glenohumeral joint dynamics during the push phase, shoulder flexor muscle activity were compared across gear conditions. To investigate the difference of using the geared wheels versus standard wheels, the combined metrics including the normalized integrated hand-rim resultant forces and propulsive moment, the normalized integrated glenohumeral resultant force and moment, and the normalized integrated muscle activity for the anterior deltoid and pectoralis major were compared across gear conditions. Because of the sample size and since the data did not have a normal distribution the differences of the dependent variables across gear conditions were analyzed using separate Wilcoxon Signed-Rank tests, and test statistics z , significance (p), and effect size (r) were reported for each metric. The effect size was calculated as the ratio of the z -value to the square root of the number of observations (number of subjects times two). Statistical analyses were done in SPSS 25 and a p -value less than 0.05 was considered statistically significant.

Results

Group mean values and the statistical results for the temporal-spatial parameters and the rate of perceived exertion for both gear conditions are reported in Table 13. The group mean results for the hand-rim kinetics are reported in Tables 15,16. The group mean joint angles, forces, and moments of the glenohumeral joint were characterized in all three planes of motion over the wheelchair stroke cycle (Figure 32). The group mean sternoclavicular and acromioclavicular joint angles in all three planes of motion are depicted in Figure 33. The group mean peak glenohumeral joint angles (Table 14), joint forces (Table 15), and joint moments (Table 16) were also calculated. The group mean values and the statistical results for the shoulder flexor muscles' peak and integrated activity are depicted in Figure 34. The box plot graphs combined with the individual measurements for the metrics significantly affected by the gear condition are depicted in Figures 35-37. The results for the combined metrics are reported in Table 17.

The average propulsion speed, stroke distance, and normalized stroke cycle frequency were all significantly less during the low gear condition than the standard gear condition (Table 13). The perceived exertion reduced significantly from a hard task (15 Borg scale) during the standard gear condition to a relatively light task (11.6 Borg scale) during the low gear condition (Table 13). The peak hand-rim resultant force and propulsive moment decreased significantly by 17% and 22%, respectively.

The peak glenohumeral joint angles in all planes of motion were similar during both conditions (Figure 32, Table 14). Using the geared wheel in lower gear condition was not significantly effective on the kinematics of sternoclavicular and acromioclavicular joints during wheelchair propulsion (Figure 33).

The peak glenohumeral anterior, inferior and medial forces as well as flexion, adduction, and internal rotation moments occurred during the push phase for both wheel conditions (Figure 32, Tables 15, 16). The peak glenohumeral inferior force significantly decreased by 26% and flexion moment decreased significantly by 33% during the low gear condition compared with the standard gear condition (Tables 15, 16).

The anterior deltoid and pectoralis major peak muscle activity decreased by 31% and 35%, respectively, during low gear condition (Figure 34). The anterior deltoid and pectoralis major integrated muscle activity decreased by 30% (Figure 34); however, the normalized integrated muscle activity was not significantly different for either of the shoulder flexors between the gear conditions (Figure 34).

The box plot graphs combined with the individual measurements (Figures 35-37) indicate that for the kinetic and muscle activity metrics which their group means were significantly decreased during the low gear condition in comparison to the standard gear condition, majority of subjects individually follow the group trends.

The results for the combined metrics (Table 17) demonstrate that using the geared wheels in the low gear condition significantly decreased the hand-rim normalized integrated propulsive moment by 15%. However, the other combined metrics were not significantly affected by the gear condition.

Table 13. Group mean temporal-spatial parameters and rate of perceived exertion for the standard gear and low gear conditions.

	Standard Gear	Low Gear	Statistical Results		
	Mean \pm SD	Mean \pm SD	<i>z</i>	<i>p</i>	<i>r</i>
Stroke Distance (m)	0.98 \pm 0.21	0.77 \pm 0.15	2.37	0.018*	0.63
Push Time (%)	53.51 \pm 3.44	49.14 \pm 2.94	1.86	0.063	0.50
Speed (m/s)	0.95 \pm 0.11	0.76 \pm 0.12	2.37	0.018*	0.63
Stroke Cycle Frequency (Hz)	0.99 \pm 0.17	1.03 \pm 0.23	1.18	0.237	0.32
Normalized Stroke Cycle Frequency (1/m.s)	1.11 \pm 0.51	1.47 \pm 0.76	2.37	0.018*	0.63
Rate of perceived exertion	15.0 \pm 1.5	11.6 \pm 1.9	2.37	0.018*	0.63

z = test statistics; *p* = significance level; *r* = effect size; *: *p* < 0.05.

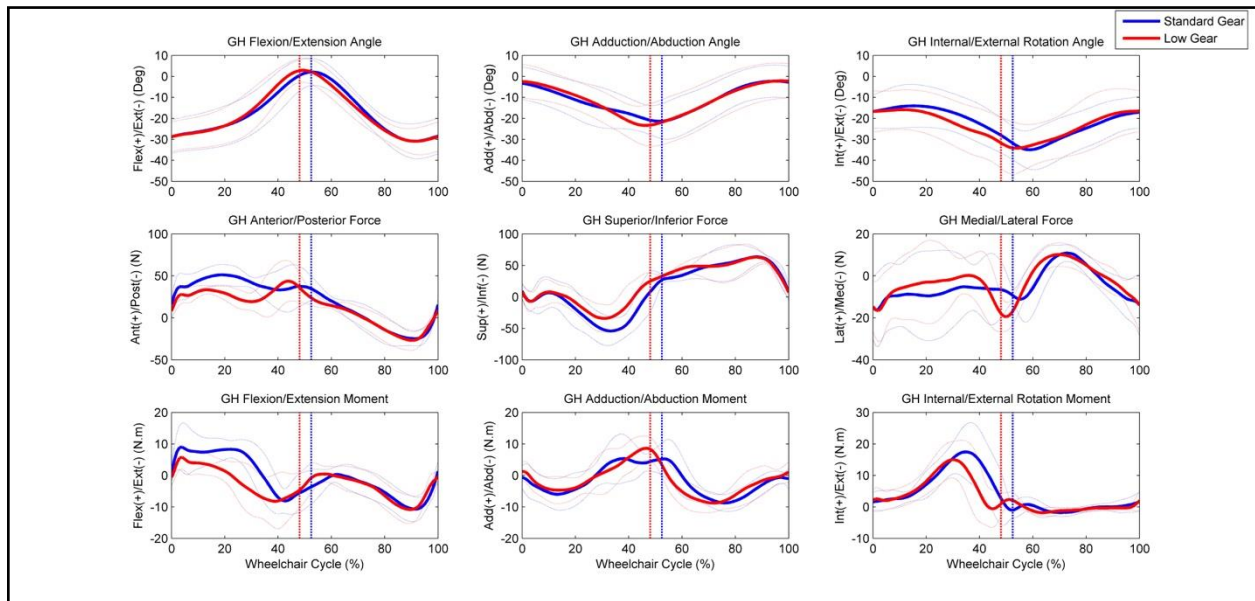


Figure 32. Three-dimensional glenohumeral joint angles, forces and moments. Group mean profiles (solid line) \pm one standard deviation (dotted line) of seven subjects (dominant side) for the standard gear and low gear conditions are depicted. The vertical dash-dot lines indicate the transition from the end of the push phase to the start of the recovery phase for each condition.

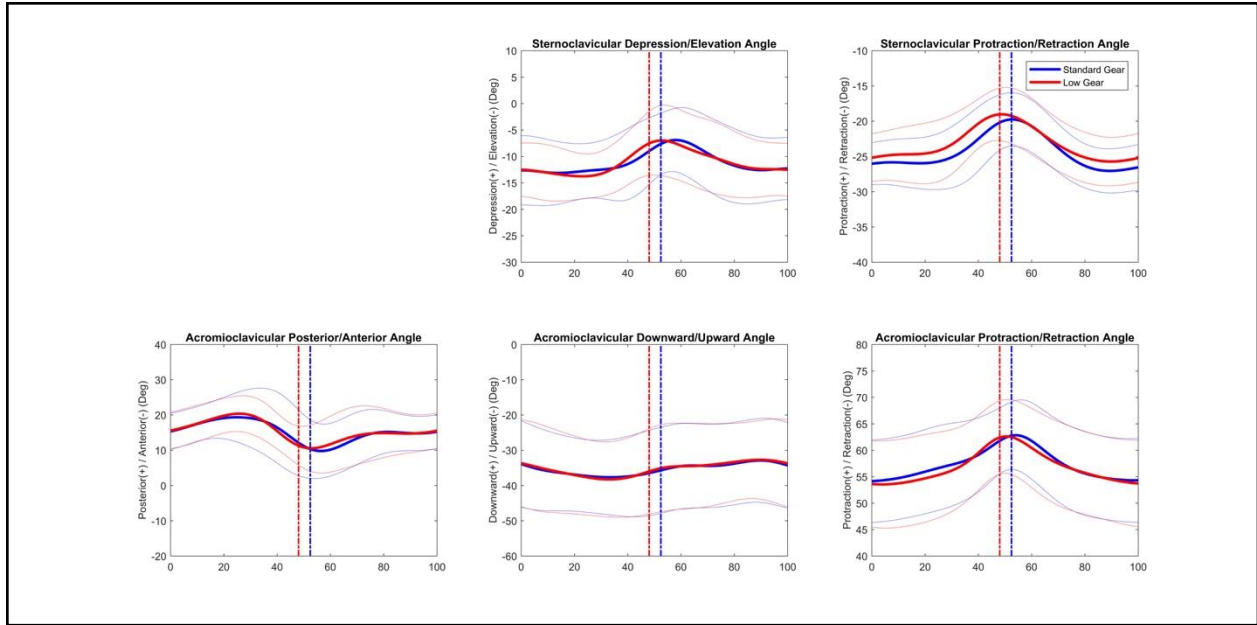


Figure 33. Three-dimensional sternoclavicular (top row) and acromioclavicular (bottom row) joint angles. Group mean profiles (solid line) +/- one standard deviation (dotted line) of seven subjects (dominant side) for the standard gear and low gear conditions are depicted. The vertical dash-dot lines indicate the transition from the end of the push phase to the start of the recovery phase for each condition.

Table 14. Group mean peak glenohumeral joint kinematics for the standard gear and low gear conditions.

		Standard Gear	Low Gear	Statistical Results		
		Mean \pm SD	Mean \pm SD	<i>z</i>	<i>p</i>	<i>r</i>
Sagittal Plane	Max Flexion	3.7 \pm 6.4	4.3 \pm 5.4	0.68	0.499	0.18
	Max Extension	31.4 \pm 7.7	31.7 \pm 6.4	0.17	0.866	0.05
Coronal Plane	Min Abduction	1.5 \pm 7.5	1.25 \pm 8.4	0.68	0.499	0.18
	Max Abduction	23.5 \pm 9.0	24.4 \pm 9.5	1.02	0.310	0.27
Transverse Plane	Min Ext. Rotation	12.6 \pm 9.6	13.4 \pm 10.6	1.18	0.237	0.32
	Max Ext. Rotation	36.5 \pm 9.0	36.7 \pm 10.6	0.17	0.866	0.05

z = test statistics; *p* = significance level; *r* = effect size; *: *p* < 0.05.

Table 15. Group mean peak hand-rim (HR) resultant force and peak glenohumeral (GH) joint forces during push phase for the standard gear and low gear conditions.

	Standard Gear	Low Gear	Statistical Results		
	Mean \pm SD	Mean \pm SD	<i>z</i>	<i>p</i>	<i>r</i>
Peak HR Resultant Force (N)	125.4 \pm 25.5	104.2 \pm 25.1	2.37	0.018*	0.63
Peak GH Anterior Force (N)	63.0 \pm 15.8	59.1 \pm 22.1	1.18	0.237	0.32
Peak GH Inferior Force (N)	74.3 \pm 16.5	54.9 \pm 15.4	2.03	0.043*	0.54
Peak GH Medial Force (N)	28.7 \pm 10.2	28.8 \pm 9.6	0.34	0.735	0.09

z = test statistics; *p* = significance level; *r* = effect size; *: *p* < 0.05.

Table 16. Group mean peak hand-rim (HR) propulsive moment and peak glenohumeral (GH) joint moments during push phase for the standard gear and low gear conditions.

	Standard Gear	Low Gear	Statistical Results		
	Mean \pm SD	Mean \pm SD	<i>z</i>	<i>p</i>	<i>r</i>
Peak HR Propulsive Moment (N · m)	29.2 \pm 4.3	22.8 \pm 3.9	2.37	0.018*	0.63
Peak GH Flexion Moment (N · m)	13.9 \pm 6.3	9.3 \pm 3.4	2.37	0.018*	0.63
Peak GH Adduction Moment (N · m)	13.1 \pm 3.12	12.8 \pm 3.9	0.51	0.612	0.14
Peak GH Internal Rotation Moment (N · m)	22.8 \pm 6.9	19.9 \pm 5.5	1.69	0.091	0.45

z = test statistics; *p* = significance level; *r* = effect size; *: *p* < 0.05.

Table 17. Group mean hand-rim (HR) normalized integrated resultant force and propulsive moment, and group mean glenohumeral (GH) normalized integrated resultant force and resultant moment during push phase for the standard gear and low gear conditions.

	Standard Gear	Low Gear	Statistical Results		
	Mean \pm SD	Mean \pm SD	<i>z</i>	<i>p</i>	<i>r</i>
HR Normalized Integrated Resultant Force ([N] · s/m)	45.4 \pm 10.3	42.9 \pm 9.3	0.85	0.398	0.22
HR Normalized Integrated Propulsive Moment ([N · m] · s/m)	10.3 \pm 2.0	8.7 \pm 1.4	2.20	0.028*	0.58
GH Normalized Integrated Resultant Force ([N] · s/m)	34.0 \pm 8.1	29.8 \pm 7.6	1.69	0.091	0.45
GH Normalized Integrated Resultant Moment ([N · m] · s/m)	8.0 \pm 2.1	8.3 \pm 1.9	0.51	0.612	0.13

z = test statistics; *p* = significance level; *r* = effect size; *: *p* < 0.05.

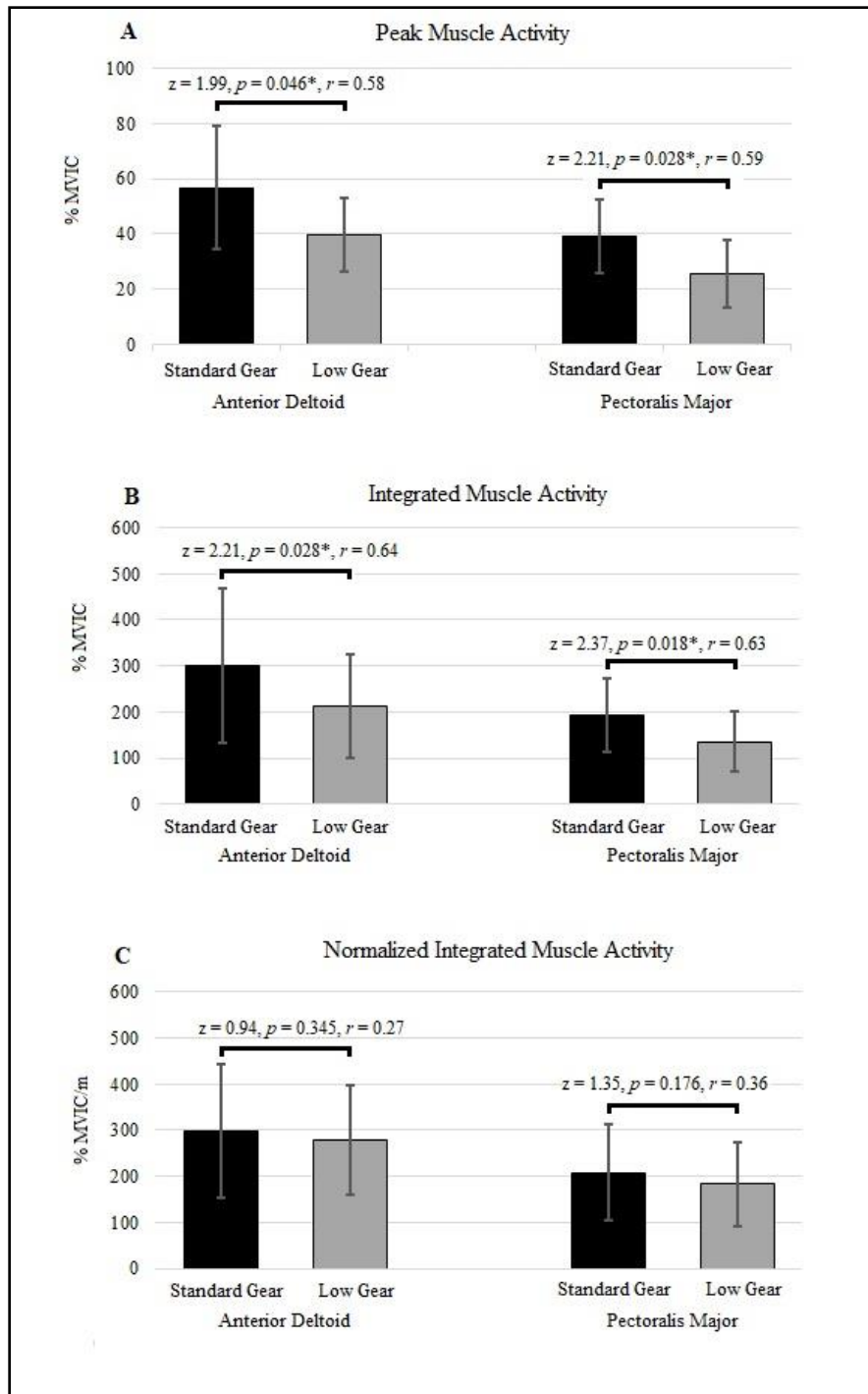


Figure 34. (A-C) Muscle activity of the anterior deltoid and pectoralis major muscles during manual wheelchair propulsion. (A) Group mean peak muscle activity, (B) integrated muscle activity, and (C) normalized integrated activity of the anterior deltoid and pectoralis major during the stroke cycle of the standard gear and low gear conditions. Error bars indicate the standard deviations as reported as percent of maximum voluntary isometric contraction (MVIC) for the peak and integrated muscle activity and as percent of maximum voluntary contraction per meter (%MVIC/m) for the normalized integrated muscle activity. Statistical results (z = test statistics; p = significance level; r = effect size; *: $p < 0.05$) are reported for each muscle.

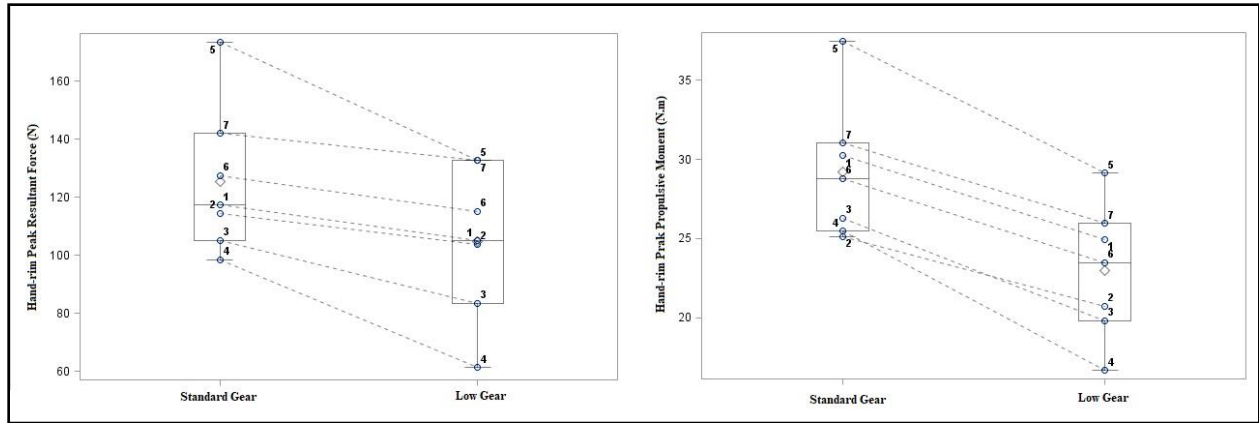


Figure 35. Peak hand-rim resultant force (left) and peak hand-rim propulsive moment (right). The bottom and top edges of the box indicate the intra-quartile range between the first and third quartiles (25th and 75th percentiles). The diamond inside the box indicates the mean value. The line inside the box indicates the median value. The whiskers that extend from each box indicate the entire range of values. The metrics for each subject are shown with a circle and the corresponding subject number.

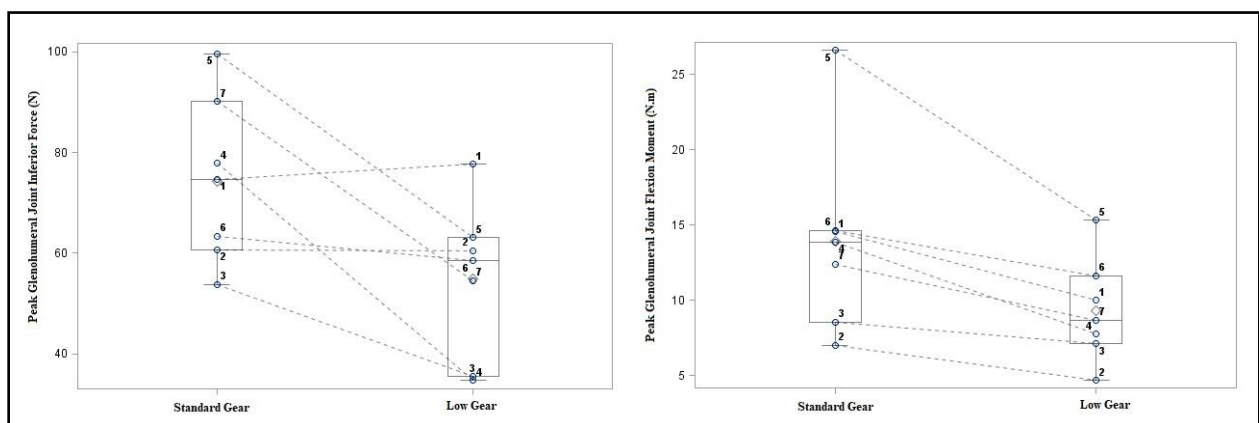


Figure 36. Peak glenohumeral joint inferior force (left) and peak glenohumeral joint flexion moment (right). The bottom and top edges of the box indicate the intra-quartile range between the first and third quartiles (25th and 75th percentiles). The diamond inside the box indicates the mean value. The line inside the box indicates the median value. The whiskers that extend from each box indicate the entire range of values. The metrics for each subject are shown with a circle and the corresponding subject number.

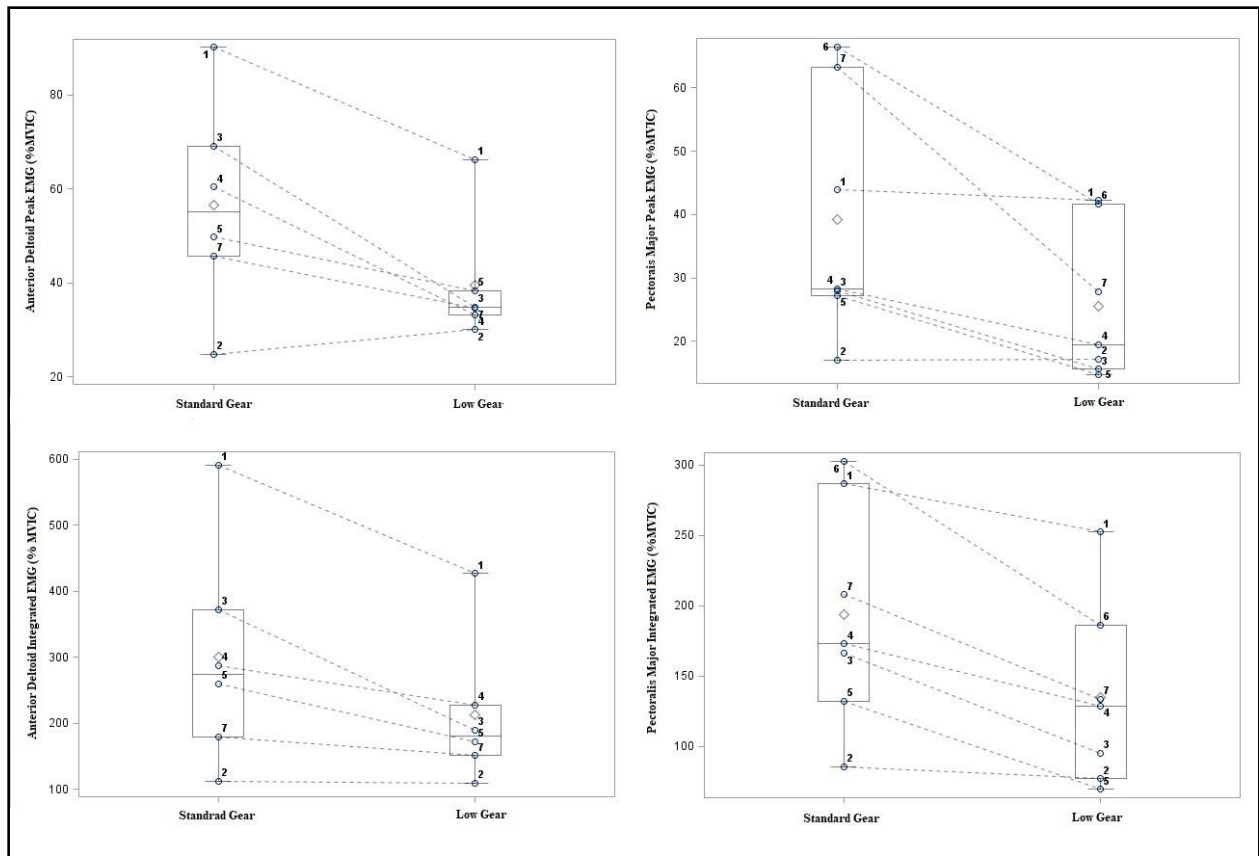


Figure 37. Peak glenohumeral joint inferior force (left) and peak glenohumeral joint flexion moment (right). The bottom and top edges of the box indicate the intra-quartile range between the first and third quartiles (25th and 75th percentiles). The diamond inside the box indicates the mean value. The line inside the box indicates the median value. The metrics for each subject are shown with a circle and the corresponding subject number.

Discussion

We successfully characterized the spatiotemporal parameters, glenohumeral joint dynamics, and shoulder muscle activity during geared manual wheelchair propulsion on a carpeted floor in veterans with SCI. Similar to previous studies, we found that high hand-rim kinetics occur during manual wheelchair propulsion (standard gear) on carpeted floor (Hurd et al., 2008; Koontz et al., 2005). The results for the propulsion speed and hand-rim kinetics during the standard gear

condition were similar to previously reported values for standard manual wheelchair propulsion on high-pile carpet (Koontz et al., 2005). As expected, the glenohumeral joint forces and moments during manual wheelchair propulsion in the standard gear condition on carpet were notably higher than the values previously reported for shoulder joint kinetics during the push phase of standard manual wheelchair propulsion at self-selected speed (Kulig et al., 1998; Mercer et al., 2006; Requejo, Philip Santos et al., 2015).

Consistent with the hypotheses, using the geared wheels in the low gear condition significantly decreased the glenohumeral inferior force and flexion moment as well as the peak and integrated muscle activity of the anterior deltoid and pectoralis major muscles during propulsion on a carpeted floor. The gear condition did not significantly affect the triaxial glenohumeral joint angles during manual wheelchair propulsion on carpeted floor, which were similar during both conditions.

The glenohumeral joint normalized integrated resultant force and moment and shoulder flexors normalized integrated muscle activity were not significantly affected by the gear condition. This indicates that the shoulder demands did not significantly decrease with the use of geared wheels in the lower gear condition for propulsion on carpeted floor. The results of this study indicate that propulsion on carpeted floor in the low gear condition was accompanied by a reduced perception of effort as compared to the standard gear condition.

The results of the hand-rim kinetics indicated that using the geared wheels in the low gear condition requires significantly less amount of hand-rim forces and moments. This finding combined with the observed results for the shoulder muscle activity and glenohumeral joint kinetics prove that manual wheelchair propulsion on carpeted floor in low gear condition is less demanding than the standard gear condition. The individual measurements also indicate that all

or a pronounced majority of subjects individually followed the group trends. The significant decrease in the glenohumeral joint kinetics and specifically the significant reduction of the peak axial forces during the push phase could decrease the risk of subacromial impingement during wheelchair propulsion on carpeted floor (Mercer et al., 2006).

The shoulder biomechanics findings during the low gear condition demonstrate that the reduction in the peak glenohumeral joint inferior force (26%) and flexion moment (33%) was similar to the percent of reduction in the muscle activity of the shoulder flexors (30% - 35%). This is consistent with the percent of gear reduction (33%) in the low gear condition compared to the standard gear condition.

The significant decrease in propulsion speed during the low gear condition is primarily attributed to the significant reduction in the stroke distance. This was a direct effect of the gear reduction and a trade-off for the significant decrease in the shoulder kinetics and muscle activity. The significant increase in the normalized stroke cycle frequency during the low gear condition demonstrate that for a given distance, a higher number of stroke cycles are required. High-repetition of upper extremity joint motions have been significantly related to increased risk of upper limb injuries in manual wheelchair users (Boninger et al., 2005; Requejo et al., 2008).

Combined metrics, such as the normalized integrated resultant force and moment, and the normalized integrated muscle activity indicate the total force and moment (impulse), and total muscle activity which is required for propelling the wheelchair along a specific distance.

Quantification of these metrics provides a comprehensive characterization of the impact that the geared wheel system has on upper extremity biomechanics. In this study, the glenohumeral joint normalized integrated resultant force and moment, and the shoulder flexors normalized integrated muscle activity were not significantly different between the standard gear and low

gear conditions. This might indicate that although a higher number of stroke cycles are required for travelling a given distance in the low gear condition than the standard gear condition, the low gear condition is not more demanding than the standard gear condition.

The significant differences in the hand-rim kinetics, glenohumeral joint kinetics, and shoulder muscle activity observed between the low gear and standard gear conditions indicate the potential benefits of using the geared manual wheelchair wheels for propulsion on carpeted floor. Previous studies have indicated that significantly higher hand-rim forces and moments are necessary to overcome the greater rolling resistance of carpeted floor compared to a hard floor (e.g. tile terrain), which could increase the upper extremity joint loading during propulsion and lead to secondary injuries (Hurd et al., 2008; Koontz et al., 2005). The geared wheels have proven to significantly decrease these joint forces and moments, which may ultimately reduce the risk of musculoskeletal injuries common in wheelchair users (Boninger et al., 2005; Mercer et al., 2006; Requejo et al., 2008). Future applications of this geared wheel technology may prove to be beneficial for manual wheelchair users during the start-up phase in addition to carpet, ramps, and uneven terrain.

Conclusion

Shoulder biomechanics during geared manual wheelchair propulsion on carpeted floor were quantified in this study. Overall, the use of the geared manual wheelchair wheels in the low gear condition significantly decreased the peak hand-rim and glenohumeral joint forces and moments during push phase along with the peak and integrated muscle activity of the shoulder flexor muscles. The propulsion speed decreased, and normalized stroke frequency increased significantly. The current investigation suggests that using the geared wheels may be beneficial

for manual wheelchair users to have independent mobility on carpeted floor in their home and community, which may ultimately lead to a reduction of secondary upper extremity musculoskeletal injuries. Further investigation of the association among hand-rim biomechanics, joint dynamics, muscle activity and energetics in a larger population of manual wheelchair users is warranted to elucidate the effects of using geared wheelchair wheels during propulsion over different ground conditions and mobility tasks.

References

- Bayley, J. C., Cochran, T. P., & Sledge, C. B. (1987). The weight-bearing shoulder. the impingement syndrome in paraplegics. *The Journal of Bone and Joint Surgery.American Volume*, 69(5), 676-678.
- Beres-Jones, J. A., & Harkema, S. J. (2004). The human spinal cord interprets velocity-dependent afferent input during stepping. *Brain*, 127(10), 2232-2246.
- Boninger, M. L., Koontz, A. M., Sisto, S. A., & Dyson-Hudson, T. A. (2005). Pushrim biomechanics and injury prevention in spinal cord injury: Recommendations based on CULP-SCI investigations. *Journal of Rehabilitation Research and Development*, 42(3), 9.
- Boninger, M. L., Towers, J. D., Cooper, R. A., Dicianno, B. E., & Munin, M. C. (2001). Shoulder imaging abnormalities in individuals with paraplegia. *Journal of Rehabilitation Research and Development*, 38(4), 401.
- Borg, G. (1998). *Borg's perceived exertion and pain scales*. Human kinetics.
- Chow, J. W., Millikan, T. A., Carlton, L. G., Morse, M. I., & Chae, W. S. (2001). Biomechanical comparison of two racing wheelchair propulsion techniques. *Medicine and Science in Sports and Exercise*, 33(3), 476-484.
- Collinger, J. L., Fullerton, B., Impink, B. G., Koontz, A. M., & Boninger, M. L. (2010). Validation of grayscale-based quantitative ultrasound in manual wheelchair users: Relationship to established clinical measures of shoulder pathology. *American Journal of Physical Medicine & Rehabilitation*, 89(5), 390-400.
- Cowan, R. E., Nash, M. S., Collinger, J. L., Koontz, A. M., & Boninger, M. L. (2009). Impact of surface type, wheelchair weight, and axle position on wheelchair propulsion by novice older adults. *Archives of Physical Medicine and Rehabilitation*, 90(7), 1076-1083.
- Criswell, E. (2010). *Cram's introduction to surface electromyography* Jones & Bartlett Publishers.
- Curtis, K., Roach, K., Applegate, E. B., Amar, T., Benbow, C., Genecco, T., et al. (1995). Development of the wheelchair user's shoulder pain index (WUSPI). *Spinal Cord*, 33(5), 290-293.
- Dubowsky, S. R., Sisto, S. A., & Langrana, N. A. (2009). Comparison of kinematics, kinetics, and EMG throughout wheelchair propulsion in able-bodied and persons with paraplegia: An integrative approach. *Journal of Biomechanical Engineering*, 131(2), 021015.
- Dyson-Hudson, T. A., & Kirshblum, S. C. (2004). No title. *Shoulder Pain in Chronic Spinal Cord Injury, Part 1: Epidemiology, Etiology, and Pathomechanics*,

- Finley, M. A., & Rodgers, M. M. (2007). Effect of 2-speed geared manual wheelchair propulsion on shoulder pain and function. *Archives of Physical Medicine and Rehabilitation*, 88(12), 1622-1627.
- Flemmer, C. L., & Flemmer, R. C. (2016). A review of manual wheelchairs. *Disability and Rehabilitation: Assistive Technology*, 11(3), 177-187.
- Gaglio, A., Daigle, S., Gacek, E., Jahanian, O., Slavens, B., Rice, I., et al. (2017). Validation of an instrumented wheelchair hand rim. *2017 Design of Medical Devices Conference*, pp. V001T05A012.
- Gaglio, A., Liang, J., Daigle, S., & Hsiao-Weckslar, E. (2016). Design of a universal instrumented wheelchair hand rim. *Journal of Medical Devices*, 10(3), 030956.
- Goosey-Tolfrey, V., Lenton, J., Goddard, J., Oldfield, V., Tolfrey, K., & Eston, R. (2010). Regulating intensity using perceived exertion in spinal cord-injured participants. *Medicine & Science in Sports & Exercise*, 42(3), 608-613.
- Hodges, P. W., & Bui, B. H. (1996). A comparison of computer-based methods for the determination of onset of muscle contraction using electromyography. *Electroencephalography and Clinical Neurophysiology/Electromyography and Motor Control*, 101(6), 511-519.
- Howarth, S. J., Pronovost, L. M., Polgar, J. M., Dickerson, C. R., & Callaghan, J. P. (2010). Use of a geared wheelchair wheel to reduce propulsive muscular demand during ramp ascent: Analysis of muscle activation and kinematics. *Clinical Biomechanics*, 25(1), 21-28.
- Hurd, W. J., Morrow, M. M., Kaufman, K. R., & An, K. (2008). Biomechanic evaluation of upper-extremity symmetry during manual wheelchair propulsion over varied terrain. *Archives of Physical Medicine and Rehabilitation*, 89(10), 1996-2002.
- Karmarkar, A., Cooper, R., Liu, H., Connor, S., & Puhlman, J. (2008). Evaluation of pushrim-activated power-assisted wheelchairs using ANSI/RESNA standards. *Archives of Physical Medicine and Rehabilitation; Arch.Phys.Med.Rehabil.*, 89(6), 1191-1198.
- Kaye, H. S., Kang, T., & LaPlante, M. P. (2000). Mobility device use in the united states. disability statistics report 14.
- Kloosterman, M. G., Snoek, G. J., van der Woude, L H, Buurke, J. H., & Rietman, J. S. (2013). A systematic review on the pros and cons of using a pushrim-activated power-assisted wheelchair. *Clinical Rehabilitation*, 27(4), 299-313.
- Kloosterman, M. G., Buurke, J. H., de Vries, W., van der Woude, Lucas HV, & Rietman, J. S. (2015). Effect of power-assisted hand-rim wheelchair propulsion on shoulder load in experienced wheelchair users: A pilot study with an instrumented wheelchair. *Medical Engineering & Physics*, 37(10), 961-968.

- Kloosterman, M. G., Buurke, J. H., Schaake, L., van der Woude, Lucas HV, & Rietman, J. S. (2016). Exploration of shoulder load during hand-rim wheelchair start-up with and without power-assisted propulsion in experienced wheelchair users. *Clinical Biomechanics*, *34*, 1-6.
- Koontz, A. M., Cooper, R. A., Boninger, M. L., & Yang, Y. (2005). A kinetic analysis of manual wheelchair propulsion during start-up on select indoor and outdoor surfaces. *Journal of Rehabilitation Research and Development*, *42*(4), 447.
- Kulig, K., Rao, S. S., Mulroy, S. J., Newsam, C. J., Gronley, J. K., Bontrager, E. L., et al. (1998). Shoulder joint kinetics during the push phase of wheelchair propulsion. *Clinical Orthopaedics and Related Research*®, *354*, 132-143.
- Mercer, J. L., Boninger, M., Koontz, A., Ren, D., Dyson-Hudson, T., & Cooper, R. (2006). Shoulder joint kinetics and pathology in manual wheelchair users. *Clinical Biomechanics*, *21*(8), 781-789.
- Morrow, M. M., Kaufman, K. R., & An, K. (2011). Scapula kinematics and associated impingement risk in manual wheelchair users during propulsion and a weight relief lift. *Clinical Biomechanics*, *26*(4), 352-357.
- Mulroy, S. J., Gronley, J. K., Newsam, C. J., & Perry, J. (1996). Electromyographic activity of shoulder muscles during wheelchair propulsion by paraplegic persons. *Archives of Physical Medicine and Rehabilitation*, *77*(2), 187-193.
- Paralyzed Veterans of America Consortium for Spinal Cord Medicine. (2005). Preservation of upper limb function following spinal cord injury: A clinical practice guideline for health-care professionals. *The Journal of Spinal Cord Medicine*, *28*(5), 434-470.
- Requejo, P. S., Mulroy, S. J., Ruparel, P., Hatchett, P. E., Haubert, L. L., Eberly, V. J., et al. (2015). Relationship between hand contact angle and shoulder loading during manual wheelchair propulsion by individuals with paraplegia. *Topics in Spinal Cord Injury Rehabilitation*, *21*(4), 313-324.
- Requejo, P., Mulroy, S., Haubert, L. L., Newsam, C., Gronley, J., & Perry, J. (2008). Evidence-based strategies to preserve shoulder function in manual wheelchair users with spinal cord injury. *Topics in Spinal Cord Injury Rehabilitation*, *13*(4), 86-119.
- Sabick, M. B., Kotajarvi, B. R., & An, K. (2004). A new method to quantify demand on the upper extremity during manual wheelchair propulsion. *Archives of Physical Medicine and Rehabilitation*, *85*(7), 1151-1159.
- Sawatzky, B., DiGiovine, C., Berner, T., Roesler, T., & Katte, L. (2015). The need for updated clinical practice guidelines for preservation of upper extremities in manual wheelchair users: A position paper. *American Journal of Physical Medicine & Rehabilitation*, *94*(4), 313-324.

- Schnorenberg, A. J., Slavens, B. A., Wang, M., Vogel, L. C., Smith, P. A., & Harris, G. F. (2014). Biomechanical model for evaluation of pediatric upper extremity joint dynamics during wheelchair mobility. *Journal of Biomechanics*, 47(1), 269-276.
- van der Woude, L., Veeger, H., Dallmeijer, A., Janssen, T., & Rozendaal, L. (2001). Biomechanics and physiology in active manual wheelchair propulsion. *Medical Engineering & Physics*, 23(10), 713-733.
- van der Woude, Lucas HV, de Groot, S., & Janssen, T. W. (2006). Manual wheelchairs: Research and innovation in rehabilitation, sports, daily life and health. *Medical Engineering & Physics*, 28(9), 905-915.
- van Drongelen, S., De Groot, S., Veeger, H., Angenot, E., Dallmeijer, A., Post, M., et al. (2006). Upper extremity musculoskeletal pain during and after rehabilitation in wheelchair-using persons with a spinal cord injury. *Spinal Cord*, 44(3), 152.
- Ward, D. S., Bar-Or, O., Longmuir, P., & Smith, K. (1995). Use of rating of perceived exertion (RPE) to prescribe exercise intensity for wheelchair-bound children and adults. *Pediatric Exercise Science*, 7(1), 94-102.
- Winter, D. A. (2009). *Biomechanics and motor control of human movement* John Wiley & Sons.
- Woltring, H. J. (1986). A fortran package for generalized, cross-validatory spline smoothing and differentiation. *Advances in Engineering Software* (1978), 8(2), 104-113.
- Yeadon, M. R., & Morlock, M. (1989). The appropriate use of regression equations for the estimation of segmental inertia parameters. *Journal of Biomechanics*, 22(6-7), 683-689.
- Zhao, K. D., Van Straaten, M. G., Cloud, B. A., Morrow, M. M., An, K. N., & Ludewig, P. M. (2015). Scapulothoracic and glenohumeral kinematics during daily tasks in users of manual wheelchairs. *Frontiers in Bioengineering and Biotechnology*, 3, 183.

Chapter 5

The Effects of Using Geared Wheelchair Wheels on Energy Cost of Propulsion in Adults with Spinal Cord Injury

Introduction

Approximately 1% of the world's population needs a wheelchair for daily mobility (Flemmer & Flemmer, 2016); substantial growth of wheelchair use far exceeds the rates of population growth (LaPlante & Kaye, 2010). In the U.S., an estimated 3.7 million people used a wheelchair in 2010 (Brault, 2012). Among working-age adults (18-64 years), wheelchairs are the second most prevalent mobility device, with 90% of all users using a manual wheelchair (Kaye, Kang, & LaPlante, 2000). Spinal cord injury (SCI) is one of the leading conditions associated with wheelchair use (Kaye et al., 2000). More than half of the estimated 358,000 individuals with SCI in the U.S. are non-ambulatory and are wheelchair users (Stover, DeLisa, & Whiteneck, 1995); manual wheelchairs are the most common alternative mode of mobility chosen by people with SCI (Beekman, Miller-Porter, & Schoneberger, 1999). The annual incidence of SCI is approximately 17,700 new cases each year (White & Black, 2016).

Wheelchair propulsion is an efficient form of locomotion for people with SCI, however, when compared to normal walking, wheelchair propulsion is relatively inefficient (Beekman et al., 1999; Cerny, Waters, Hislop, & Perry, 1980; Gordon & Vanderwalde, 1956; Hussey & Stauffer, 1973; Waters & Lunsford, 1985). The inefficiency is attributed to the small muscle mass of the upper limbs which are not specialized for ambulatory activities and the biomechanical disadvantages of using hand-rims for propulsion (Sawka, Glaser, Wilde, & von Lührte, 1980;

van der Woude, Lucas HV & de Groot, 2005). The health conditions of people with SCI contribute to additional propulsion inefficiencies as well.

The effects of different wheelchair types on energy expenditure and efficiency influences wheelchair prescription for individuals with SCI. Energy expenditure and efficiency factors are also necessary for evaluation of function and participation of manual wheelchair users with SCI and the assessment of their physical fitness (Hayes, Myers, Ho, & Lee, 2005; Mukherjee, Bhowmik, & Samanta, 2005). The effects of different models of standard manual wheelchairs (Beekman et al., 1999) and alternative propulsion mechanisms (e.g. lever and crank propelled wheelchairs (Dallmeijer, Zentgraaff, Zijp, & van der Woude, 2004; van der Woude, Lucas HV, Botden, Vriend, & Veeger, 1997), as well as pushrim-activated power assist wheelchairs (Kloosterman, Snoek, van der Woude, L H, Buurke, & Rietman, 2013; Nash et al., 2008) on energy expenditure and efficiency in wheelchair users have been previously investigated.

Geared manual wheelchairs (GMWs) are a promising alternative propulsion mechanism that may reduce the biomechanical demands of the upper extremity while maximizing function. Similar to multi-speed bicycles, geared wheels allow individuals to utilize a lower gear to reduce propulsion effort. Studies on non-wheelchair users and the preliminary results of our study on people with SCI have shown that using geared manual wheelchairs could be beneficial for strenuous tasks such as ramp ascent (Howarth, Pronovost, Polgar, Dickerson, & Callaghan, 2010; Jahanian, Schnorenberg, & Slavens, 2016) and propulsion on carpeted floors (Jahanian et al.; Jahanian, Schnorenberg, Hawi, & Slavens, 2015). One potential advantage of geared manual wheelchair use is decreased shoulder pain (Finley & Rodgers, 2007). However, the effects of geared wheelchair wheels on energy expenditure and propulsion efficiency in manual wheelchair

users has not yet been evaluated. The aim in this study was to quantify the effects of geared wheelchair wheels on energy cost of propulsion in adults with SCI. The related hypotheses were:

1. Using geared wheels in the low gear condition will significantly increase energy cost of propulsion in comparison to the standard gear condition.
2. Using geared wheels in the low gear condition will significantly decrease the intensity of wheelchair propulsion in comparison to the standard gear condition.

The measures, distance travelled and energy cost of transport during the low gear and standard gear conditions were used to test the first hypothesis. The rate of oxygen consumption, average heart rate, and rate of perceived exertion were contrasted during the low gear and the standard gear conditions to test the second hypothesis.

Pilot work on the impact of geared wheels on energy expenditure during manual wheelchair mobility was done to investigate the feasibility of Aim #4 (Jahanian, Rowley, Strath, Silver-Thorn, & Slavens, 2017). Three able-bodied individuals (males, age: 21 years) participated in this pilot study. The results indicated that the rate of oxygen consumption and total energy expenditure for a seven-minute wheelchair propulsion on passive wheelchair rollers at constant speeds (1.5 and 2 mph) increased during the low gear condition compared to the standard gear condition. The notable increase in the stroke frequency during the low gear condition could be the main reason for the observed increase in the rate of oxygen consumption and energy expenditure. The results from this pilot study also suggested that to test the hypotheses for Aim #4, it is more appropriate to test individuals with SCI during propulsion at a self-selected speed rather than a constant speed to better reflect demands during propulsion (Beekman et al., 1999).

Methods

This study was approved by the Department of Veterans Affairs (DVA, Milwaukee, WI) and the University of Wisconsin-Milwaukee (UWM) Institutional Review Boards (IRBs). Prior to research participation, all subjects submitted written informed consent.

Subjects

Veterans with paraplegic SCI who met the inclusion criteria (18 to 70 years of age, manual wheelchair used as the primary mode of mobility, minimum 6 months post-injury, and ability to perform independent transfers) were examined by a physician in the SCI Unit at the Clement J Zablocki VA Medical Center (Milwaukee, WI) to confirm eligibility. Eleven adult male manual wheelchair users with SCI were recruited. As noted in Table 18, the subjects' average age was 47.2 ± 13.1 years and their average duration as a manual wheelchair user was 16.4 ± 13.1 years; their SCI levels ranged from T1 to L2. Their mean body mass index (BMI) was 26.7 ± 4.4 kg/m^2 . SCI levels ranged from T1 to L2. Their mean body mass index (BMI) was 26.7 ± 4.4 kg/m^2 .

Experimental protocol and instrumentatin

Participants were instructed to refrain from caffeine and energy beverages (for 6 hours) and vigorous exercise (for 12 hours) prior to wheelchair propulsion testing at the UWM Mobility Lab. After collection of anthropometric and demographic information, subjects transferred from their wheelchair to a medical adjustable height exam table (Intensa, High Point, NC). The geared wheels (IntelliWheels, Inc., Champaign, IL) were then mounted on their personal wheelchairs. The subjects then returned to their wheelchairs. The tire pressure was adjusted to approximately

100 psi. After a 15-minute acclimation period to propulsion with the new wheels on passive rollers (McLAIN, Traverse City, MI), subjects were instrumented with the portable metabolic system (COSMED K4b², Rome, Italy), the heart rate monitor (T34, Polar Electro Inc., Lake Success, NY), and retroreflective markers (see Table 19). The test procedures were reviewed, and subjects were given additional time to acclimate to wearing the COSMED mask and data acquisition unit (Figure 38).

Table 18. Subjects characteristics

#	Subject ID	Age (years)	Weight (kg)	Height (cm)	Arm Dominance	SCI level	Years as wheelchair user
1	3	53	87	178	Left	T4, ASIA <u>A</u>	27
2	4	42	84.8	188	Right	T10, ASIA <u>C</u>	21
3	5	55	97.7	185	Right	T5, ASIA <u>A</u>	31
4	6	36	80.2	175	Right	L2, ASIA <u>C</u>	12
5	7	68	73	170	Right	T10, ASIA <u>A</u>	1.5
6	8	57	81.2	180	Right	T11, ASIA <u>C</u>	0.6
7	9	50	66	180	Right	T6, ASIA <u>C</u>	9.5
8	10	24	71.2	180	Right	T5, ASIA <u>A</u>	2
9	11	51	112	188	Left	T12, ASIA <u>C</u>	30
10	12	29	93	188	Right	T1, ASIA <u>A</u>	10
11	13	54	136	193	Right	T12, ASIA <u>A</u>	36
	Mean ± SD	47.2 ± 13.1	89.3 ± 20.2	182.3 ± 6.8	-----	-----	16.4±13.1

T#: Thoracic spinal injury level, L#: Lumbar spinal injury level; ASIA A: Complete spinal cord injury; ASIA C: Incomplete spinal cord injury

The geared wheels supported both the standard gear (gear ratio of 1:1) and low gear (gear ratio of 1.5:1) propulsion conditions. The test protocol included six-minute trials at the subject’s self-selected speed (e.g. “normal comfortable” pace) in both the standard and low gear conditions, in a random order. A mandatory ten-minute rest period separated test conditions. Measurements of energy expenditure (breath by breath measures of O₂ and CO₂ to estimate oxygen uptake

[ml/min] and energy expenditure [kcal/min]) and heart rate were conducted during wheelchair propulsion. Hand-rim kinematics and spatiotemporal parameters were also collected using a 15-camera motion capture system (Vicon Motion Systems, Oxford, UK; 120 Hz) and a cycling speedometer (Bell Dashboard 100, city, state).



Figure 38. Energy expenditure assessment during manual wheelchair propulsion on passive wheelchair rollers; the COSMED mask and data acquisition Holter are also shown.

All tests were conducted in the morning; the relative humidity was 40-60% and air temperature ranged from 20-22 °C. The $K4b^2$ system, used for this study, has been reported as a valid and reliable measure of oxygen uptake (McLaughlin, King, Howley, Bassett Jr, & Ainsworth, 2001)

and has been effectively used to measure energy costs of individuals with SCI (Abel, Platen, Vega, Schneider, & Strüder, 2008; Collins et al., 2010). The system analyzer (k4b2 device) was calibrated before each test and verified with reference gasses and room air according to the manufacturer's guidelines.

At the end of each task or test condition, the rate of perceived exertion was measured using the Borg 6-20 scale, see Table 20 (Borg, 1998). Borg 6-20 is a subjective rating scale that has been used as a valid method for rating the perceived exertion and measuring exercise intensity in people with SCI (Goosey-Tolfrey et al., 2010) and manual wheelchair users (Ward, Bar-Or, Longmuir, & Smith, 1995).

Table 19. Locations of retroreflective markers for calculation of the distance traveled and stroke cycle frequency, as well as characterization of propulsion pattern.

Marker	Location
M3	Dorsal aspect of the dominant hand on the third metacarpal joint, dominant side
Wrist	Dorsal aspect of the dominant wrist midway between the radial and ulnar styloid processes, dominant side
WHEEL	Center of wheel hub, non-dominant side
Off-Center	On the wheel, at the distance of 15 cm from the center of the wheel hub, non-dominant side

Table 20. The Borg RPE scale, the 15-grade scale for ratings of perceived Exertion (RPE)

RPE Scale	Level of Exertion
6	No exertion at all
7	Extremely Light
8	
9	Very Light, "like wheeling slowly on a hard floor"
10	
11	Light
12	
13	Somewhat Hard. "Somewhat hard but it still feels OK to continue"
14	
15	Hard (heavy)
16	
17	Very hard, "Very strenuous, it feels very heavy and tiring"
18	
19	Extremely hard, "the most strenuous experience you have ever experienced"
20	Maximal exertion

Data processing

The outcome measures for each subject and test condition included distance travelled, energy expenditure, cost of transport, and rate of perceived exertion during the 6-minute push test, as well as rate of oxygen consumption, average heart rate, and stroke cycle frequency during the steady state phase of wheelchair propulsion. The distance travelled was based on the vertical displacement of Off-Center marker; the number of full wheel rotations was based on the number of observed local maxima. The kinematic data were smoothed using a 400 msec moving average filter prior to calculating the number of peaks for each minute. The distance travelled for each minute of propulsion was the product of the number of wheel cycles times the wheel circumference. For one subject, the distance travelled was calculated using the cycle speedometer mounted on the front roller of the passive wheelchair dynamometer. The average deviation (for ten subjects) in the distance measured using the speedometer and the distance calculated based on the kinematic data was less than 2.9 %.

The COSMED $K4b^2$ software was used to establish summary estimates of energy expenditure including oxygen uptake (VO_2), and CO_2 production (VCO_2), and rate of energy expenditure.

The rate of energy expenditure (EE, Kcal/min) was calculated based on the measured VO_2 (l/min) and VCO_2 (l/min), calculated breath by breath (Equation 1) (Elia & Livesey, 1992) .

$$\text{EE} = 3.781 * \text{VO}_2 + 1.237 * \text{VCO}_2 \quad (1)$$

The rate of energy expenditure data was then used to calculate the total energy expenditure during the 6-minute push test on the passive wheelchair ergometer.

The cost of transport (cal/m) was the ratio of total energy expenditure to distance travelled.

The oxygen consumption was normalized by subject's weight (VO_2/kg , ml/min/kg). Steady state values were reviewed during minutes 2 through 5 of the 6-minute trial (coefficient of variation < 10%); these normalized steady state values were averaged across 30-second periods.

As per Collins et al., (2010), one metabolic equivalent (MET) for SCI individuals is 2.7 ml/kg/min (for able-bodied adults, one MET is 3.5 ml/kg/min). Therefore, the normalized steady state values of oxygen consumption were averaged across 30-second periods and divided by 2.7 to determine the SCI MET during propulsion for both gear conditions. The average heart rate was also calculated for the period of steady state (e.g. oxygen consumption coefficient of variation less than 10%).

The sagittal plane kinematics of the wrist marker were used to evaluate the stroke cycle frequency. Specifically, the number of stroke cycles per minute was computed based on the number of the local maxima in the horizontal motion of the wrist marker trajectory. The average stroke cycle frequency during the steady state phase was then computed for each task. To characterize the subject's stroke pattern, the sagittal plane kinematics of the M3 marker were

reviewed; patterns were classified as semicircular (SC), single-looping over propulsion (SLOP), double-looping over propulsion (DLOP), or arcing (ARC) (Boninger et al., 2002).

Statistical analysis

To test the respective research hypotheses and evaluate the effect of geared wheel use on energy expenditure, the differences between the distance travelled, cost of transport, SCI MET, heart rate, stroke cycle frequency, and rate of perceived exertion were compared across gear conditions. Because of the small sample size and because the data did not have a normal distribution, the differences of the dependent variables across gear conditions were analyzed using separate Wilcoxon Signed-Rank tests. Test statistics (Z), significance (p), and effect size (r) were reported for each metric. The effect size was calculated as the ratio of the Z -value to the square root of the number of observations (number of subjects times two). Statistical analyses were done in SPSS 25 (IBM Corporation) and the level of significance was reduced from 0.05 to 0.0083, using a Bonferroni correction for six dependent variables.

Results

The data from wheelchair propulsion testing were analyzed using wheel condition as the independent variable and distance travelled, cost of transport, SCI MET, heart rate, stroke cycle frequency, and rate of perceived exertion as the main dependent variables.

All subjects performed the wheelchair propulsion tasks. The heart rate data during wheelchair propulsion from two subjects (subjects 10 and 12) were not analyzed due to technical issues which occurred during testing.

The results from the 6-minute push test on the passive wheelchair ergometer indicated that the distance travelled, and SCI MET were significantly less during the low gear condition compared to the standard gear condition (Table 21). The cost of transport was significantly higher during the geared condition (Table 21). The gear condition did not significantly affect heart rate, cadence, or the rate of perceived exertion.

Propulsion on the passive rollers was significantly slower during the geared condition in comparison to standard gear condition. The mean total distance travelled for six-minute propulsion in the low gear condition was significantly less (-34.3 %, $p = 0.003$), and the mean total energy expenditure was markedly less (Table 21 and Figure 39). The results for the cost of transport indicated that wheelchair propulsion in the low gear condition was significantly more energy demanding (29.5%, $p < 0.003$); however, the SCI MET was significantly less (-13.3%, $p = 0.006$), (Table 21 and Figure 40).

The wheel condition was moderately effective on the level of exertion (Table 4, Figure 41). The perceived exertion during the low gear condition decreased by 11.8%; however, it was not statistically significant ($p = 0.085$). The wheel condition had a small effect size on heart rate (Table 21). The average heart rate slightly decreased during the geared condition (-1.8 %, $p = 0.47$). The wheel condition did not alter the stroke cycle frequency during wheelchair propulsion on passive roller at normal comfortable speed (Table 21). Subjects used the same propulsion pattern during both the standard gear and low gear conditions (Table 22). The box plot graphs combined with the individual measurements for the metrics affected strongly ($r > 0.5$) to moderately ($0.2 < r < 0.5$) with gear condition are depicted in Figure 42.

Table 21. Mean and standard deviation of total distance (Tot. Distance), cost of transport (CT), metabolic equivalent (SCI MET), average heart rate (HR), stroke cycle frequency (cadence), and rate of perceived exertion (RPE) for the standard gear and low gear conditions.

	Standard gear	Geared	Statistical Results			
	Mean \pm SD	Mean \pm SD	N	Z	<i>p</i>	<i>r</i>
Tot. Distance (m)	341.11 \pm 144.59	224.11 \pm 91.77	11	2.93	0.003 *	0.62
CT (cal/m)	98.33 \pm 36.71	127.33 \pm 42.71	11	2.93	0.003 *	0.62
SCI MET	4.33 \pm 1.24	3.76 \pm 0.98	11	2.75	0.006 *	0.59
HR (bpm)	102 \pm 16	100 \pm 19	9	0.71	0.47	0.17
Cadence (cycle/min)	55 \pm 9	54 \pm 10	11	0.76	0.45	0.16
RPE	12.36 \pm 2.81	10.90 \pm 1.92	11	1.72	0.085	0.37

N = number of subjects; Z= test statistic; *p* = significance level; *r* = effect size; *: *p* < 0.0083.

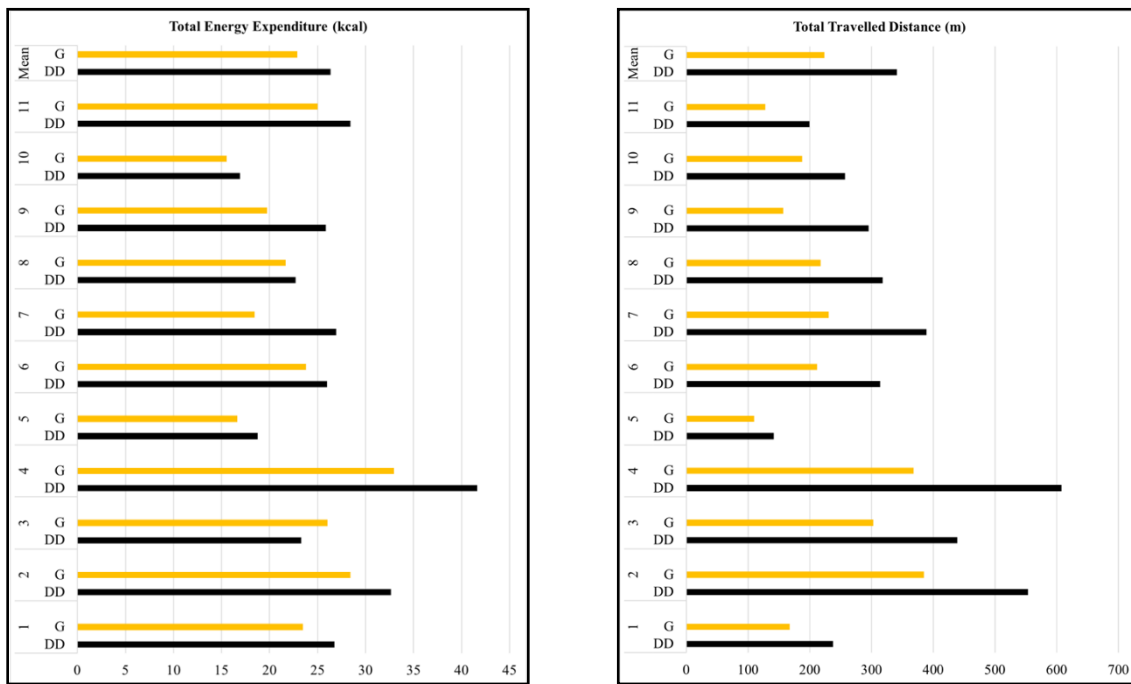


Figure 39. Total energy expenditure (left) and distance travelled for the low gear (G) and standard gear (DD) conditions. Each bar along the y-axis represents an individual participant, the first set of bars show the group mean values.

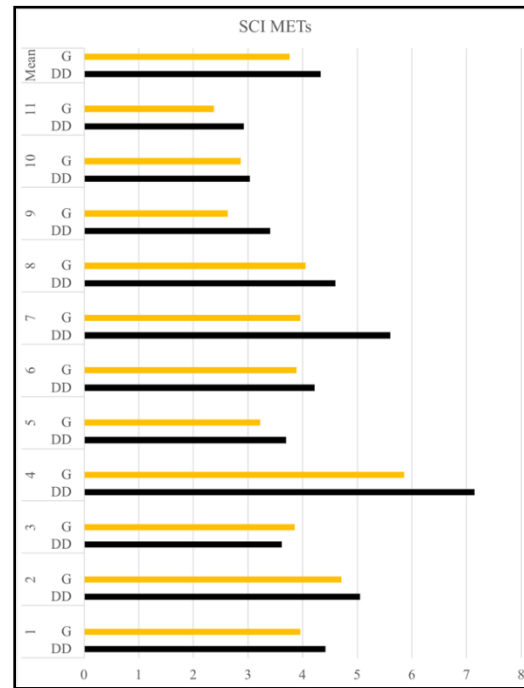
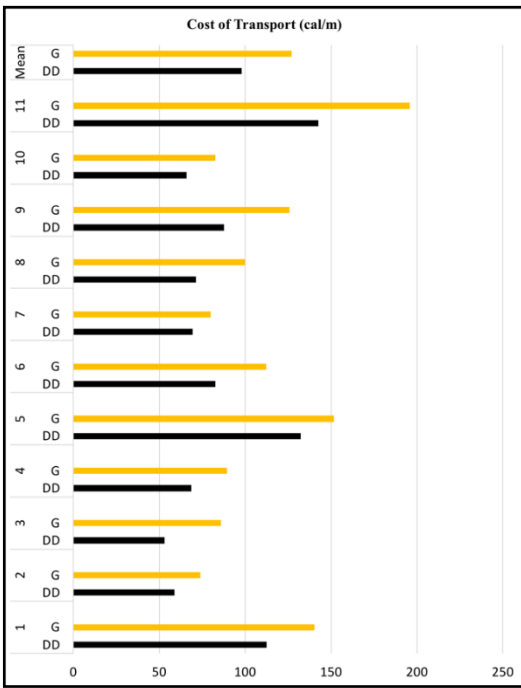


Figure 40. Cost of transport (left) and rate of oxygen consumption (SCI METs) for the low gear (G) and standard gear (DD) conditions. Each bar along the y-axis represents an individual participant, the first set of bars show the group mean values.

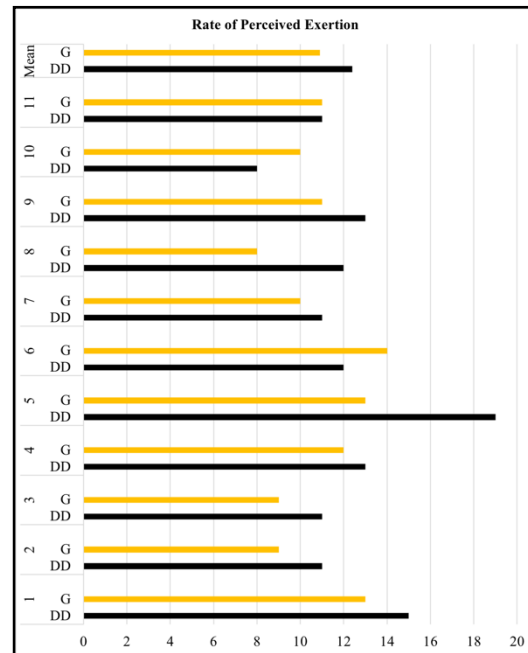
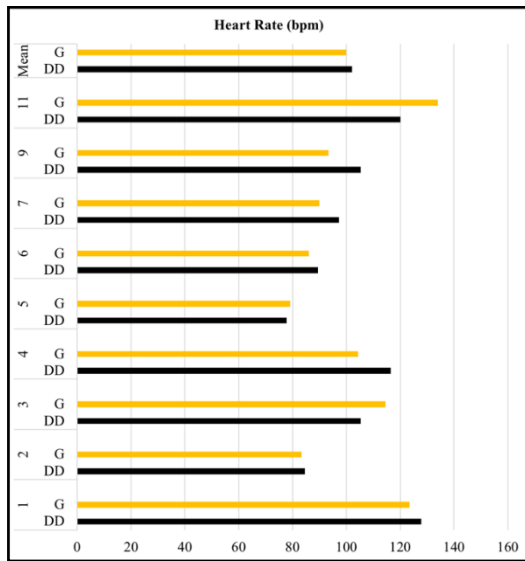


Figure 41. Average heart rate (left) and rate of perceived exertion for the low gear (G) and standard gear (DD) conditions. Each bar along the y-axis represents an individual participant, the first set of bars show the group mean values.

Table 22. Propulsion patterns during standard gear and geared conditions.

Subject	1	2	3	4	5	6	8	9	10	11
Standard gear	ARC	DLOP	DLOP	DLOP	ARC	ARC	DLOP	DLOP	DLOP	ARC
Low gear	SC→ARC	DLOP	DLOP	DLOP	ARC	ARC	DLOP	DLOP	DLOP	ARC

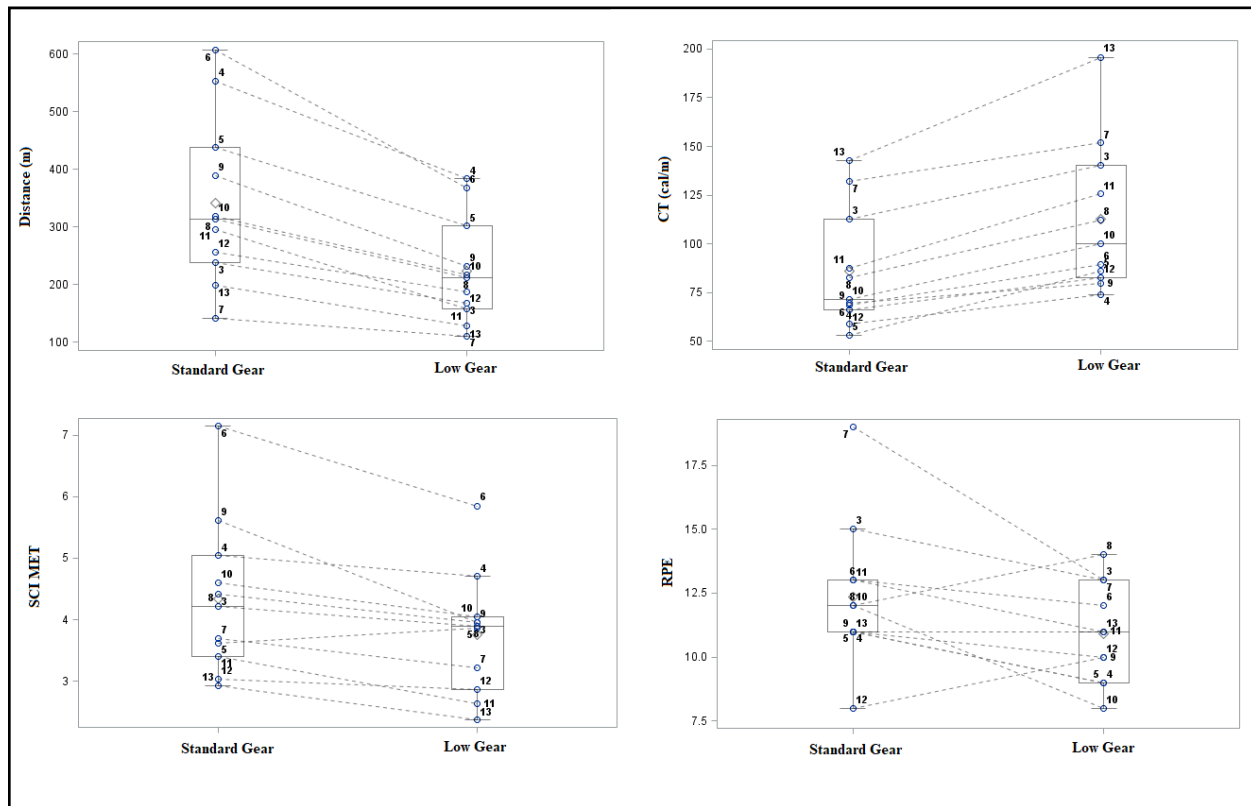


Figure 42. Distance travelled (top left), cost of transport (top right), rate of oxygen consumption (SCI MET, bottom left), and rate of perceived exertion (RPE, bottom right) which was measured for each subject during the standard gear and low gear conditions. In each graph the box plot on the left is for the standard gear and on the right is for the low gear condition. In each graph the measurements for each subject are shown with a circle and the subject ID next to it.

Discussion

We successfully characterized the effects of using geared wheelchair wheels on wheelchair propulsion energy cost and efficiency in manual wheelchair users with paraplegic SCI. To the

author's knowledge it is for the first time that energy cost and efficiency of geared manual wheelchair propulsion is being studied with experienced manual wheelchair users. The results of the study supported both hypotheses that using the geared wheels in the low gear condition significantly increased the energy cost of propulsion and decreased the intensity of wheelchair propulsion.

The propulsion speed decreased significantly during the low gear condition and the distance travelled in six-minute propulsion on the passive rollers was significantly less compared to the standard gear condition. This could be primarily attributed to the reduction in the stroke distance, a direct effect of the gear reduction (1.5:1). The total energy expenditure for wheelchair propulsion on passive rollers for six minutes was significantly lower for the low gear condition; however, the cost of transport was significantly higher. This means that using the geared wheels in the low gear condition is significantly more energy demanding for propelling a given distance in comparison to the standard gear condition. The significant decrease in distance traveled and the significant increase in energy cost of transport support the hypothesis that using the geared wheels in the low gear condition significantly increases the energy cost of propulsion in manual wheelchair users with SCI. The decrease in wheelchair propulsion energy efficiency in the low gear condition was consistent with what we had observed in a pilot study with able-bodied subjects.

Using the geared wheels in the low gear condition significantly decreased oxygen consumption rate (SCI MET) in comparison to standard gear condition. This could be interpreted as a significant decrease in the intensity of the wheelchair propulsion task using the geared wheels in the low gear condition. The substantial decrease in the perceived exertion is consistent with this interpretation, although it was not statistically significant. The significant decrease in oxygen consumption rate

and substantial decrease in the rate of perceived exertion support the hypothesis that using the geared wheels in the low gear condition decreases the intensity of wheelchair propulsion.

The energy expenditure results indicated that for the standard gear condition the mean oxygen consumption rate for 11 adult male manual wheelchair users with SCI was 4.33 ± 1.24 SCI METS which is in the range of 3.35 – 6.22 SCI METs, which was reported for wheeling on carpet/grass by Collins and colleagues (Collins et al., 2010) . The results for oxygen consumption cost for both tasks indicate that propulsion on the passive rollers can be classified as a moderate intensity (3.0 – 6.0 METs) physical activity (Haskell et al., 2007).

The reason that the average heart rate was not significantly different between the low gear and standard gear conditions could be explained by the similar stroke cycle frequency that subjects used for wheelchair propulsion in both conditions. Subjects were instructed to propel their wheelchair at their normal comfortable speed, the similar stroke cycle frequency in both wheel conditions indicate that participants performed both tasks at their comfortable stroke cycle frequency (optimum frequency) rather than their comfortable speed. Previous studies have reported optimal energy cost and efficiency at the stroke cycle frequencies close to the self-selected frequency (Lenton et al., 2013; van der Woude, LHV, Veeger, Rozendal, & Sargeant, 1989).

Conclusions

The findings of this study demonstrated that using the geared wheels in the low gear condition in people with paraplegic SCI reduced the energy efficiency of wheelchair propulsion. However, using the geared wheels in the low gear condition at a self-selected stroke cycle frequency was significantly less intense (easier) and accompanied by a reduced perception of effort.

The current investigation and the findings from the previous studies on biomechanical effects of using geared wheelchair wheels suggest that using the geared wheels in the low gear condition could be beneficial for manual wheelchair users with SCI to independently accomplish more strenuous tasks such as propulsion on carpeted floor or grass, while increasing their physical activity. On the other hand, using the low geared wheels is not recommended for long distance propulsion as it can be fatiguing and increases the risk of repetitive strain injuries.

References

- Abel, T., Platen, P., Vega, S. R., Schneider, S., & Strüder, H. (2008). Energy expenditure in ball games for wheelchair users. *Spinal Cord*, *46*(12), 785-790.
- Beekman, C. E., Miller-Porter, L., & Schoneberger, M. (1999). Energy cost of propulsion in standard and ultralight wheelchairs in people with spinal cord injuries. *Physical Therapy*, *79*(2), 146-158.
- Boninger, M. L., Souza, A. L., Cooper, R. A., Fitzgerald, S. G., Koontz, A. M., & Fay, B. T. (2002). Propulsion patterns and pushrim biomechanics in manual wheelchair propulsion. *Archives of Physical Medicine and Rehabilitation*, *83*(5), 718-723.
- Borg, G. (1998). *Borg's perceived exertion and pain scales*. Human kinetics.
- Brault, M. W. (2012). Americans with disabilities: 2010. *Current Population Reports*, *7*, 0-131.
- Cerny, K., Waters, R., Hislop, H., & Perry, J. (1980). Walking and wheelchair energetics in persons with paraplegia. *Physical Therapy*, *60*(9), 1133-1139.
- Collins, E. G., Gater, D., Kiratli, J., Butler, J., Hanson, K., & Langbein, W. E. (2010). Energy cost of physical activities in persons with spinal cord injury. *Medicine and Science in Sports and Exercise*, *42*(4), 691-700.
- Dallmeijer, A., Zentgraaff, I., Zijp, N., & van der Woude, L. (2004). Submaximal physical strain and peak performance in handcycling versus handrim wheelchair propulsion. *Spinal Cord*, *42*(2), 91-98.
- Elia, M., & Livesey, G. (1992). Energy expenditure and fuel selection in biological systems: The theory and practice of calculations based on indirect calorimetry and tracer methods. *Metabolic control of eating, energy expenditure and the bioenergetics of obesity* (pp. 68-131) Karger Publishers.
- Finley, M. A., & Rodgers, M. M. (2007). Effect of 2-speed geared manual wheelchair propulsion on shoulder pain and function. *Archives of Physical Medicine and Rehabilitation*, *88*(12), 1622-1627.
- Flemmer, C. L., & Flemmer, R. C. (2016). A review of manual wheelchairs. *Disability and Rehabilitation: Assistive Technology*, *11*(3), 177-187.
- Goosey-Tolfrey, V., Lenton, J., Goddard, J., Oldfield, V., Tolfrey, K., & Eston, R. (2010). Regulating intensity using perceived exertion in spinal cord-injured participants. *Medicine & Science in Sports & Exercise*, *42*(3), 608-613.
- Gordon, E. E., & Vanderwalde, H. (1956). Energy requirements in paraplegic ambulation. *Archives of Physical Medicine and Rehabilitation*, *37*(5), 276-285.

- Haskell, W. L., Lee, I., Pate, R. R., Powell, K. E., Blair, S. N., Franklin, B. A., et al. (2007). Physical activity and public health: Updated recommendation for adults from the American College of Sports Medicine and the American Heart Association. *Circulation*, 116(9), 1081.
- Hayes, A. M., Myers, J. N., Ho, M., & Lee, M. Y. (2005). Heart rate as a predictor of energy expenditure in people with spinal cord injury. *Journal of Rehabilitation Research and Development*, 42(5), 617.
- Howarth, S. J., Pronovost, L. M., Polgar, J. M., Dickerson, C. R., & Callaghan, J. P. (2010). Use of a geared wheelchair wheel to reduce propulsive muscular demand during ramp ascent: Analysis of muscle activation and kinematics. *Clinical Biomechanics*, 25(1), 21-28.
- Hussey, R. W., & Stauffer, E. S. (1973). Spinal cord injury: Requirements for ambulation. *Archives of Physical Medicine and Rehabilitation*, 54(12), 544-547.
- Jahanian, O., Gaglio, A., Daigle, S., Muqet, V., Schnorenberg, A. J., Hsiao-Wecksler, E. T., et al. Hand-rim biomechanics of geared manual wheelchair mobility.
- Jahanian, O., Rowley, T., Strath, S., Silver-Thorn, B. & Slavens, B. (2017). Impact of Geared Wheels on Energy Expenditure during Manual Wheelchair Mobility. *Proceeding of the 41st Annual Meeting of American Society of Biomechanics, Boulder, CO.*
- Jahanian, O., Schnorenberg, A. J., Hawi, L., & Slavens, B. A. (2015). Upper extremity joint dynamics and electromyography (EMG) during standard and geared manual wheelchair propulsion. *Proceeding of the 39th Annual Meeting of American Society of Biomechanics, Columbus, OH.*
- Jahanian, O., Schnorenberg, A. J., & Slavens, B. A. (2016). Evaluation of shoulder joint kinematics and muscle activity during geared and standard manual wheelchair mobility. *Engineering in Medicine and Biology Society (EMBC), 2016 IEEE 38th Annual International Conference of The*, pp. 6162-6165.
- Kaye, H. S., Kang, T., & LaPlante, M. P. (2000). Mobility device use in the United States. *Disability Statistics Report 14.*
- Kloosterman, M. G., Snoek, G. J., van der Woude, L. H., Buurke, J. H., & Rietman, J. S. (2013). A systematic review on the pros and cons of using a pushrim-activated power-assisted wheelchair. *Clinical Rehabilitation*, 27(4), 299-313.
- LaPlante, M. P., & Kaye, H. S. (2010). Demographics and trends in wheeled mobility equipment use and accessibility in the community. *Assistive Technology*®, 22(1), 3-17.
- Lenton, J., van der Woude, L., Fowler, N., Nicholson, G., Tolfrey, K., & Goosey-Tolfrey, V. (2013). Hand-rim forces and gross mechanical efficiency at various frequencies of wheelchair propulsion. *International Journal of Sports Medicine*, 34(02), 158-164.

- McLaughlin, J., King, G., Howley, E., Bassett Jr, D., & Ainsworth, B. (2001). Validation of the COSMED K4 b2 portable metabolic system. *International Journal of Sports Medicine*, 22(04), 280-284.
- Mukherjee, G., Bhowmik, P., & Samanta, A. (2005). Effect of chronic use of different propulsion systems in wheelchair design on the aerobic capacity of indian users. *Indian Journal of Medical Research*, 121(6), 747.
- Nash, M. S., Koppens, D., van Haaren, M., Sherman, A. L., Lippiatt, J. P., & Lewis, J. E. (2008). Power-assisted wheels ease energy costs and perceptual responses to wheelchair propulsion in persons with shoulder pain and spinal cord injury. *Archives of Physical Medicine and Rehabilitation*, 89(11), 2080-2085.
- Sawka, M. N., Glaser, R. M., Wilde, S. W., & von Lührte, T. C. (1980). Metabolic and circulatory responses to wheelchair and arm crank exercise. *Journal of Applied Physiology: Respiratory, Environmental and Exercise Physiology*, 49(5), 784-788.
- Stover, S. L., DeLisa, J. A., & Whiteneck, G. G. (1995). *Spinal cord injury: Clinical outcomes from the model systems* Aspen Publishers.
- van der Woude, L., Veeger, H., Rozendal, R., & Sargeant, A. (1989). Optimum cycle frequencies in hand-rim wheelchair propulsion. *European Journal of Applied Physiology and Occupational Physiology*, 58(6), 625-632.
- van der Woude, Lucas HV, Botden, E., Vriend, I., & Veeger, D. (1997). Mechanical advantage in wheelchair lever propulsion: Effect on physical strain and efficiency. *Journal of Rehabilitation Research and Development*, 34(3), 286.
- van der Woude, Lucas HV, & de Groot, S. (2005). Wheelchair propulsion: A straining form of ambulation. *Indian Journal of Medical Research*, 121(6), 719.
- Ward, D. S., Bar-Or, O., Longmuir, P., & Smith, K. (1995). Use of rating of perceived exertion (RPE) to prescribe exercise intensity for wheelchair-bound children and adults. *Pediatric Exercise Science*, 7(1), 94-102.
- Waters, R. L., & Lunsford, B. R. (1985). Energy cost of paraplegic locomotion. *The Journal of Bone and Joint Surgery.American Volume*, 67(8), 1245-1250.
- White, N., & Black, N. (2016). Spinal cord injury (SCI) facts and figures at a glance.

Chapter 6

Overall Summary and Conclusions

Summary and Discussion

The purpose of this dissertation was to quantitatively investigate the effects of using geared wheelchair wheels on biomechanics, physiology, and function in individuals with spinal cord injury (SCI). To evaluate the biomechanical effects of geared wheels, first we investigated in able-bodied, non-wheelchair users. Eventually, the effects of the new propulsion mechanism were quantitatively evaluated in experienced wheelchair users.

The first aim of this study was to evaluate and compare the upper extremity joint kinematics and muscle activity during standard and geared manual wheelchair propulsion in able-bodied subjects. We successfully characterized the spatiotemporal parameters, glenohumeral joint kinematics and shoulder muscle activity during manual wheelchair propulsion on level floor and up a ramp in 14 able-bodied individuals using geared and standard manual wheelchair wheels. Use of the geared wheels reduced the stroke distance, speed, and increased the stroke frequency when compared to the use of the standard manual wheelchair wheels. The stroke distance decreased significantly during geared wheel use similar to the results reported in the literature (Howarth, Pronovost, Polgar, Dickerson, & Callaghan, 2010). This indicates that for propulsion along a given distance substantially higher repetitions are required when using the geared wheels in comparison to standard wheels. Using the geared manual wheelchair resulted in a substantial reduction in the peak muscle activity of the primary shoulder flexors (pectoralis major, anterior deltoid), and infraspinatus compared to the standard wheels. A reduction in the peak muscular

demands might lead to a reduction in peak forces applied to the glenohumeral joint and consequently a reduction in the risk of shoulder secondary injury and pain. This might be the primary benefit of using geared manual wheelchair wheels. The normalized integrated muscle activity for the shoulder flexor muscles was not significantly different between the geared and standard wheel conditions. However, the normalized muscle activity was significantly higher for the geared condition in the investigation by (Howarth et al., 2010). The difference in gear ratio (2:1 vs. 1.6:1) and slower velocity with the geared wheel with larger gear reduction (2:1) could be the main reasons for this difference. This might be evidence that the smaller gear reduction (1.6:1) could be a more optimized gear ratio for manual wheelchair users, particularly for longer distances. The results of this study were used to refine the data collection protocol for the main study with individuals with SCI.

The second aim of this study was to evaluate the hand-rim biomechanics during geared manual wheelchair propulsion over different ground conditions in adults with SCI. We successfully characterized the hand-rim kinetics and stroke cycle characteristics during geared manual wheelchair propulsion on tile and carpeted level floors and up a ramp in seven veterans with SCI. Using the geared wheels in the low gear condition significantly decreased the propulsion speed, and the hand-rim kinetics including the peak hand-rim resultant force, peak hand-rim propulsive moment, and peak rate of rise of the hand-rim resultant force, in comparison with the standard gear condition in all ground conditions. The significant differences in hand-rim kinetics seen between the standard gear and low gear conditions indicate potential benefits of using geared wheels regardless of the terrain. Previous studies have shown that the reduction of hand-rim propulsion forces, wheel torque, and rate of force application could increase the manual wheelchair efficiency and decrease the risk of development of upper extremity limb injuries such

as carpal tunnel syndrome (Boninger, Cooper, Baldwin, Shimada, & Koontz, 1999; Boninger, Koontz, Sisto, & Dyson-Hudson, 2005; Jahanian, Gaglio, Schnorenberg, Muqet, Hsiao-Wecksler, & Slavens, 2019). The stroke distance decreased significantly during the low gear condition. This demonstrates that for a given distance, a higher number of stroke cycles are required to move the same distance. High-repetition of upper extremity joint motions have been significantly related to increased risk of upper limb injuries in manual wheelchair users (Boninger et al., 2005; Requejo et al., 2008). The results for the combined metrics indicated a significant decrease in the normalized integrated hand-rim propulsive moment regardless of the ground condition. This might indicate that although a higher number of stroke cycles are required for travelling a given distance in the low gear condition than the standard gear condition, the low gear condition might be less demanding than the standard gear condition. This might be interpreted as lower cumulative load during the low gear condition than the standard gear condition which might lead to lower biomechanical demands of upper extremity joints during strenuous tasks such as propulsion on carpeted floor.

The third aim of this study was to evaluate the glenohumeral joint dynamics and shoulder muscle activity during geared manual wheelchair propulsion on carpeted level floors in seven adults with SCI. We successfully characterized the spatiotemporal parameters, glenohumeral joint dynamics, and shoulder muscle activity during geared manual wheelchair propulsion on a carpeted floor in veterans with SCI. Using the geared wheels in the low gear condition significantly decreased the glenohumeral joint inferior force and flexion moment as well as the peak and integrated muscle activity of the anterior deltoid and pectoralis major muscles during propulsion on a carpeted floor. This could decrease the risk of subacromial impingement during wheelchair propulsion on carpeted floor (Mercer et al., 2006). The glenohumeral joint

normalized integrated resultant force and moment and shoulder flexors normalized integrated muscle activity were not significantly affected by the gear condition. This indicates that the shoulder demands did not significantly decrease with the use of geared wheels in the lower gear condition for propulsion on carpeted floor. This might indicate that although a higher number of stroke cycles are required for travelling a given distance in the low gear condition than the standard gear condition, the low gear condition is not more demanding than the standard gear condition. The results of this study demonstrate that using the geared wheels may be beneficial for manual wheelchair users to have independent mobility on carpeted floor in their home and community, which may ultimately lead to a reduction of secondary upper extremity musculoskeletal injuries.

The fourth aim of this study was to quantify the effects of using the geared wheelchair wheels on energy cost and intensity of propulsion in eleven adults with SCI. We successfully characterized the effects of using geared wheelchair wheels on wheelchair propulsion energy cost and efficiency in manual wheelchair users with paraplegic SCI during six-minute push test on passive rollers. The results indicated that using the geared wheels in the low gear condition significantly increased the energy cost of propulsion and decreased the intensity of wheelchair propulsion. The propulsion speed decreased significantly during the low gear condition and the distance travelled in six-minute propulsion on the passive rollers was significantly less compared to the standard gear condition. The total energy expenditure for wheelchair propulsion on passive rollers for six minutes was significantly lower for the low gear condition; however, the cost of transport was significantly higher. This means that using the geared wheels in the low gear condition is significantly more energy demanding for propelling a given distance in comparison to the standard gear condition. Using the geared wheels in the low gear condition significantly

decreased oxygen consumption rate (SCI MET) in comparison to standard gear condition. This could be interpreted as a significant decrease in the intensity of the wheelchair propulsion task using the geared wheels in the low gear condition. The substantial decrease in the perceived exertion is consistent with this interpretation. In this study subjects were instructed to propel their wheelchair at their normal comfortable speed, the similar stroke cycle frequency in both wheel conditions indicates that participants performed both tasks at their comfortable stroke cycle frequency (optimum frequency) rather than their comfortable speed. The energy expenditure results for the standard gear condition were similar to what previously reported for wheeling on carpet/grass (Collins et al., 2010) .

Practical Implications

Our findings indicate that using the geared manual wheelchair wheels could decrease the biomechanical demands of upper extremity joints which are required for manual wheelchair propulsion. The current investigation suggests that using geared wheels could be effective in reducing the risk factors of secondary upper extremity musculoskeletal injuries common in manual wheelchair users, such as subacromial impingement and carpal tunnel syndrome. The significant decrease in the hand-rim kinetics regardless of the terrain condition indicates the potential of these wheels in reducing the biomechanical demands of manual wheelchair propulsion over different terrains.

As we expected, we found that high hand-rim kinetics, and high glenohumeral joint kinetics and shoulder muscle activity, occurred during manual wheelchair propulsion on carpeted floor. This could increase the risk of injury in manual wheelchair users and further deteriorate their function and quality of life. Our findings demonstrated that using the geared wheels in the low gear

condition could significantly reduce the hand-rim kinetics, glenohumeral joint kinetics, and shoulder muscle activity. Ultimately, this will lead to increased home and community mobility, independence and quality of life.

The findings of this study demonstrated that using the geared wheels in the low gear condition in people with paraplegic SCI reduced the energy efficiency of wheelchair propulsion. However, using the geared wheels in the low gear condition at a self-selected stroke cycle frequency was significantly less intense (easier) and accompanied by a reduced perception of effort. Because in daily life, short and slow bouts of active propulsion dominate the manual wheelchair usage (Kloosterman, Buurke, Schaake, van der Woude, Lucas HV, & Rietman, 2016; Sonenblum, Sprigle, & Lopez, 2012), using the geared wheels in the low gear condition could be beneficial for manual wheelchair users with SCI to independently accomplish strenuous tasks such as propulsion on carpeted floor or grass, while increasing their physical activity.

The use of the geared wheels has the potential to preserve the upper limb function of manual wheelchair users and delay transition to a powered wheelchair. This allows them to maintain an optimal level of activity and independence that is necessary for high quality of life. Transition to a geared manual wheelchair might be an interesting alternative in the context of the preservation of the upper limb function as well as the need to remain physically active.

The results of this study and the participants' feedback indicate that specific groups of individuals with paraplegic SCI might benefit from using geared manual wheelchairs more than other groups. The results from energy expenditure and participants' feedback on use of geared wheels suggest that older individuals with paraplegic SCI might benefit from using geared wheels more than younger individuals. Previous studies have shown that forward lean of the trunk and the trunk muscular demand increase significantly during manual wheelchair ramp

ascent in comparison to manual wheelchair propulsion over level floor (Chow, Millikan, Carlton, Chae, Lim, & Morse, 2009; Howarth, Polgar, Dickerson, & Callaghan, 2010). Injury to the thoracic nerves- T1 to T5 usually affect the abdominal and lower back muscles as well as the legs. Therefore, paraplegic SCI patients with a higher level of injury (injury to the thoracic nerves- T1 to T5) might benefit from using the geared wheels more than those with lower level injury (injury to thoracic nerves- T6 to T12) during functional mobility tasks such as wheelchair ramp ascent.

Using geared manual wheelchair wheels might be beneficial for different groups of people with locomotive disability, which were not investigated in this study. The use of geared manual wheelchairs has the potential to decrease the period of time in which manual wheelchair propulsion should be avoided after shoulder surgery in wheelchair dependent patients. This could significantly help them to return to independence quicker postoperatively.

The integrative approach used in this study for quantitative evaluation of geared manual wheelchair mobility could be implemented for evaluation of other recently developed adaptive equipment and assistive technologies. The combined biomechanical metrics which were introduced in this study provide a comprehensive characterization of the impact that using geared wheels could have on upper extremity biomechanics and the risk factors (loading and repetition) for the incidence of overuse injuries in manual wheelchair users. These combined metrics might be used as an index characterizing the effects of using the geared wheels on both upper extremity joint loading and repetition over distance. These metrics could be implemented for developing commercially available toolkits to assist clinicians with manual wheelchair prescription, use, training, and transition. The outcomes of this study could be helpful for clinicians (therapists and physicians), wheelchair users, rehabilitation engineers, manufacturers, and insurers. The

outcomes from this research will have clinical implications for augmenting manual wheelchair prescription and transition guidelines. The results from this study could also be used for design modifications and development of new geared wheels for manual wheelchair users.

Limitations and Future Directions

The wide variety (large standard deviations) in the observations across subjects in this study is mainly due to the heterogeneity of the subjects in terms of their age, weight, level of injury, and years as manual wheelchair users. We included a large range of age, level of injury, and years of wheelchair use to demonstrate the application of this technology to a wide variety of patients, as well as to allow feasible human subjects recruitment. The wide range of age and years as wheelchair users is not a concerning limitation since in this study we used a repeated measures design and statistical methods using non-parametric within-subject comparisons. This research was a cross-sectional study and subjects had limited time to acclimate to the geared wheels. Population and sample size might be a limitation in this study. Since our sample only included adult male manual wheelchair users with different levels of paraplegic SCI, we couldn't investigate the effects of the level of injury on the observed results. Future work is required to address the effects of level of injury and age on biomechanical demands and propulsion efficiency during manual wheelchair use. In addition, we are unable to generalize the findings to pediatric and female wheelchair users or individuals with other disabilities than paraplegic SCI. Evaluation of geared manual wheelchair mobility in pediatric and female manual wheelchair users are directions for future investigation.

The scope of this dissertation was evaluation of geared manual wheelchair biomechanics during steady-state propulsion. In daily life, short and slow bouts of active propulsion dominate manual

wheelchair usage, which makes the number of starts/stops notably high during a day. The loads being applied on the upper extremity joints have been reported up to 3.5 times higher during the start-up phase than steady-state propulsion (Koontz et al., 2005). These facts demonstrate the clinical significance of future investigation on the effects of a geared wheel system on wheelchair biomechanics during the start-up phase of manual wheelchair use.

Our objective in this dissertation was to investigate the difference between geared and standard manual wheelchair wheels. Although the investigation regarding cumulative loading is outside of the scope of this study, the evaluation of the combined metrics is the first step towards quantification using this technology and provides valuable insight about the effects of the geared wheel system on cumulative loading. We will aim to investigate cumulative loading in a future study with a modified study design and methodology to comprehensively investigate joint forces and repetition. All tasks in the energy expenditure part of this study were performed on a passive wheelchair roller system, which is different from over ground propulsion. To minimize the difference, the rear roller of the passive dynamometer was connected to a flywheel to provide momentum during the recovery phase, similar to propulsion over carpeted floor or grass. Finally, since we used a passive wheelchair ergometer and we did not measure the hand-rim kinetics during the six-minute push test, we were unable to calculate the gross mechanical efficiency; this can be an area for further research.

Further investigation of hand-rim biomechanics, upper extremity joint dynamics, muscle activity, and energetics is warranted to elucidate the effects of using geared wheelchair wheels during propulsion over different ground conditions and mobility tasks.

References

- Boninger, M. L., Cooper, R. A., Baldwin, M. A., Shimada, S. D., & Koontz, A. (1999). Wheelchair pushrim kinetics: Body weight and median nerve function. *Archives of Physical Medicine and Rehabilitation*, 80(8), 910-915.
- Boninger, M. L., Koontz, A. M., Sisto, S. A., & Dyson-Hudson, T. A. (2005). Pushrim biomechanics and injury prevention in spinal cord injury: Recommendations based on CULP-SCI investigations. *Journal of Rehabilitation Research and Development*, 42(3), 9.
- Chow, J. W., Millikan, T. A., Carlton, L. G., Chae, W., Lim, Y., & Morse, M. I. (2009). Kinematic and electromyographic analysis of wheelchair propulsion on ramps of different slopes for young men with paraplegia. *Archives of Physical Medicine and Rehabilitation*, 90(2), 271-278.
- Collins, E. G., Kiratli, J., Butler, J., Hanson, K., Langbein, W. E., & Gater, D. (2010). Energy cost of physical activities in persons with spinal cord injury.(report). *Medicine and Science in Sports and Exercise*, 42(4), 691-700.
- Howarth, S. J., Polgar, J. M., Dickerson, C. R., & Callaghan, J. P. (2010). Trunk muscle activity during wheelchair ramp ascent and the influence of a geared wheel on the demands of postural control. *Archives of Physical Medicine and Rehabilitation*, 91(3), 436-442.
- Howarth, S. J., Pronovost, L. M., Polgar, J. M., Dickerson, C. R., & Callaghan, J. P. (2010). Use of a geared wheelchair wheel to reduce propulsive muscular demand during ramp ascent: Analysis of muscle activation and kinematics. *Clinical Biomechanics*, 25(1), 21-28.
- Jahani, O., Gaglio, A., Schnorenberg, A. J., Muqet, V., Hsiao-Wecksler, E. T., & Slavens, B. A. (2019). Evaluation of Hand-rim and Wrist Joint Kinetics During Geared Manual Wheelchair Propulsion in Veterans with Spinal Cord Injury. *Biomedical sciences instrumentation*, 55(2), 324-329.
- Kloosterman, M. G., Buurke, J. H., Schaake, L., van der Woude, Lucas HV, & Rietman, J. S. (2016). Exploration of shoulder load during hand-rim wheelchair start-up with and without power-assisted propulsion in experienced wheelchair users. *Clinical Biomechanics*, 34, 1-6.
- Mercer, J. L., Boninger, M., Koontz, A., Ren, D., Dyson-Hudson, T., & Cooper, R. (2006). Shoulder joint kinetics and pathology in manual wheelchair users. *Clinical Biomechanics*, 21(8), 781-789.
- Requejo, P., Mulroy, S., Haubert, L. L., Newsam, C., Gronley, J., & Perry, J. (2008). Evidence-based strategies to preserve shoulder function in manual wheelchair users with spinal cord injury. *Topics in Spinal Cord Injury Rehabilitation*, 13(4), 86-119.
- Sonenblum, S. E., Sprigle, S., & Lopez, R. A. (2012). Manual wheelchair use: Bouts of mobility in everyday life. *Rehabilitation Research and Practice*, 2012

Curriculum Vitae

Education

PhD: Health Sciences 2013 - 2019

University of Wisconsin-Milwaukee

Dissertation: Quantitative Evaluation of Geared Manual Wheelchair Mobility in Individuals with Spinal Cord Injury, Using an Integrative Approach

MSc: Mechanical Engineering – Applied Mechanics 2007-2010

Azad University of Mashhad, Iran

Thesis: Optimization of Biped Locomotion System by Intelligent Mechanical Designs and Considering Biological Elements

BSc: Mechanical Engineering – Fluid Mechanics 2001-2006

Azad University of Mashhad, Iran

Peer-Reviewed Publications & Conference Proceedings

Slavens, B. A., Jahanian, O., Schnorenberg, A. J., & Hsiao-Wecksler, E. A. (Under Review). Comparison of Glenohumeral Joint Kinematics and Muscle Activation During Standard and Geared Manual Wheelchair Mobility. *Medical engineering & physics*.

Jahanian O., Schnorenberg, A. J., Muqet V., Hsiao-Wecksler, E., & Slavens B. (Under Review). Glenohumeral Joint Dynamics and Shoulder Muscle Activity During Geared Manual Wheelchair Propulsion on Carpeted Floor in Individuals with Spinal Cord Injury. *Journal of Electromyography and Kinesiology*.

Jahanian, O., Gaglio, A., Schnorenberg, A. J., Muqet, V., Hsiao-Wecksler, E. T., & Slavens, B. A. (2019, April). Evaluation of Hand-rim and Wrist Joint Kinetics During Geared Manual Wheelchair Propulsion in Veterans with Spinal Cord Injury. *Biomedical sciences instrumentation*, 55(2), 324-329.

Jahanian O., Schnorenberg A., Riebe J., Gaglio A., Muqet V., Hsiao-Wecksler, E., and Slavens B. (2019, March). Glenohumeral Joint Dynamics During Geared Manual Wheelchair Propulsion in Individuals with Spinal Cord Injury. *Gait and Clinical Movement Analysis Society (GCMAS) 2019 Conference, Frisco, TX.*

Jahanian O., Silver-Thorn B., Strath S., Muqet V., Hsiao-Wecksler, E., and Slavens B. (2018, August) Energy Expenditure during Manual Wheelchair Propulsion in Individuals with Spinal Cord Injury. *The 42nd Annual Meeting of American Society of Biomechanics, ASB2018, Rochester, MN.*

Jahanian O., Muqet V., Hsiao-Wecksler, E., and Slavens B. (2018, August) Shoulder Muscle Activity in Individuals with Spinal Cord Injury Using Geared Manual Wheelchairs during Start-UP. *The 12th Annual Meeting of the International Shoulder Group, ISG2018, Rochester, MN.*

Jahanian O., Gaglio A., Daigle S., Muqet V., Schnorenberg A., Hsiao-Wecksler, E., and Slavens B. (2018, July) Hand-rim Biomechanics of Geared Manual Wheelchair Mobility. *Rehabilitation Engineering and Assistive Technology Society of North America (RESNA) 2018 Annual Conference, Arlington, VA.*

Jahanian O., Rowley T., Strath S., Silver-Thorn B. Slavens B. (2017, August) Impact of Geared Wheels on Energy Expenditure during Manual Wheelchair Mobility. *The 41st Annual Meeting of American Society of Biomechanics, ASB2017, Boulder, CO.*

Xiao C., Liang, Jahanian O, Slavens B. & Hsiao-Wecksler, E. (2017, August). Biomechanical Evaluation of Pneumatic Sleeve Orthosis for Lofstrand Crutch-Assisted Gait. *The 41st Annual Meeting of American Society of Biomechanics, ASB2017, Boulder, CO.*

Jahanian O., Schnorenberg A., Kempfer J., Silver-Thorn B., and Slavens B. (2017, May). Walker Assisted Amputee Gait Analysis Using a Mobile Prosthesis Integrated Sensor System. *Gait and Clinical Movement Analysis Society (GCMAS) 2017 Conference, Salt Lake City, UT.*

Xiao C., Liang, Jahanian O., Schnorenberg A., Slavens B. & Hsiao-Wecksler, E. (2017, April). Design and Biomechanical Evaluation of Pneumatic Ergonomic Crutch. *2017 Design of Medical Devices Conference.*

Gaglio, A., Daigle, S., Gacek E., Jahanian O., Slavens B., Rice I. & Hsiao-Wecksler, E. (2017, April). Validation of an Instrumented Wheelchair Hand Rim. *2017 Design of Medical Devices Conference.*

Jahanian, O., Schnorenberg, A. J., & Slavens, B. A. (2016, October). Evaluation of shoulder joint kinematics and muscle activity during geared and standard manual wheelchair mobility. *In Engineering in Medicine and Biology Society (EMBC), 2016 IEEE 38th Annual International Conference, 6162-6165.*

Farooq, D., Jahanian, O., Slavens, B. A., & Hsiao-Wecksler, E. T. (2016, August). Evaluation of a wrist orthosis on lofstrand crutch-assisted gait. *In Engineering in Medicine and Biology Society (EMBC), 2016 IEEE 38th Annual International Conference, 5042-5045.*

Jahanian O., Schnorenberg A., Hawi L., Slavens B. (2016, July) Evaluation of Shoulder Joint Kinematics and Stroke Cycle Characteristics During Geared and Standard Manual Wheelchair Mobility. *Rehabilitation Engineering and Assistive Technology Society of North America (RESNA) 2016 Annual Conference, Arlington, VA.*

Kopf, M., Jahanian, O., Schnorenberg, A. J., Silver-Thorn, B., Kempfer, J., Smith, R. O., & Slavens, B. A. (2016, July) Quantitative Assessment of Walker-Assisted Gait in Transtibial Amputees. *Rehabilitation Engineering and Assistive Technology Society of North America (RESNA) 2016 Annual Conference, Arlington, VA.*

Jahanian O., Schnorenberg A., Hawi L., Slavens B. (2015, August) Upper Extremity Joint Dynamics and Electromyography (EMG) During Standard and Geared Manual Wheelchair Propulsion. *The 39th Annual Meeting of American Society of Biomechanics, ASB2015, Columbus, OH.*

Karimi, G., & Jahanian, O. (2012). Genetic Algorithm Application in Swing Phase Optimization of AK Prosthesis with Passive Dynamics and Biomechanics Considerations. *Chapter 5, Genetic Algorithms in Applications book, ISBN: 978-953-51-0400-1, INTECH Open Access Publisher.*

Jahanian, O., Falahi, M., & Karimi, M. (2011, December). Warehousebot, An Automated Material Handling Machine. *In The 3rd International Conference on Manufacturing Engineering (ICME), Tehran, Iran.*

Farshidianfar A., Jahanian O. (2010) Passive Dynamic Robots; *ISME Mechanical Engineering Magazine*, No:72, 19th ,2010 (In Persian).

Jahanian, O., & Karimi, G. (2006, December). Locomotion systems in robotic application. *In 2006 IEEE International Conference on Robotics and Biomimetics*, 689-696.

Journal Articles (In Preparation)

Jahanian O., Silver-Thorn B., Muqet V., Hsiao-Wecksler, E., Strath S., and Slavens B. (In Preparation). The Effects of Using Geared Wheelchair Wheels on Energy Cost of Propulsion in Adults with Spinal Cord Injury. *Journal of Spinal Cord.*

Jahanian O., Gaglio A., Cho C., Muqet V., Hsiao-Wecksler, E., and Slavens B. (In preparation). Hand-Rim Biomechanics of Geared Manual Wheelchair Mobility in Veterans with Spinal Cord Injury. *PLOS ONE, Veterans Disability & Rehabilitation Research Channel.*

Silver-Thorn B., Jahanian O., Kempfer J., Schnorenberg A., and Slavens B. (In Preparation). Comparison of Kinetic Data for Various Prosthetic Components during Sit-to-Stand and Stand-to-Sit Trials for Lower Limb Amputees: A Pilot Study. *Journal of Prosthetics & Orthotics.*

Xiao C., Liang, Jahanian O, Slavens B. & Hsiao-Wecksler, E. (In Preparation). Design and Biomechanical Evaluation of Pneumatic Sleeve Orthosis for Lofstrand Catches. *IEEE Transactions on Neural Systems and Rehabilitation Engineering.*

Presentations

Jahanian O., Xiao C., Farooq D., Hsiao-Wecksler, E., and Slavens B. (2017, March), Evaluation of Passive and Active Orthoses for Lofstrand Crutch-Assisted Gait. 2017 Health Research Symposium, University of Wisconsin Milwaukee. (Podium).

Gacek E, Pakeltis A., Jahanian O., Gaglio A., Daigle S., Rice I, Slavens B., Hsiao-Wecksler E. (2017, March), An Investigation of the Effect of Gear Ratio on Manual Wheelchair Kinetics. 2017 Midwest Regional Meeting of the American Society of Biomechanics, Grand Valley State University, MI. (Poster).

Jahanian O., Slavens B. (2016, October). An Integrative Approach for Quantitative Evaluation of Manual Wheelchair Mobility. Wisconsin Occupational Therapy Association (WOTA) 95th Conference. (Workshop).

Jahanian O., Schnorenberg A., Slavens B. (2016, May) Evaluation of Stroke Cycle Characteristics, Shoulder Joint Kinematics and Muscle Activity during Geared and Standard Manual Wheelchair Mobility. College of Health Sciences Spring 2016 Research Symposium, University of Wisconsin Milwaukee. (Poster).

Engels E., Silver-Thorn B., Kempfer J., Jahanian O., Schnorenberg A., Smith R., and Slavens B. (2016, September) Kinetic Visualization of the iPecsTM Lab Sensor System to Assess Prosthetic Componentry for Lower-Limb Amputees. The 99th American Orthotic & Prosthetic Association (AOPA) National Assembly. (Poster).

Jahanian O., Slavens B. (2016, May). Evaluation of Upper Extremity Muscle Activation during Geared Manual Wheelchair Propulsion on Ramp. The 5th Annual Occupational Therapy Summit, Pittsburg. (Poster).

Jahanian O., Simpson E., Slavens B. (2015, December) Evaluation of Energy Cost During Standard and Geared Manual Wheelchair Propulsion; College of Health Sciences Fall 2015 Research Symposium, University of Wisconsin Milwaukee. (Poster).

Jahanian O., Schnorenberg A., Hawi L., Slavens B. (2015, May) Evaluation of Upper Extremity Biomechanics during Standard and Geared Manual Wheelchair Propulsion. College of Health Sciences Spring 2015 Research Symposium, University of Wisconsin Milwaukee. (Podium).

Jahanian O., Schnorenberg A., Hawi L., Slavens B. (2014, December) How Do Geared Manual Wheelchairs Influence Wheelchair Propulsion Biomechanics? College of Health Sciences Fall 2014 Research Symposium , University of Wisconsin Milwaukee. (Podium).

Jahanian O., Schnorenberg A., Slavens B. (2014, May) Evaluation Methods for Comparing Joint Kinematics during Geared and Standard Manual Wheelchair Usage; College of Health Sciences Spring 2014 Research Symposium, University of Wisconsin Milwaukee. (Poster).

Funded Projects

Jahanian, O. & Slavens A.B. (2014). A Comparison of Joint Dynamics, Energetics, and Muscle Activations during Geared and Standard Manual Wheelchair Usage. UW-Milwaukee, CHS Student Research Grant. Amount \$2,000.

Jahanian, O. & Slavens A.B. (2016). Prediction of Energy Expenditure in Manual Wheelchair Users with Spinal Cord Injury. UW-Milwaukee, CHS Student Research Grant. Amount \$1,300.

Jahanian, O. & Slavens A.B. (2018). Impact of Geared Wheels on Energy Expenditure during Manual Wheelchair Mobility. UW-Milwaukee, CHS Student Research Grant. Amount \$2,000.

Scholarships & Awards

The Gait and Clinical Movement Analysis Society (GCMAS) 2019 conference student travel award (2019)

Winning Papers in Rehabilitation Engineering and Assistive Technology Society of North America's (RESNA) Annual Conference, 2018 Student Scientific Paper Competition (2018)

University of Wisconsin-Milwaukee Distinguished Dissertation Fellowship (2017-2018)

The Gait and Clinical Movement Analysis Society (GCMAS) 2017 conference student travel award (2017)

2017 UWM Health Research Symposium Best Research, 3rd Place (2017)

Honorable Mention in Rehabilitation Engineering and Assistive Technology Society of North America's (RESNA) Annual Conference, 2016 Student Scientific Paper Competition, sponsored by Paralyzed Veterans of America (2016)

Certificate of Completion Methods in Grant Preparation, May 2015, Clinical & Translational Science Institute/ Medical College of Wisconsin (2015)

UW-Milwaukee Chancellor's Graduate Student Award (2013, 2014, 2015, 2016, & 2018)

Positions Held

Graduate Research Assistant, Department of Occupational Science & Technology, University of Wisconsin Milwaukee (2018-2019)

Instructor, Department of Occupational Science & Technology, University of Wisconsin Milwaukee, Spring 2018 (OccThpy 704, Musculoskeletal Analysis and Occupational Function)

Teaching assistant (TA), Department of Occupational Science & Technology, University of Wisconsin Milwaukee, Spring 2017 (OccThpy 704, Musculoskeletal Analysis and Occupational Function)

Instructor, Department of Occupational Science & Technology, University of Wisconsin Milwaukee, Fall 2016 (OccThpy 593: Introduction to Biomedical and Rehabilitation Instrumentation)

Authorized Research Co-Investigator (WOC), Zablocki VA Medical Center, Milwaukee, WI, Since 2014

Graduate Research Assistant, Aug.2014 – Aug. 2016 (National Institute of Health)

NIH Phase 2 SBIR-IntelliWheels: The Automatic Transmission for Manually Propelled Wheelchairs, PI: Brooke A. Slavens, Ph.D.

Collaborators: IntelliWheels, Inc., University of Illinois at Urbana-Champaign, and Clement J. Zablocki VA Medical Center

Graduate Research Assistant, Department of Occupational Science & Technology, University of Wisconsin Milwaukee (2013 -2016)